CHAPTER V

RESULTS AND DISCUSSIONS

Experimental results from several tests of fiber reinforced epoxy composites are revealed and discussed in this chapter. The numerical data of these tests are detailed in Appendix A.

5.1 REGRESSION ANALYSIS

The mechanical properties from tests in Section 4.4 are analyzed based on the statistical method of 2^3 factorial design. The three factors of interest namely aging temperature (A), humidity (B) and UV (C) were designed at two levels giving eight treatment combinations as shown in Table 4.2. Therefore, there are seven degree of freedom among the eight treatment combinations in this 2^3 factorial design. Three degree of freedom are associated with the main effects of A, B and C while four are with interactions namely AB, AC, BC and ABC.

Estimation of the effects and the sum of squares can be obtained by Yates' algorithm. The determination of the main effects was achieved by plotting the estimates of the effects on a normal probability scale. Thorough calculation is shown in Appendix B. The normal probability plots of the fiber reinforced epoxy composites are shown in Appendix C.

Table 5.1 displays an example of the experimental responses of fiber reinforced epoxy composites in terms of the flexural strength. Estimates of the effects and corresponding sum of squares are exhibited in Table 5.2. Estimates of all the effects and the sum of squares are detailed in Appendix D.

Aging condition	Factors			Responses, MPa (y)
	A	B	C	
1	-	+	+	95.811
2	-	+	-	106.315
3	-	-	+	103.401
4	-	-	-	111.919
5	+	+	+	91.874
6	+	+	-	92.997
7	+	-	+	107.078
8	+	-	-	95.984

Table 5.1: Flexural strength of carbon fiber reinforced epoxy composites.

Treatment combination	Responses	Estimate of effect	Sum of squares
(1)	111.919	-	-
a	95.984	-7.3783	108.8771
b	106.315	-7.8463	123.1273
ab	92.997	-1.2493	3.1213
c	103.401	-2.2628	10.2401
ac	107.078	7.2483	105.0743
bc	95.811	-3.5508	25.2157
abc	91.874	-2.5578	13.0842

Table 5.2: Estimation of effects and sum of squares for flexural strength of carbon fiber reinforced epoxy composites.

A multiple linear regression model with k predictor variables as shown in Equation 5.1 can be applied fitting empirical model.

$$y = \beta_0 + \beta_1 x_1 + \beta_2 x_2 + ... + \beta_k x_k + \varepsilon \qquad (5.1)$$

where y represents the responses variables, $x_1, x_2, \ldots, x_k$ represents the coded variables of the independent variables. ε is the random error term. The parameter β_j is known as the regression coefficients and $j = 0, 1, 2, 3, \ldots, k$. It represents the expected change in the response (y) per unit change in x_j when all the remaining independent variables x_i ($i \neq j$) are held constant. From the normal probability plot of effects, significance effects will not lie along the straight line. Figure 5.1 depicts the normal probability plot of estimate effects for the flexural strength of the carbon fiber-reinforced epoxy composites.
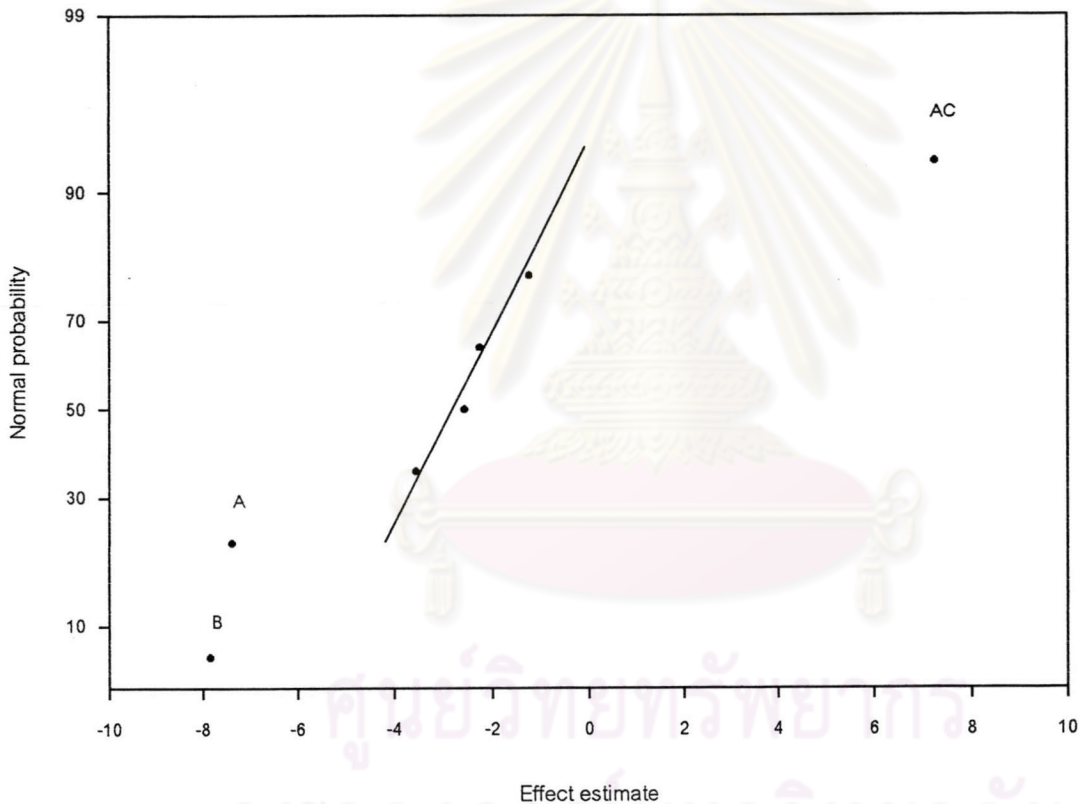
Figure 5.1: Normal probability plot of estimate effect for the flexural strength of carbon fiber reinforced epoxy composites.

It is obvious that the important factors influencing the flexural strength of the composites are aging temperature (A), humidity (B) and the interaction between aging temperature and UV (AC). Thus, the regression model for

predicting the flexural strength of carbon fiber reinforced epoxy composites can be written as shown in Equation 5.2.

$$\hat{y} = 100.6724 - \left(\frac{7.3783}{2}\right)x_1 - \left(\frac{7.8463}{2}\right)x_2 + \left(\frac{7.2483}{2}\right)x_1 x_3 \quad (5.2)$$

where the x_1, x_2 and x_3 are the coded variables of aging temperature, humidity and UV exposure, respectively. The $x_1 x_3$ term is the interaction between the aging temperature and UV exposure. The analysis of variance (ANOVA) is summarized in Table 5.3. This ANOVA table is utilized in hypothesis testing for the multiple linear regression model, Equation 5.2.

Source of variation	Sum of squares	Degree of freedom	Mean square	F_0
A	108.8771	1	108.8771	8.4301
B	123.1273	1	123.1273	9.5334
AC	105.0743	1	105.0743	8.1356
Error	51.6611	4	12.9153	
Total	388.7398	7	$R^2 = 0.8671$	

Table 5.3: ANOVA table for regression analysis of flexural strength of carbon fiber reinforced epoxy composites.

In this present study, test for the significance of the regression is applied. This is a test to decide if there is a linear relationship between the flexural strength (y) and the coded variable of the aging effects, x_1, x_2 and x_3. The proper hypotheses are

$$H_0: \beta_1 = \beta_2 = \ldots = \beta_k = 0 \quad (5.3)$$
$$H_1: \beta_j \ 0 \quad \text{for at least one } j \quad (5.4)$$

where H_0 and H_1 are used to check whether the multiple regression model is null. Rejection of H_0 in Equation 5.3 implies that at least one of the predictor

variable, x_1, x_2 and x_1x_3, contributes substantially to the model. The test procedure is to compute F_0 and to reject H_0 if F_0 exceeds $F_{\alpha, k, n-k-1}$. The confidential level in this study is set at 90%, in other word, the level of significance is at 0.1. As a result, the critical F-distribution at the level of significance at 0.1, $F_{0.1,3,4}$ is 4.19 while F_0 is at least 8.1356 for this example. Because F_0 is greater than $F_{0.1,3,4}$, the hypothesis of H_0 is rejected. Therefore, this linear regression model appropriately fits the data and the regression coefficients from the regression analysis are proper for the prediction of the flexural strength of carbon fiber-reinforced epoxy composites. Additionally, the coefficient of determination, R^2, of 0.8671 shown in the ANOVA table means that the linear regression model can explain 86.71% of the observed flexural strength data.

Before the conclusions from the analysis of variance are adopted, the adequacy of the regression model should be checked via residual analysis. The residuals can be calculated as the difference between the observed and the predicted flexural strength of carbon fiber-reinforced epoxy composites by using the empirical linear regression model. Table 5.4 lists the observed and the predicted flexural strength of carbon fiber reinforced epoxy composites and their corresponding.

Effects	Observed values	Predicted values	Residuals
(1)	111.919	111.9089	0.0102
A	95.984	97.2823	-1.2983
B	106.315	104.0626	2.2525
AB	92.997	89.436	3.5611
C	103.401	104.6606	-1.2596
AC	107.078	104.5306	2.5475
BC	95.811	96.8143	-1.0033
ABC	91.874	96.6843	-4.8103

Table 5.4: Observed and predicted flexural strength of carbon fiber reinforced epoxy composites and corresponding residuals.

A normal probability plot of these residuals is shown in Figure 5.2. The fact that the residuals remain reasonably close to a straight line supports the prior conclusion that the aging temperature (A), humidity (B) and an interaction between aging temperature and UV (AC) are the significant effects of the linear regression model for the flexural strength of carbon fiber-reinforced epoxy composites.
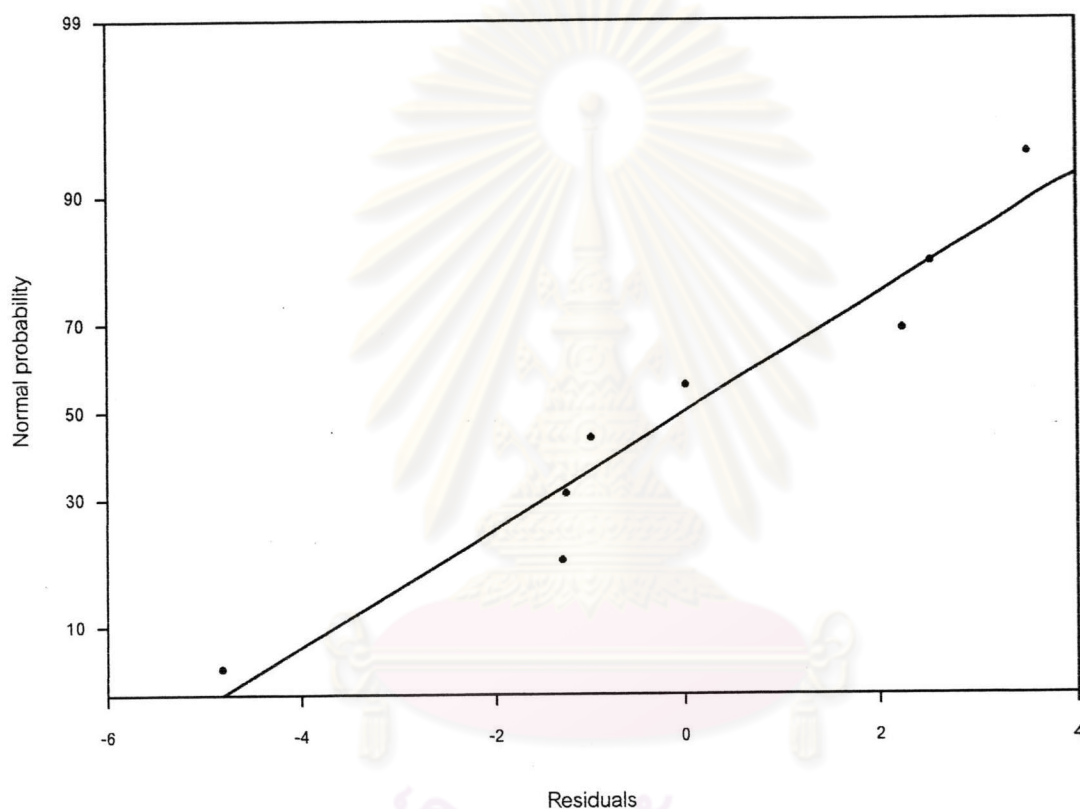

Figure 5.2: Normal probability plot of residuals for flexural strength of carbon fiber reinforced epoxy composites.

All linear regression models derived from the regression analysis of the mechanical properties in this experimental study are summarized in Table 5.5 and 5.6. These linear regression models are suitable for predicting the mechanical properties of carbon fiber-reinforced epoxy composites and aramid fiber reinforced epoxy composites that are exposed to various climatic conditions. Specifically, compressive strengths applied for

the regression analysis are values received from compressing the composites in the direction paralleled with the principal axis of anisotropy.

Mechanical properties	Linear regression model
Flexural strength (MPa)	$y = 100.6724 - \left(\dfrac{7.3783}{2}\right)x_1 - \left(\dfrac{7.8463}{2}\right)x_2 + \left(\dfrac{7.2483}{2}\right)x_1x_3$
Compressive strength (MPa)	$y = 83.862 - \left(\dfrac{4.155}{2}\right)x_2 + \left(\dfrac{3.848}{2}\right)x_3 - \left(\dfrac{3.362}{2}\right)x_1x_2 + \left(\dfrac{3.872}{2}\right)x_2x_3$
Fracture toughness (MPa/m$^{1/2}$)	$y = 3.0683 + \left(\dfrac{0.441}{2}\right)x_1 + \left(\dfrac{0.7565}{2}\right)x_3 + \left(\dfrac{1.025}{2}\right)x_1x_3$
Fracture energy (J/m^2)	$y = 2.7291 + \left(\dfrac{1.2663}{2}\right)x_1 + \left(\dfrac{1.4108}{2}\right)x_3 + \left(\dfrac{2.3558}{2}\right)x_1x_3$

Table 5.5: Linear regression model from the mechanical properties of carbon fiber reinforced epoxy composites.

Mechanical properties	Linear regression model
Flexural strength (MPa)	$y = 108.7149 - \left(\dfrac{9.5163}{2}\right)x_2 - \left(\dfrac{7.3798}{2}\right)x_1x_2$
Compressive strength (MPa)	$y = 76.988 - \left(\dfrac{5.2533}{2}\right)x_2 - \left(\dfrac{2.2748}{2}\right)x_3 + \left(\dfrac{3.7478}{2}\right)x_2x_3$
Fracture toughness (MPa/m$^{1/2}$)	$y = 5.6093 + \left(\dfrac{2.96}{2}\right)x_1 - \left(\dfrac{0.727}{2}\right)x_2 - \left(\dfrac{0.337}{2}\right)x_1x_2x_3$
Fracture energy (J/m^2)	$y = 13.4226 + \left(\dfrac{12.7913}{2}\right)x_1$

Table 5.6: Linear regression model from the mechanical properties of aramid fiber reinforced epoxy composites.

5.2 MECHANICAL PROPERTIES OF FIBER REINFORCD EPOXY COMPOSITES

5.2.1 Flexural properties

Flexural test was performed to evaluate the modulus of elasticity and the maximum strength of the carbon fiber and aramid fiber-reinforced epoxy composites in flexural mode. Figure 5.3 illustrates the carbon fiber reinforced epoxy composites after flexural loading. The composite has a crack at the center of the specimen in the epoxy layer. The fiber is not failed. Failure has been caused by tension at the outermost layer according to the standard test method JIS K7074.

(a)

(b)
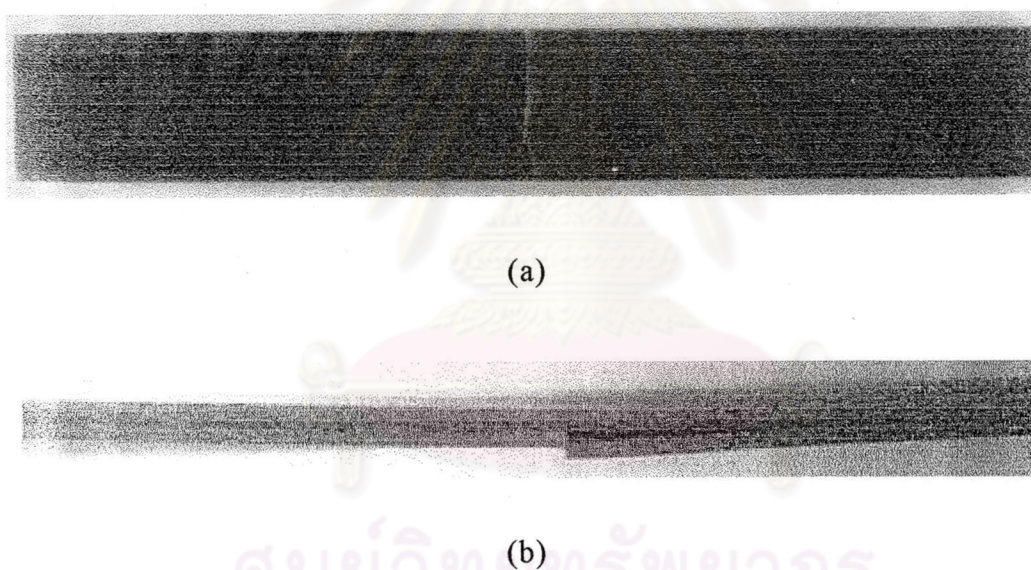
Figure 5.3: Carbon fiber reinforced epoxy composites after flexural loading; (a) top view and (b) side view.

The effects of various climatic conditions on the flexural strength of fiber reinforced epoxy composites are displayed in Figures 5.4 and 5.5.
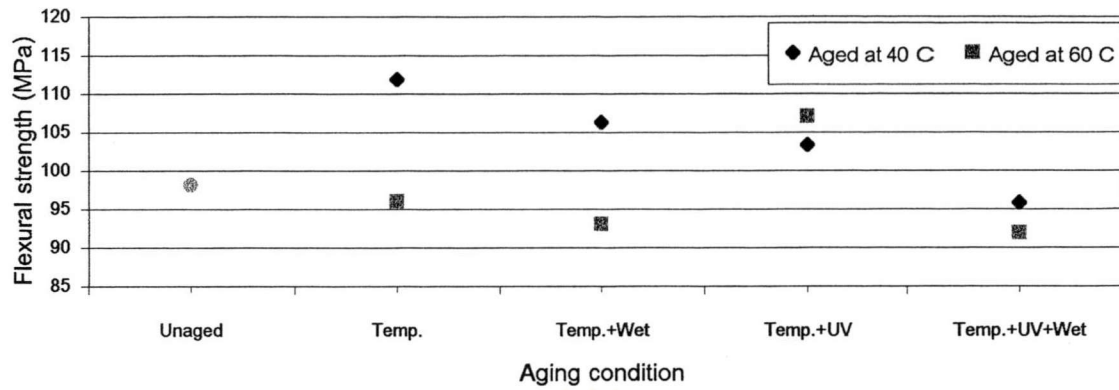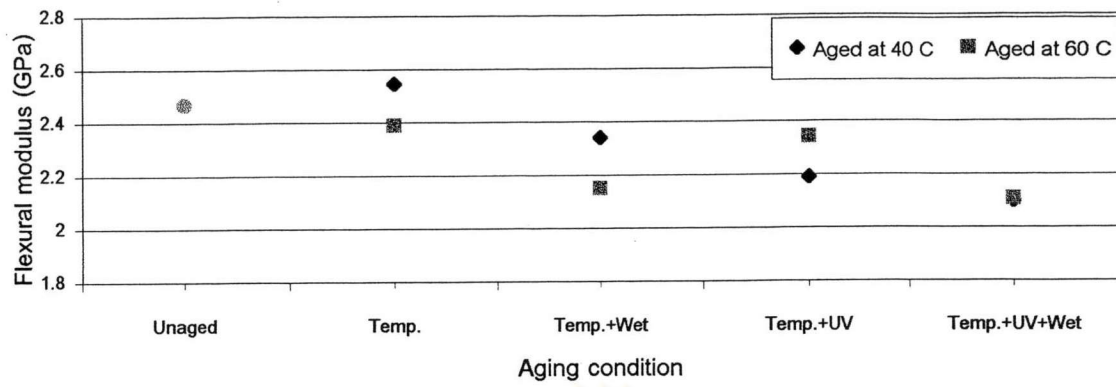
(a)
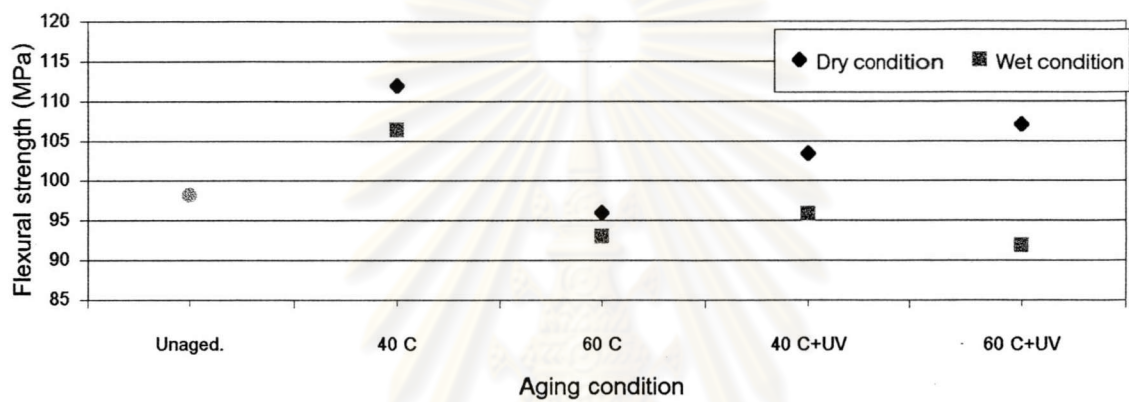
(b)
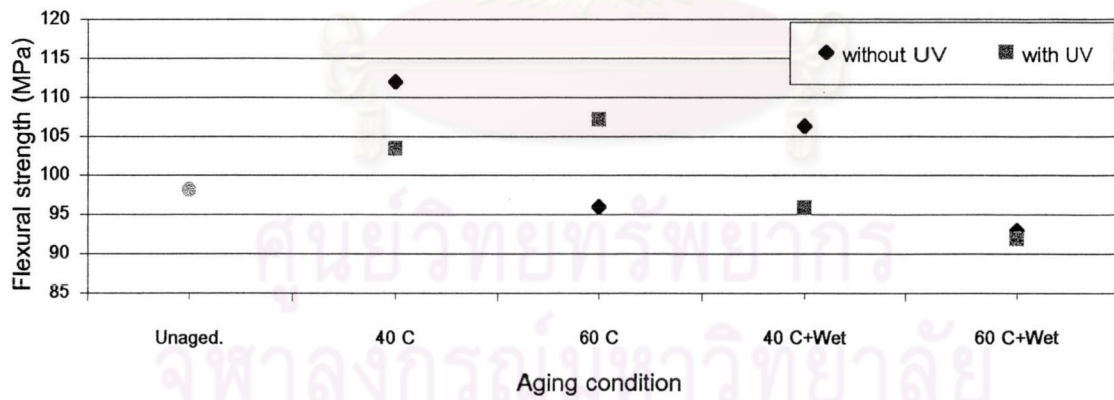
(c)

Figure 5.4: Effects of temperature (a), humidity (b) and the UV exposure (c) on the flexural strength of carbon fiber reinforced epoxy composites.
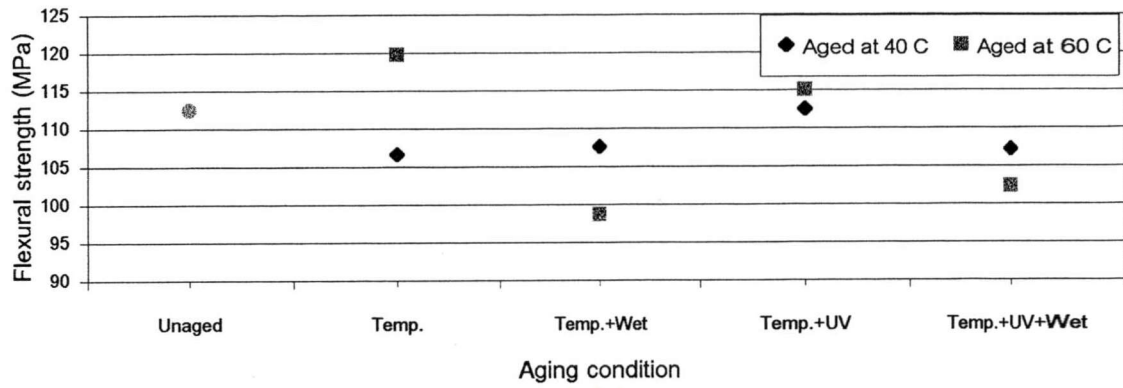
(a)
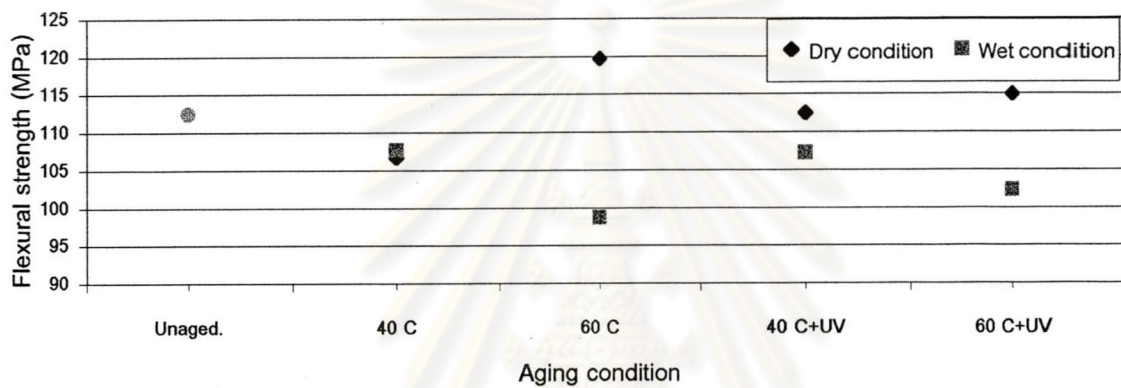
(b)
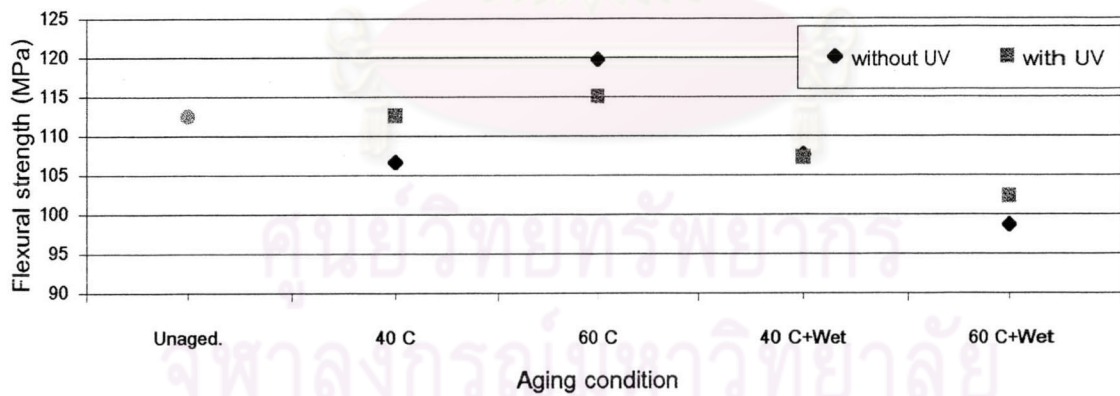
(c)

Figure 5.5: Effects of temperature (a), humidity (b) and the UV exposure (c) on the flexural strength of aramid fiber reinforced epoxy composites.

Firstly, for all results in Section 5.2, aging conditions shown in all plots are arranged from mild to severe conditions. For carbon fiber reinforced composites in Figure 5.4 (b), it is evident that the flexural strength of the specimens aged with dry condition are higher than those aged with wet condition. From Figure 5.4 (a) and (c), the flexural strength of the specimens aged at a higher temperature and aged with UV are lower than that those aged at a lower temperature and aged without UV. However, the flexural strength of the specimens aged at high temperature with UV are higher than those aged at a lower temperature with UV in Figure 5.4 (a) and higher than those aged at a higher temperature without UV in Figure 5.4 (c). Thus, the combined aging temperature and UV seems to play significant effect on the flexural strength of carbon fiber reinforced composites. The result is in agreement with the regression analysis, as shown in Figure 5.6 (a), in which the significant factors affecting the flexural strength of carbon fiber reinforce composites was found to be the humidity (B), the aging temperature (A) and the combined aging temperature and UV (AC) respectively.

For aramid fiber reinforced epoxy composites, from Figures 5.5 (a) and (c), there is no consistent trend for all four aging conditions. From Figure 5.5 (b), the flexural strength of the specimens aged with wet condition are lower than those aged with dry condition, except the specimens aged at a lower temperature with dry and wet condition. This is in agreement with the regression analysis for the flexural strength of aramid fiber reinforced composites, as shown in Figure 5.6 (b), in that the significance effects are the humidity (B) and the combined aging temperature and humidity (AB). The main factors affecting the flexural strength of aramid fiber reinforced composites are the humidity and the combined aging temperature and humidity respectively.

The effects of various climatic conditions on the flexural modulus of fiber reinforced epoxy composites are displayed in Figures 5.7 and 5.8.
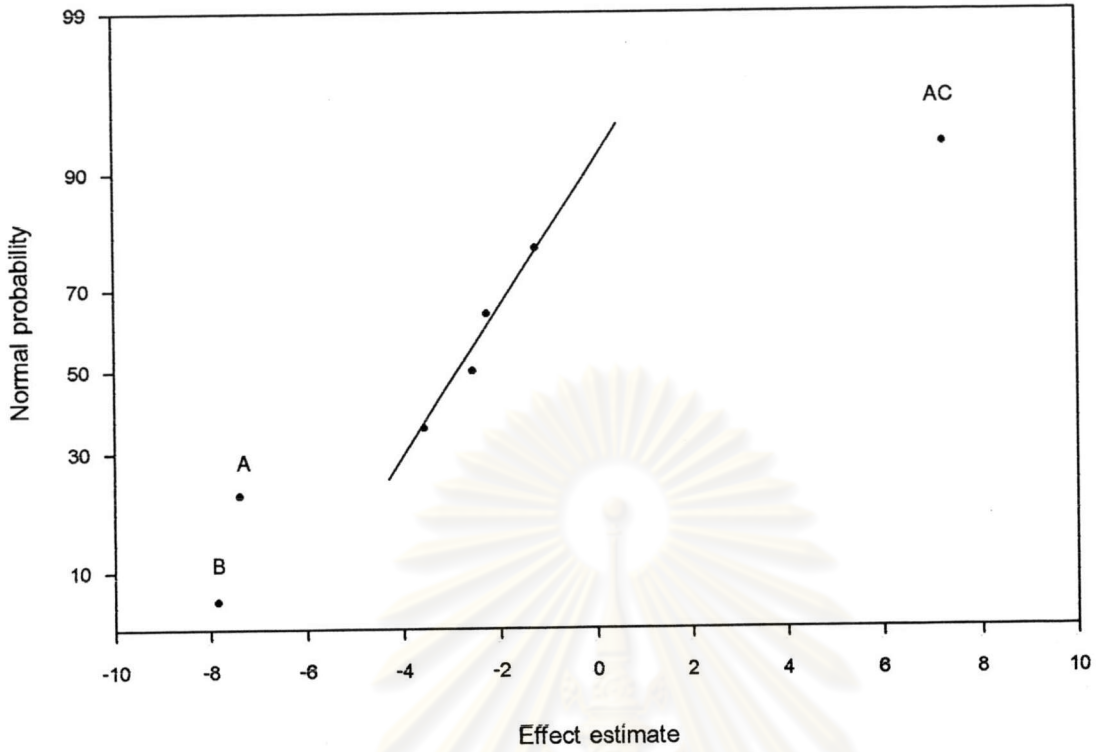
(a) carbon fiber reinforced composite
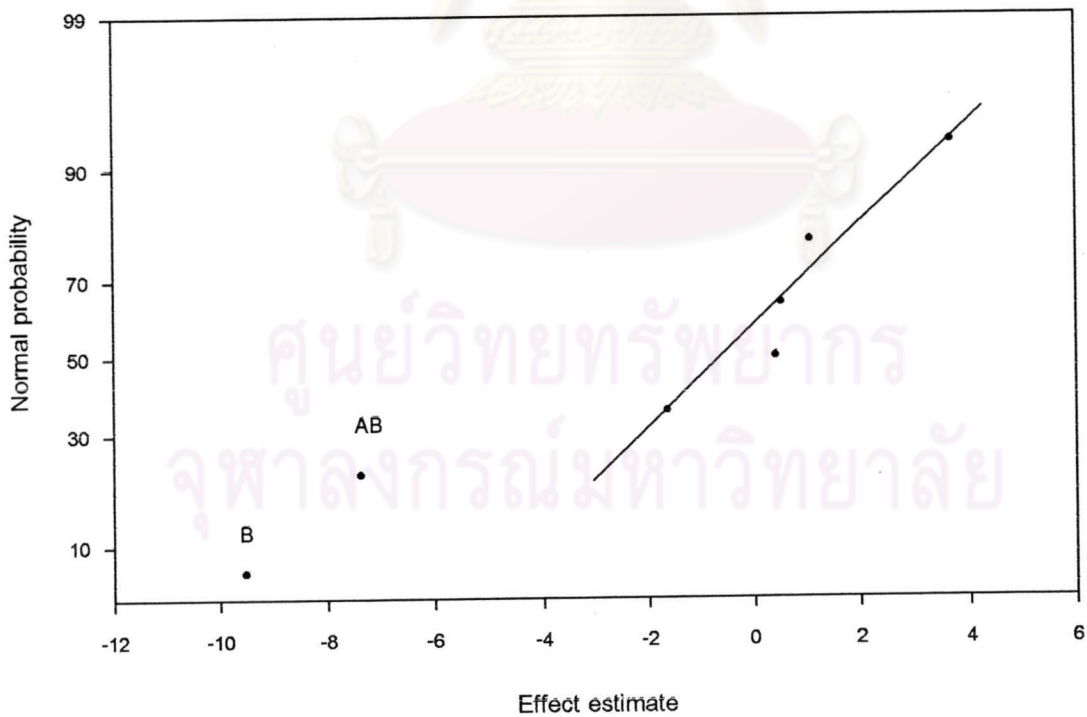
(b) aramid fiber reinforced composite

Figure 5.6: Normal probability plots of estimate effect for the flexural strength of fiber reinforced epoxy composites.
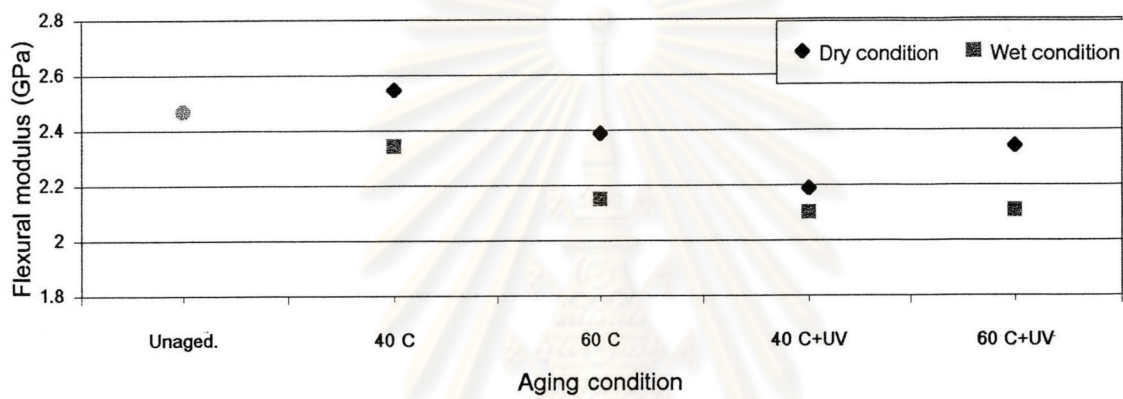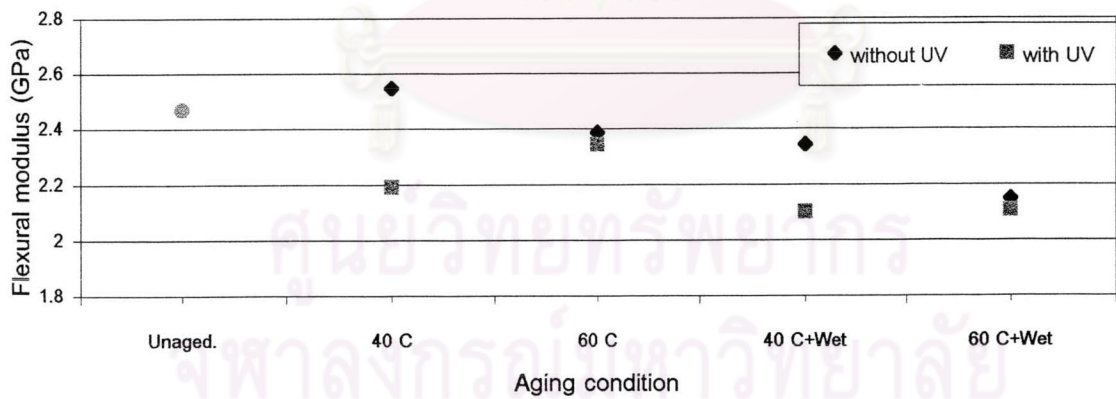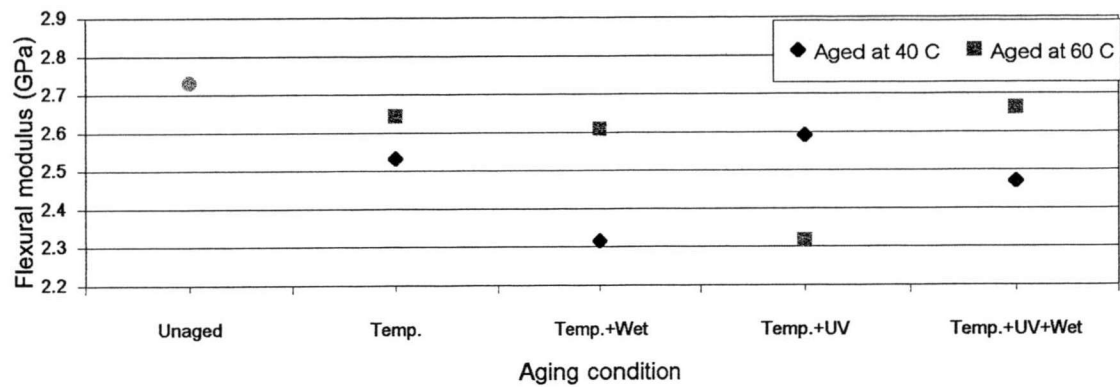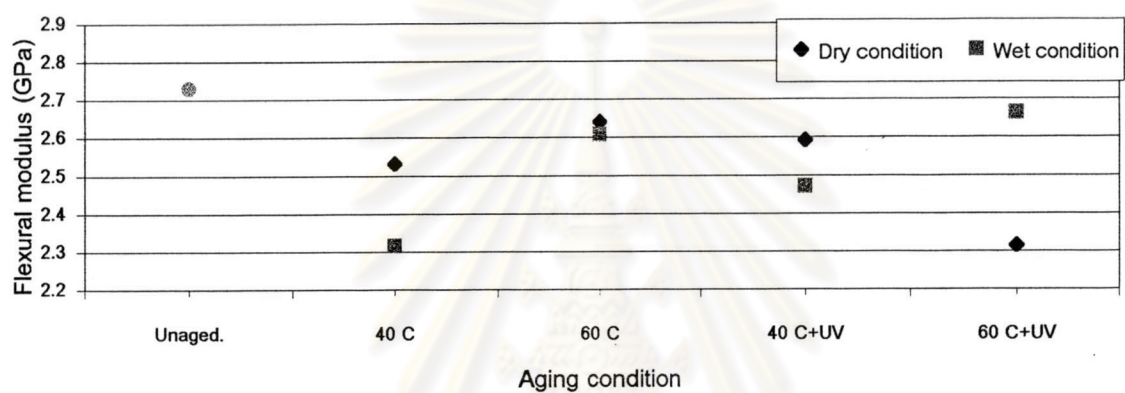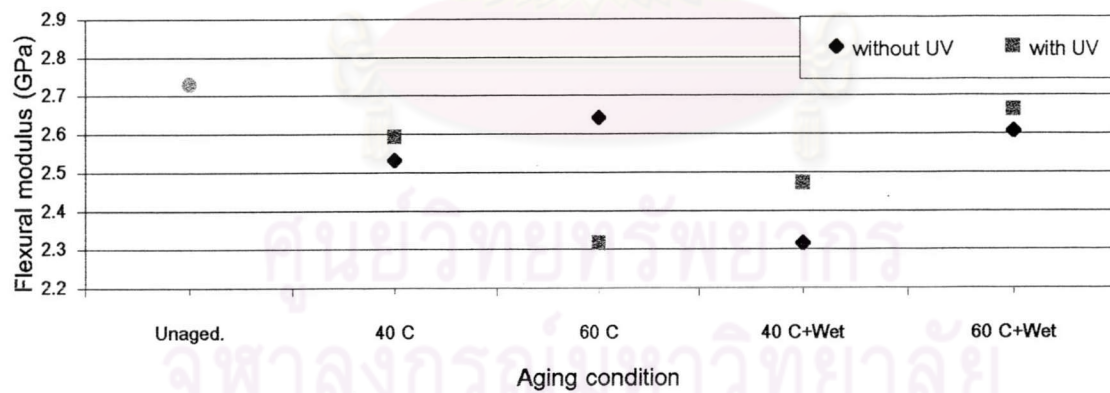
Figure 5.7: Effects of temperature (a), humidity (b) and the UV exposure (c) on the flexural modulus of carbon fiber reinforced epoxy composites.
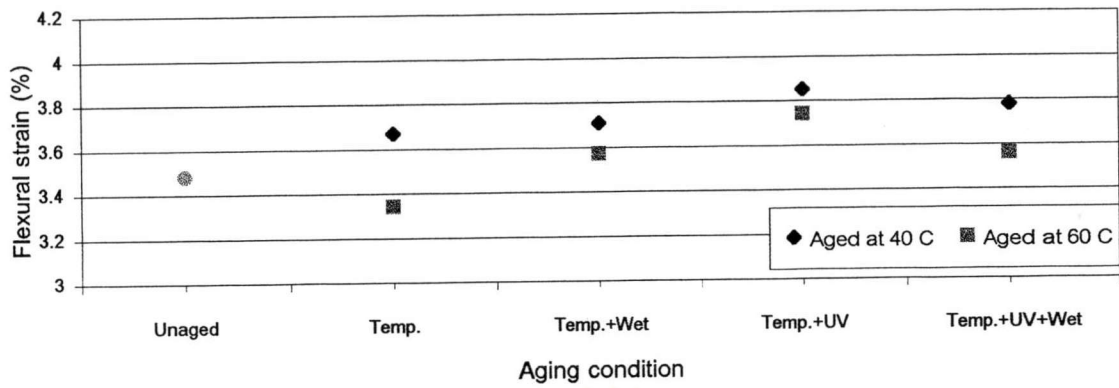
(a)
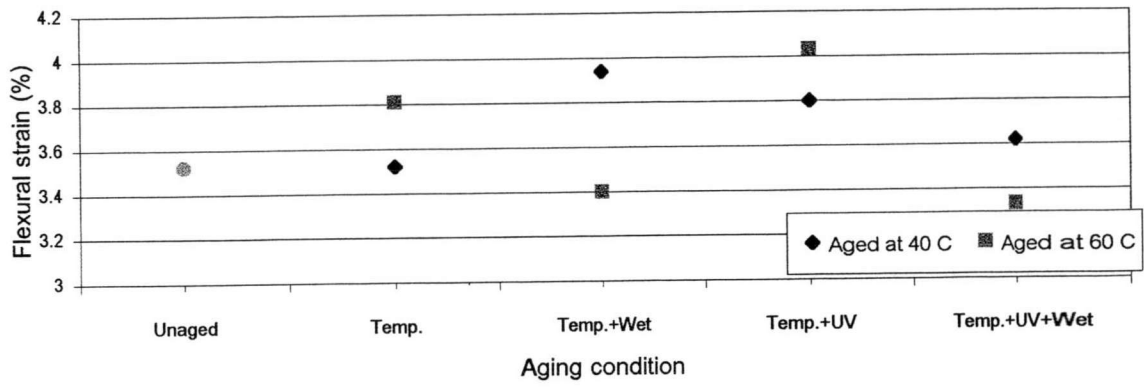
(b)

(c)

Figure 5.8: Effects of temperature (a), humidity (b) and the UV exposure (c) on the flexural modulus of aramid fiber reinforced epoxy composites.

For carbon fiber reinforced composites, from Figure 5.7 (a), it is not clearly seen which factors affect the flexural modulus of the specimens. Nevertheless, the flexural modulus tends to decrease when specimens are exposed to more severe conditions. From Figure 5.7 (b) and (c), the flexural modulus of the specimens aged with wet condition and aged with UV are lower than those aged with dry condition and aged without UV. This means that the aging temperature and UV exposure are the significant effects of the flexural modulus of carbon fiber reinforced composites.

For aramid fiber reinforced epoxy composites, from Figures 5.8 (a), the flexural modulus of the specimens aged at a higher temperature are higher than those aged at a lower temperature except the specimens aged at a higher temperature with UV. From Figure 5.8 (b), the flexural modulus of the specimens aged with dry condition are higher than those aged with wet condition, except the specimens aged at a higher temperature with dry condition. From Figure 5.8 (c), the flexural modulus of the specimens aged with UV are higher than those aged without UV except the specimens aged at a higher temperature with UV. These results imply that the aging temperature, humidity and UV exposure are the main effects of the flexural modulus of aramid fiber reinforced composites.

The effects of various aging conditions on the flexural strain at yield of fiber reinforced epoxy composites are shown in Figures 5.9 and 5.10.

For carbon fiber reinforced composites, from Figure 5.9 (a) and (c), it is apparent that the flexural strain at yield of the specimens aged at a higher temperature and aged without UV are lower than those aged at a lower temperature and aged with UV. From Figure 5.9 (b), it is not yet distinct which effects influence the flexural strain at yield for all four aging conditions.
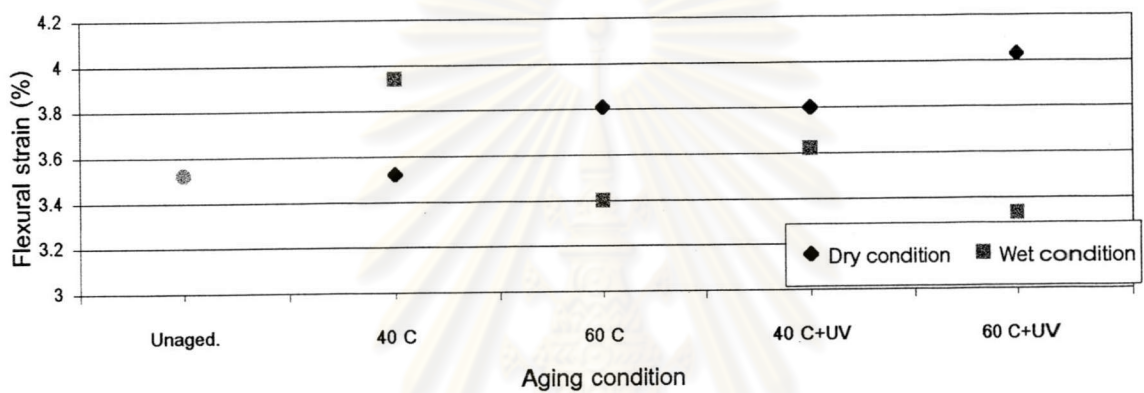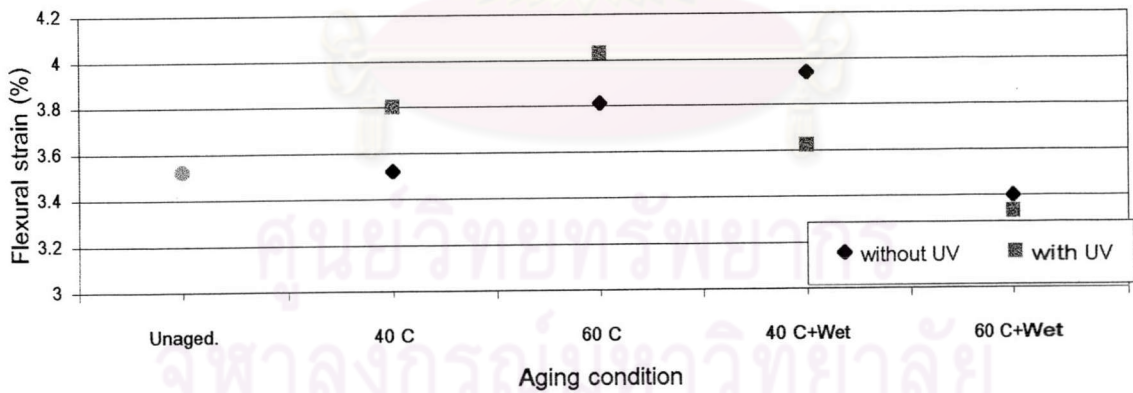
(a)
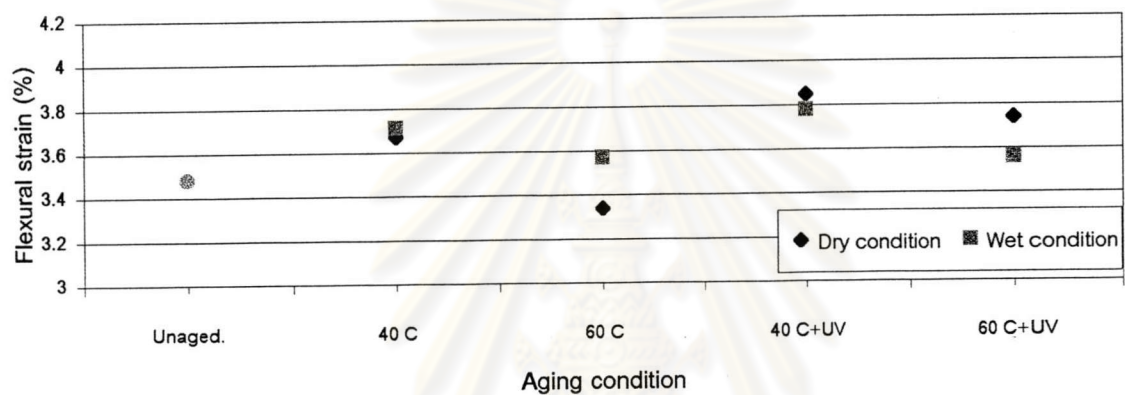
(b)
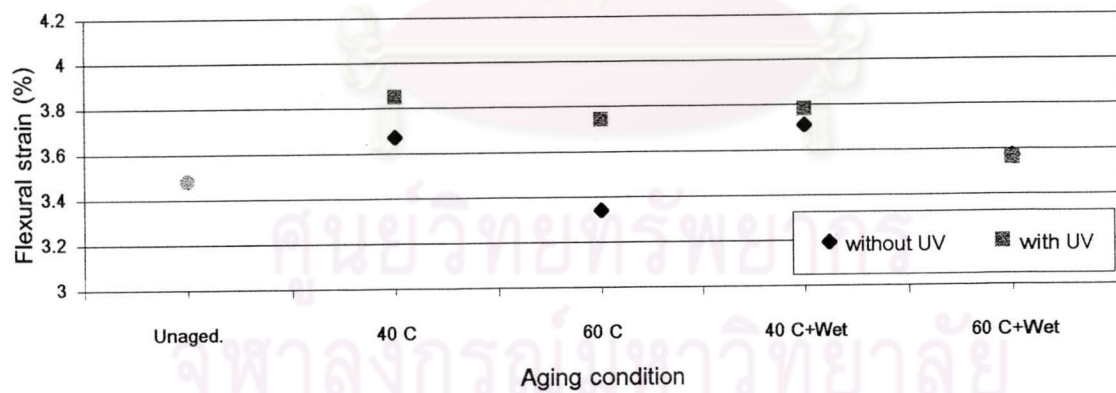
(c)

Figure 5.9: Effects of temperature (a), humidity (b) and the UV exposure (c) on the flexural strain at yield of carbon fiber reinforced epoxy composites.
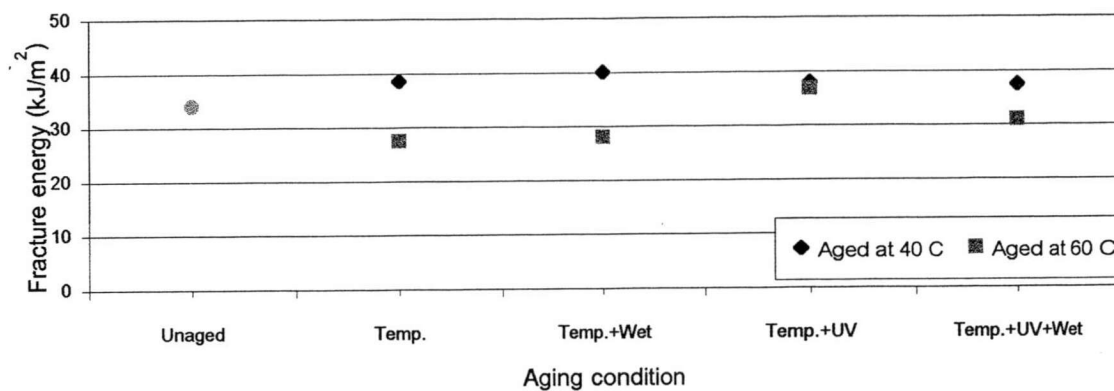
(a)

(b)

(c)

Figure 5.10: Effects of temperature (a), humidity (b) and the UV exposure (c) on the flexural strain at yield of aramid fiber reinforced epoxy composites.

For aramid fiber reinforced epoxy composites, from Figures 5.10 (a) and (c), it is also not apparent which factors affect the flexural strain at yield. From Figure 5.10 (b), the flexural strain at yield of the specimens aged with wet condition are lower than those aged with dry condition, with the exception of the specimen aged at a lower temperature with dry and wet condition. It is thus assumed that humidity seems to play a significant role on the flexural strain at yield of aramid fiber reinforced composites.

The effects of various climatic conditions on the fracture energy of fiber reinforced epoxy composites under flexural mode are shown in Figure 5.11 and 5.12.

From Figures 5.11 and 5.12, there is no significant difference for the fracture energy of fiber reinforced composites between the low level and high level of all aging conditions. For carbon fiber reinforced epoxy composites, from Figure 5.11 (a), it is seen that the flexural fracture energy of the specimens aged at a higher temperature are slightly lower than those aged at a lower temperature. It can be assumed that the aging temperature possibly is the main effect of the flexural fracture energy of carbon fiber reinforced composites. From Figures 5.11 (b) and (c), all aging conditions show the fracture energy at high level of aging conditions to be indifferent from those at low level of aging conditions.

For aramid fiber reinforced epoxy composites in Figures 5.12, all aging conditions also show the fracture energy at high level of aging conditions to be close to those at low level of aging conditions. Similar with carbon fiber reinforced composites, there is no significant factor affecting the flexural fracture energy of aramid fiber reinforced epoxy composites within the range studied.
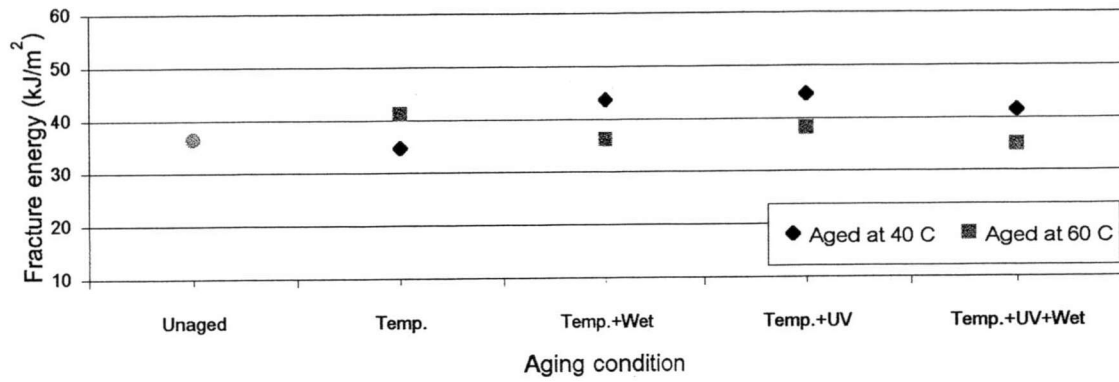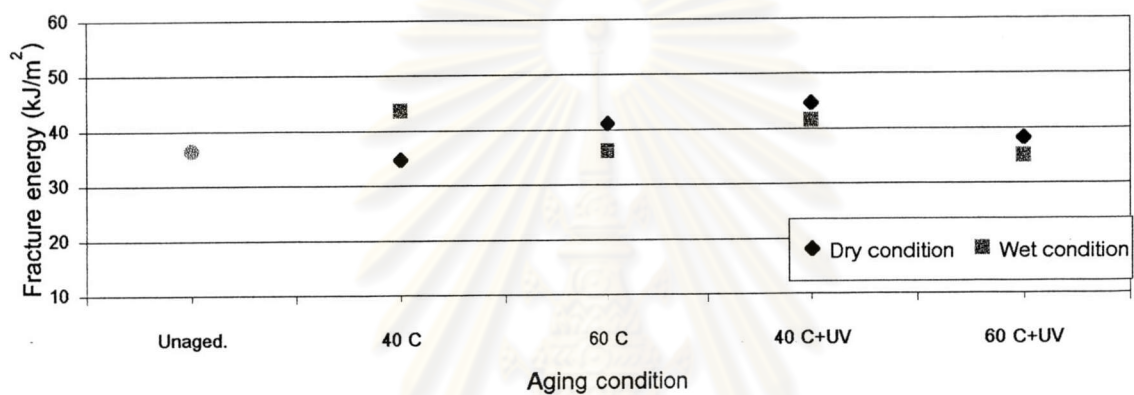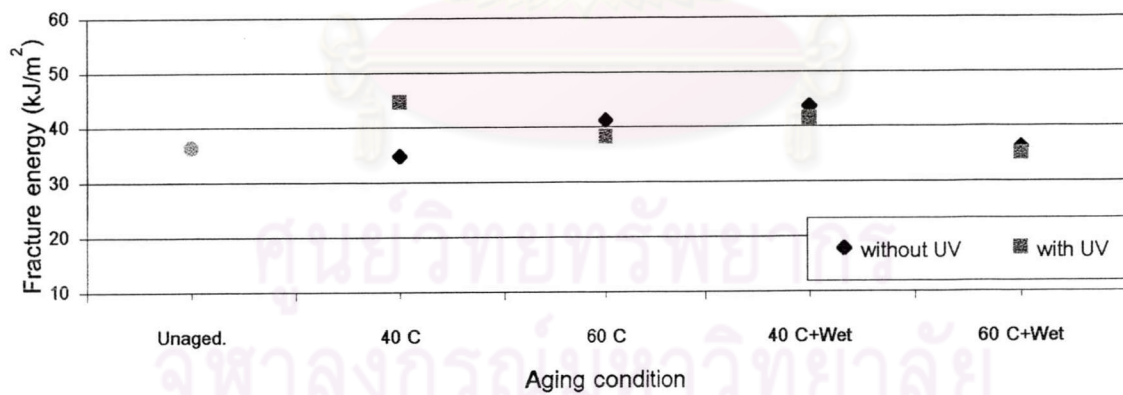
(a)
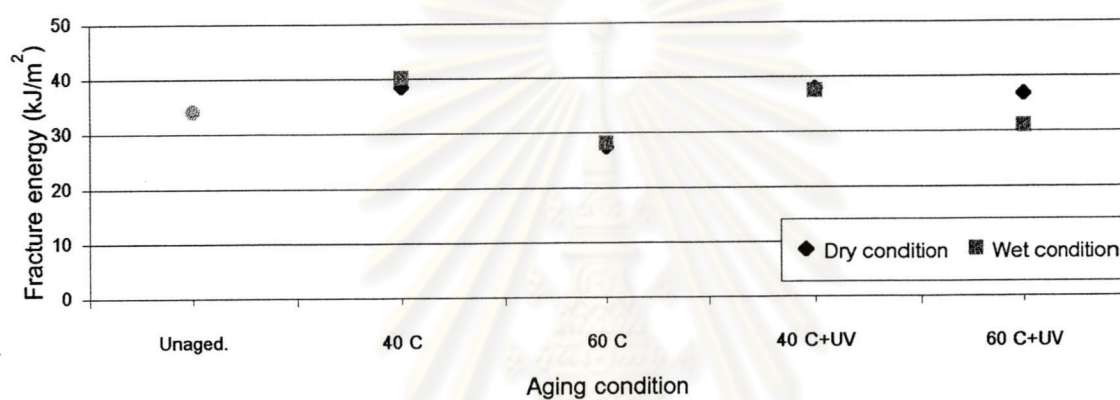
(b)
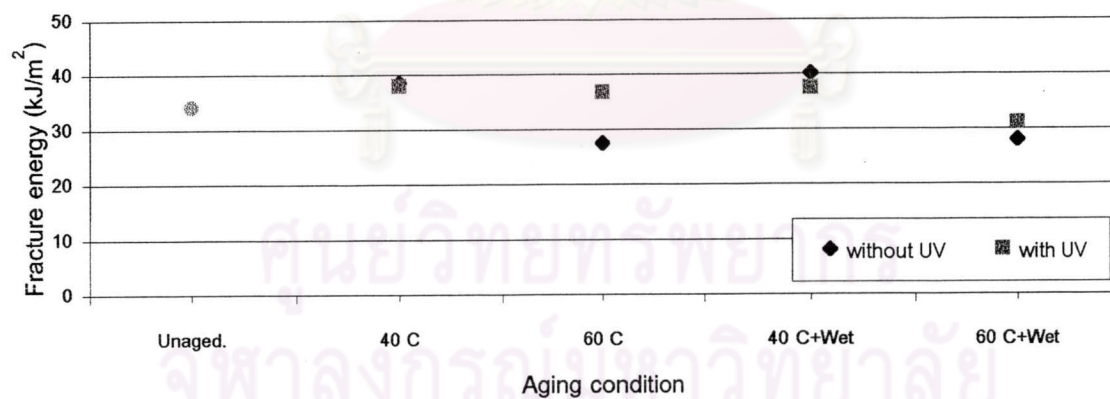
(c)

Figure 5.11: Effects of temperature (a), humidity (b) and the UV exposure (c) on
the fracture energy of carbon fiber reinforced epoxy composites under flexural mod

(a)

(b)

(c)

Figure 5.12: Effects of temperature (a), humidity (b) and the UV exposure (c) on
the fracture energy of aramid fiber reinforced epoxy composites under flexural mod

5.2.2 Compression test

Compression test is applied to estimate the maximum strength and the modulus of elasticity in compression mode. Test specimen for carbon fiber reinforced epoxy composites after compression loading is displayed in Figure 5.13. The specimen deforms and buckles during the compression test, and then it cracks at the center of the specimen. The epoxy layer is detached from the reinforcing fiber at the interface after the compression.
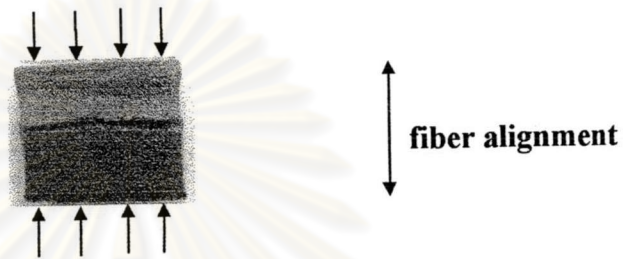
Figure 5.13: Carbon fiber reinforced epoxy composites after compression loading. The composite was compressed in the direction parallel with fiber alignment.

In this experimental work, the composites were tested in two direction, direction "1" and "2" as shown in Figure 5.14. The regression analysis for the significance of the aging conditions will be based on compressive properties in direction "1", i.e. parallel with the principal axis of anisotropy only.
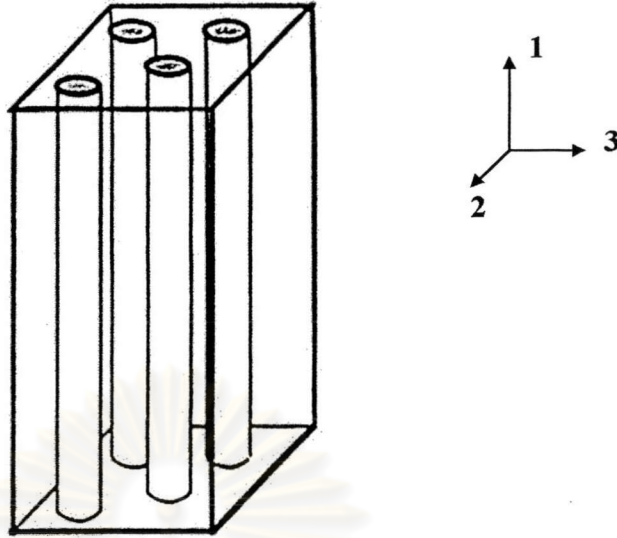
Figure 5.14: The compressive direction.

5.2.2.1 Compressive properties in direction "1"

The effects of various aging conditions on the compressive strength of fiber reinforced epoxy composites are shown in Figure 5.15 and 5.16.

For carbon fiber reinforced epoxy composites in Figure 5.15 (a), the compressive strength does not exhibit a consistent trend for all aging conditions. From Figures 5.15 (b), the compressive strength of the specimens aged with wet condition are lower than those aged with dry condition except the specimens aged at a lower temperature with UV exposure in dry and wet condition. This can be assumed that humidity is one of the significant factors for the compressive strength. From Figure 5.15 (c), the compressive strength of the specimens aged with UV are higher than those aged without UV except the specimens aged at a higher temperature with and without UV. This implies that UV exposure is one important factor affecting the compressive strength of carbon fiber reinforced composites. The regression analysis, as shown in Figure 5.17 (a), confirms this implication, it reveals all the significant factors affecting the compressive strength of carbon fiber reinforced composites to be humidity (B), the combined humidity and UV
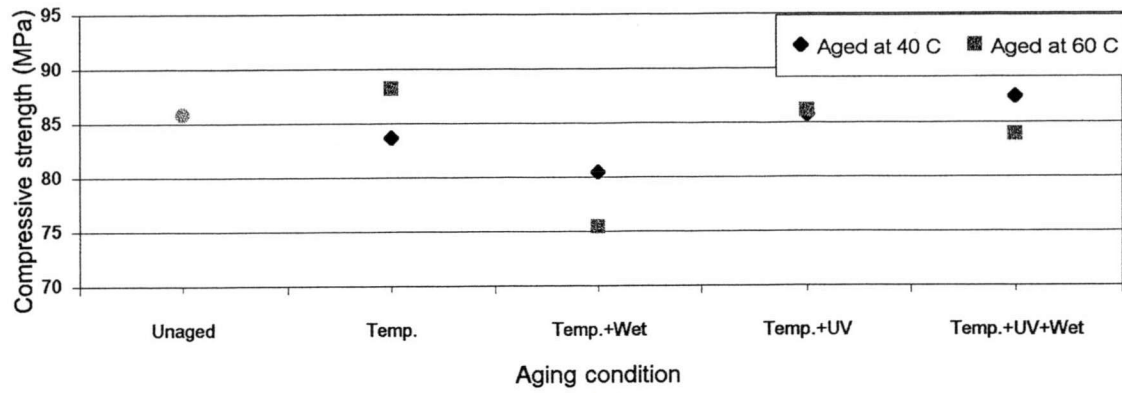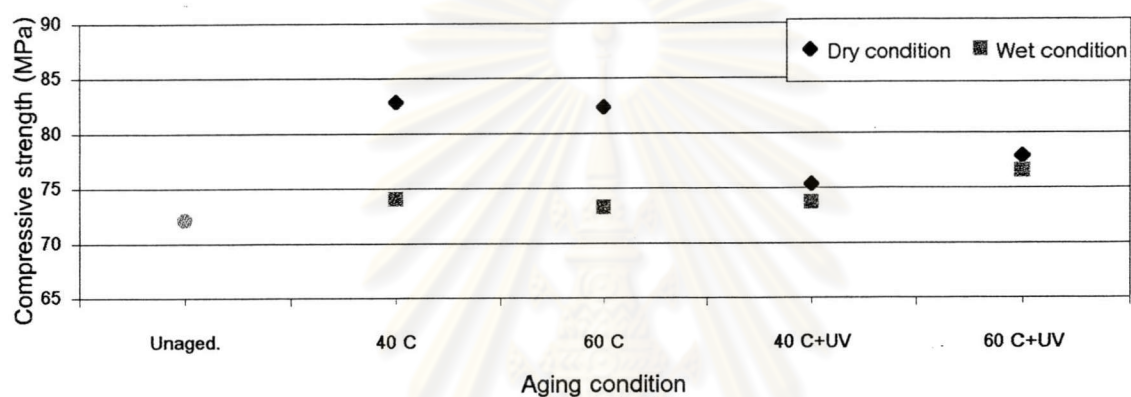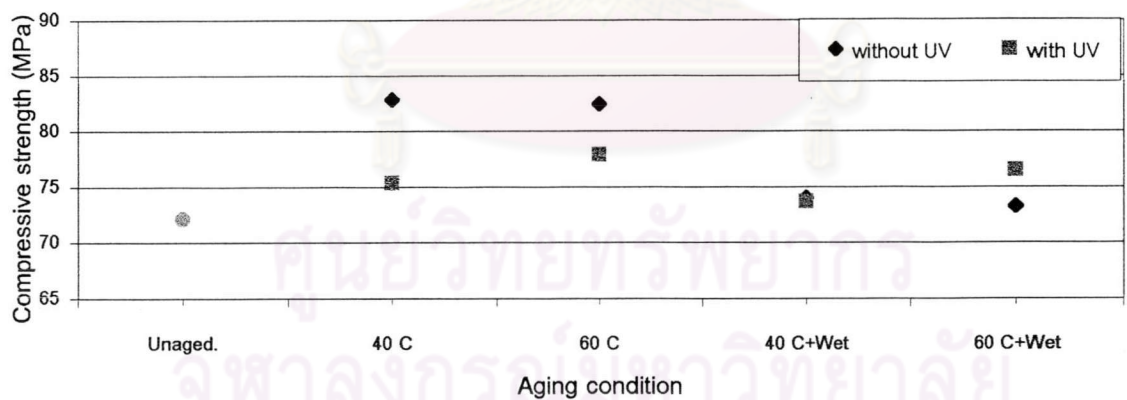
(a)
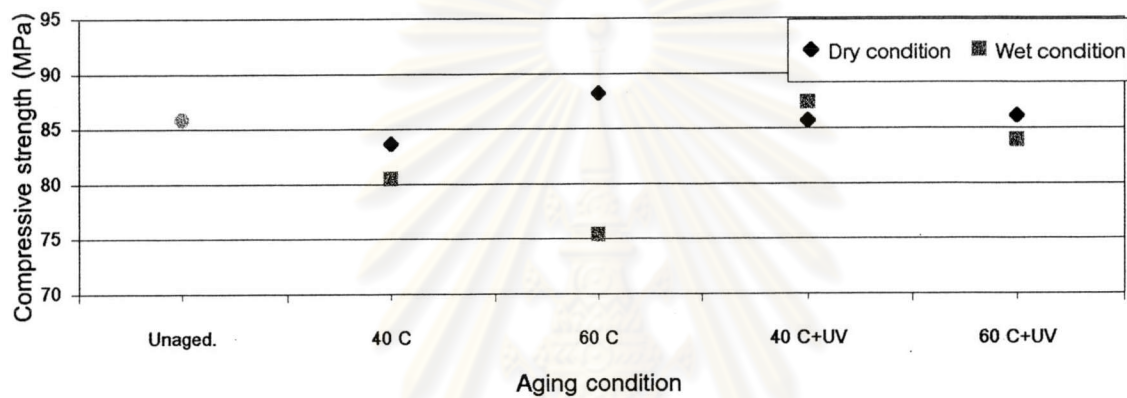
(b)
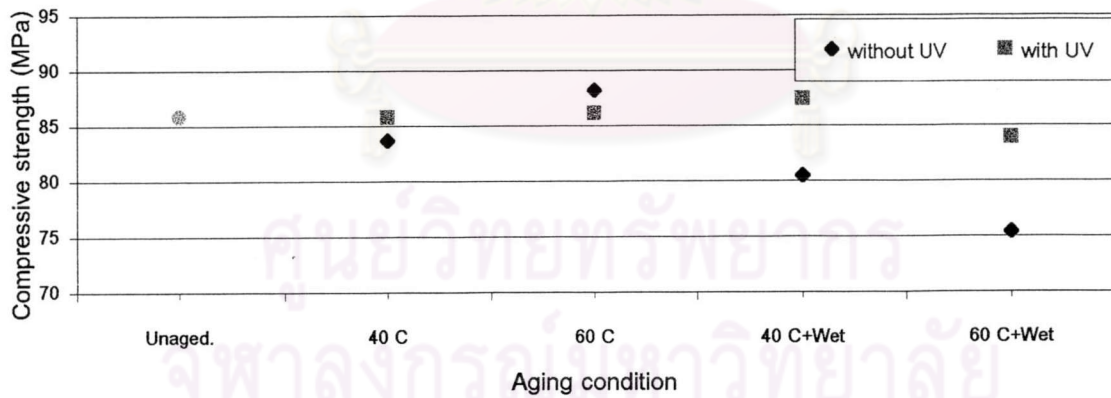
(c)

Figure 5.15: Effects of temperature (a), humidity (b) and the UV exposure (c) on the compressive strength in direction "1" of carbon fiber reinforced epoxy composite
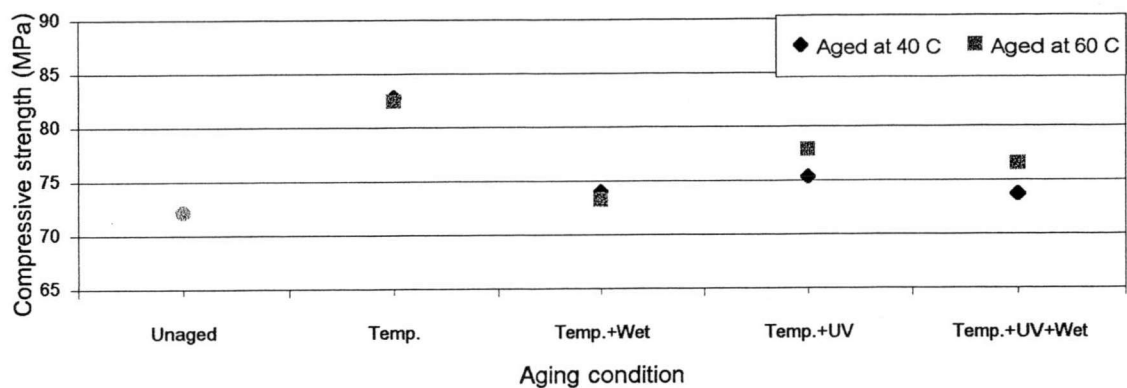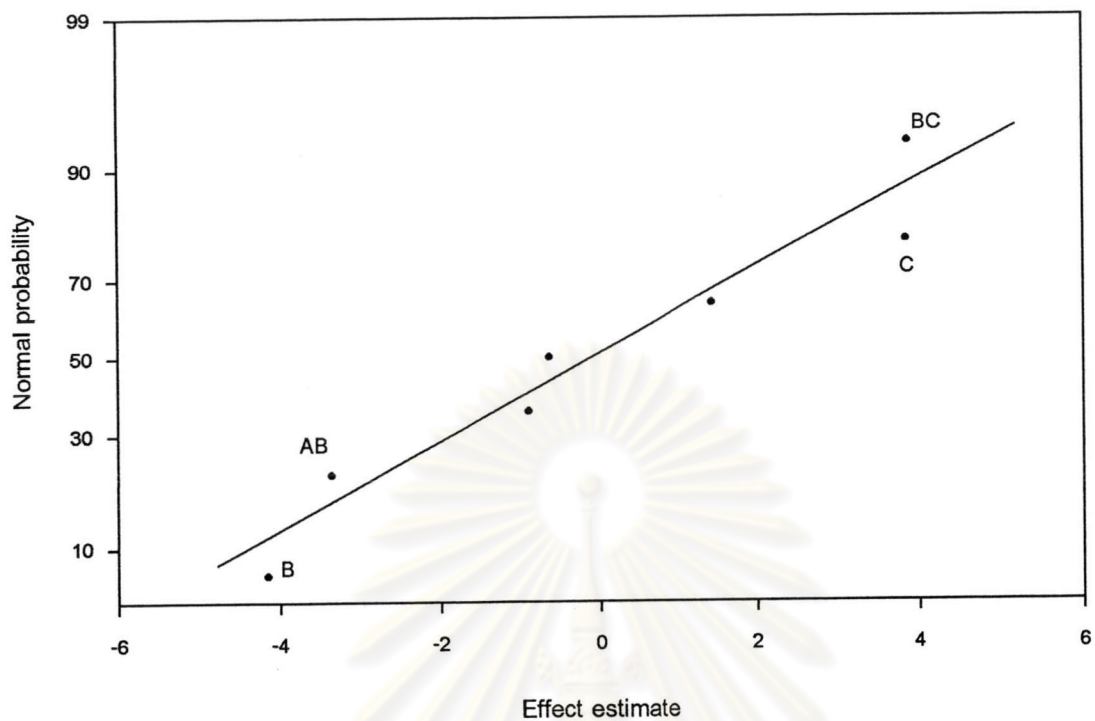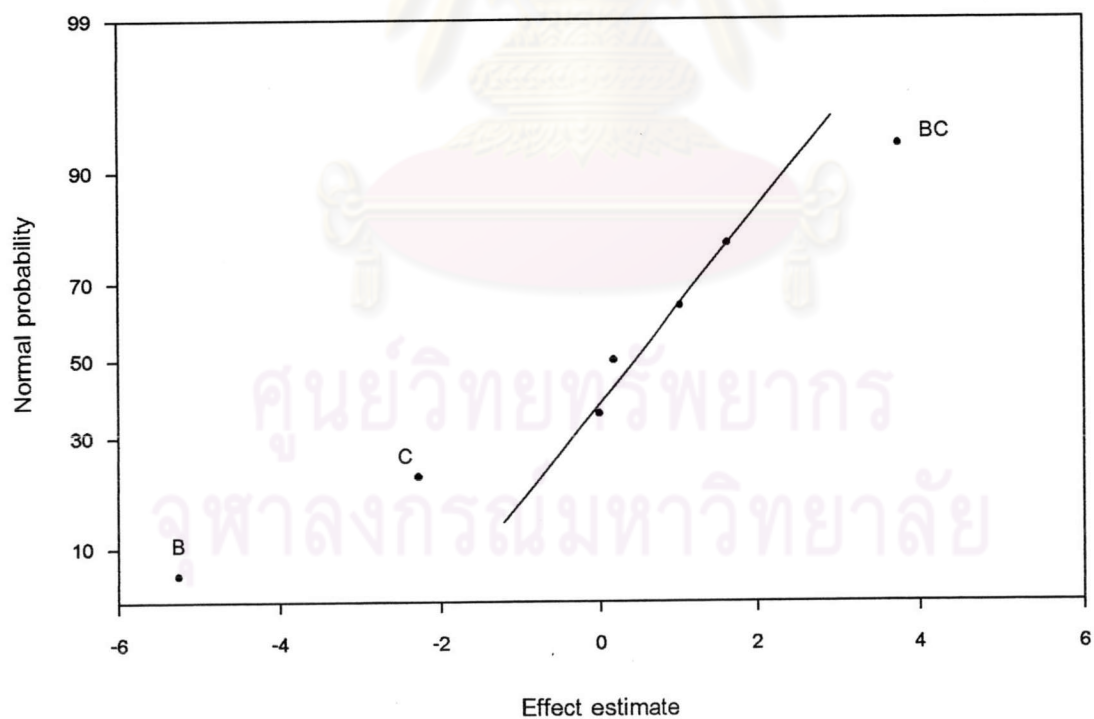
(a)

(b)

(c)

Figure 5.16: Effects of temperature (a), humidity (b) and the UV exposure (c) on the compressive strength in direction "1" of aramid fiber reinforced epoxy composite

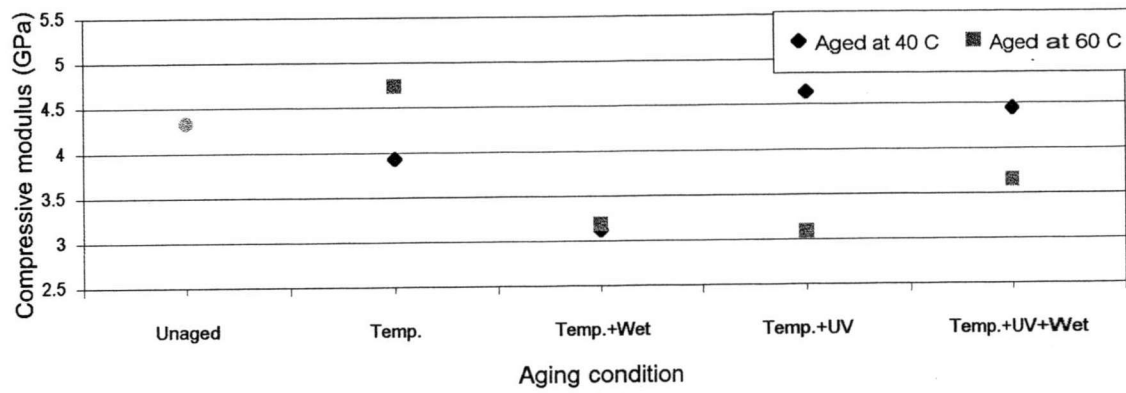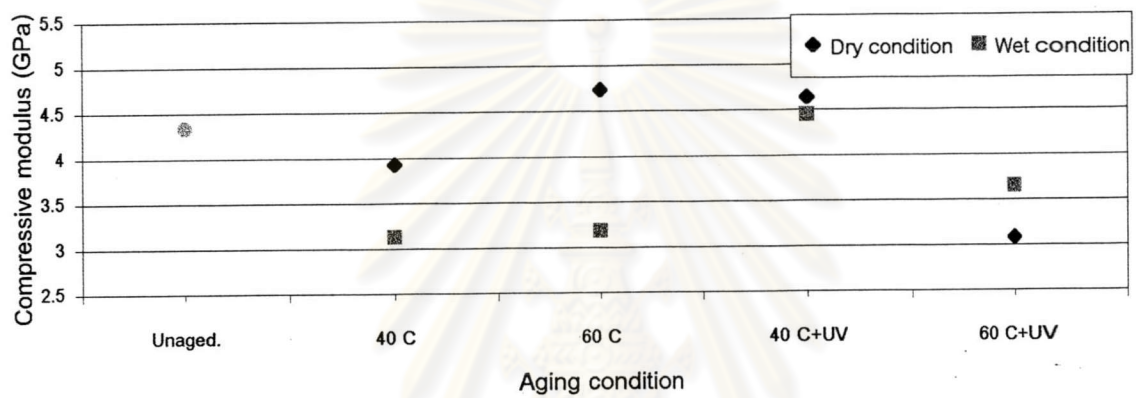**(a) carbon fiber reinforced composite**

(b) aramid fiber reinforced composite

Figure 5.17: Normal probability plots of estimate effect for the compressive strength in direction "1" of fiber reinforced epoxy composites.

(BC), UV (C) and the combined aging temperature and humidity (AB) respectively.

For aramid fiber reinforced epoxy composites in Figure 5.16 (a), the compressive strength does not show a consistent trend for all aging conditions. However, the compressive strength tends to decrease in specimens exposed to more severe conditions. From Figures 5.16 (b), it is obvious that the compressive strength of the specimens aged with wet condition are lower than those aged with dry condition. Thus, humidity is the significant factor for the compressive strength. From Figure 5.16 (c), the compressive strength of the specimens aged with UV are lower than those aged without UV except for the specimens aged at a higher temperature in wet condition with and without UV. UV exposure seems to play an important role on the compressive strength of aramid fiber reinforced composites. This was confirmed in the regression analysis, as shown in Figure 5.17 (b), in which the significant factors affecting the compressive strength of aramid fiber reinforced composites were identified. They are humidity (B), the combined humidity and UV (BC), and UV (C) respectively.

The effects of various aging conditions on the compressive modulus of fiber reinforced epoxy composites are shown in Figure 5.18 and 5.19.
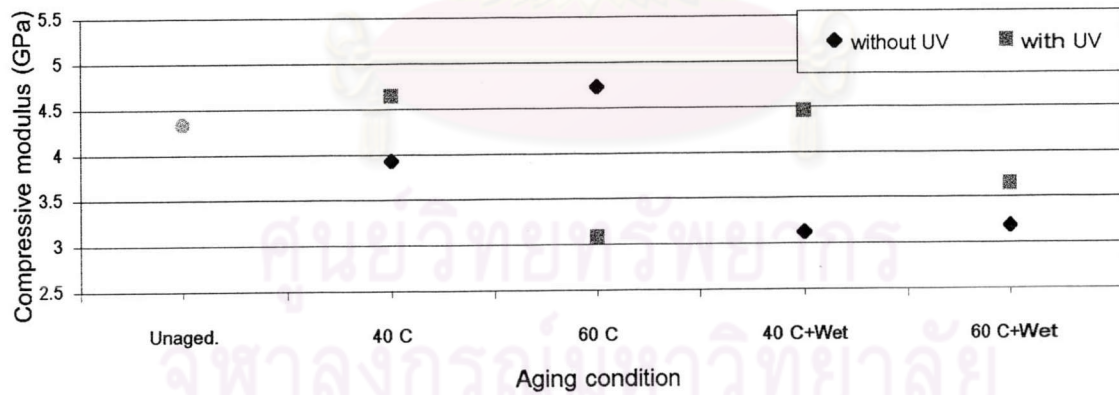
For carbon fiber reinforced composites in Figure 5.18 (b) and (c), the compressive modulus of the specimens aged in wet condition and aged without UV are lower than those aged in dry condition and aged with UV. However, the compressive modulus of those aged at a higher temperature with UV in wet condition are higher than those aged at a lower temperature with UV in dry condition as shown in Figure 5.18 (b). The compressive modulus of the specimens aged at a higher temperature without UV are higher than those aged at a higher temperature with UV as shown in Figure 5.18 (c). Therefore, humidity and UV seem to play the significant effect on the compressive modulus of carbon fiber reinforced composites.
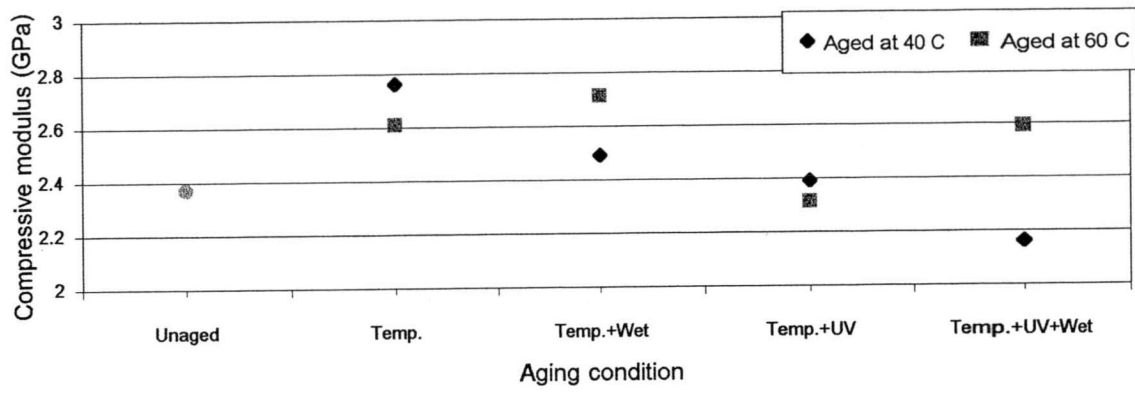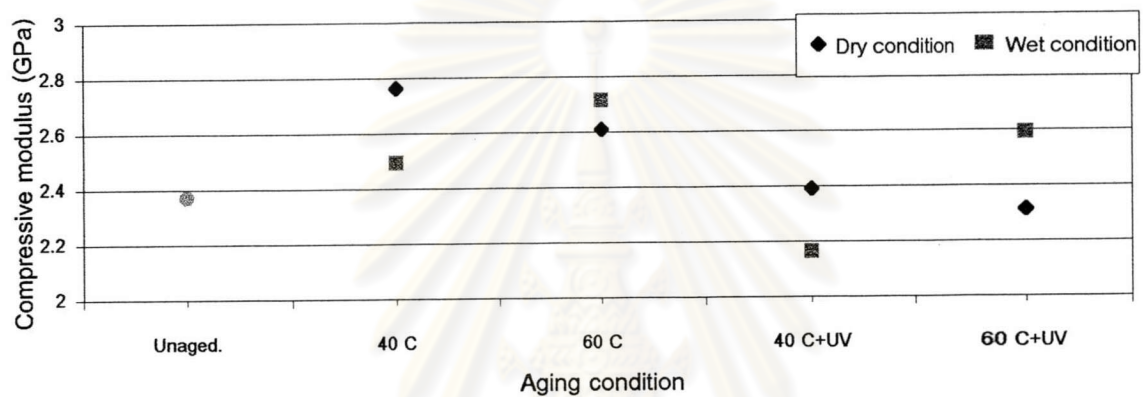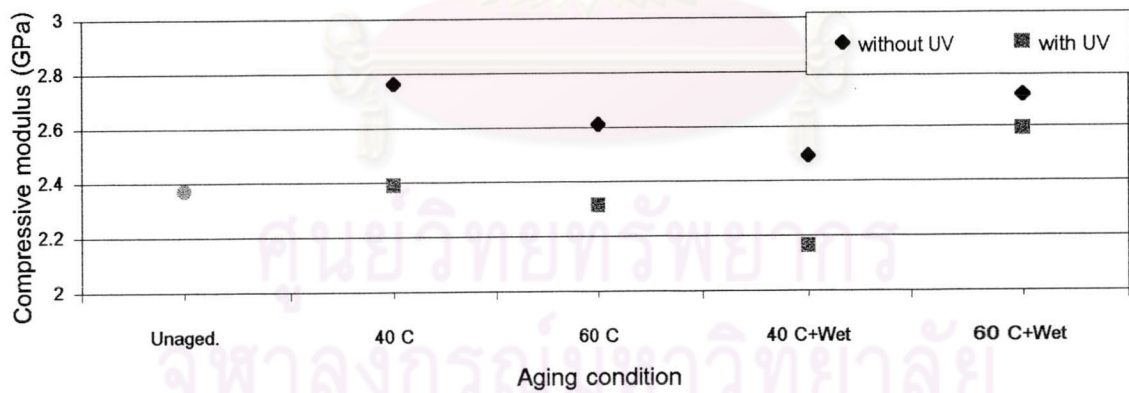
(a)

(b)

(c)

Figure 5.18: Effects of temperature (a), humidity (b) and the UV exposure (c) on the compressive modulus in direction "1" of carbon fiber reinforced epoxy composit

(a)

(b)

(c)

Figure 5.19: Effects of temperature (a), humidity (b) and the UV exposure (c) on the compressive modulus in direction "1" of aramid fiber reinforced epoxy composit

From Figure 5.18 (a), it is indistinct which factors affect the compressive strength of the specimens for all four aging conditions.

For aramid fiber reinforced epoxy composites, from Figures 5.19 (a) and (b), it is also not apparent which factors affect the compressive modulus of the specimens. However, the compressive modulus tends to decrease when the specimens were exposed to more severe conditions, especially in Figure 5.19 (a). From Figure 5.19 (c), it is clearly seen that the compressive modulus of the specimens aged with UV is lower than those aged without UV. Therefore, it can be concluded that the UV exposure is the significant factor of the compressive modulus of aramid fiber reinforced composites.

The effects of various climatic conditions on the compressive strain at yield of fiber reinforced epoxy composites are shown in Figure 5.20 and 5.21.

For carbon fiber reinforced composites in Figure 5.20 (a), the compressive strain at yield does not show the consistent trend for all aging conditions. From Figure 5.20 (b), the compressive strain at yield of the specimens aged in wet condition is higher than those aged in dry condition except for the specimen aged at a higher temperature with UV in dry and wet condition. From Figure 5.20 (c), the compressive strain at yield of the specimens aged with UV are lower than those aged without UV except for the specimen aged at a higher temperature in dry condition with and without UV. Therefore, it can be assumed that humidity and UV are significant factors on the compressive strain at yield of carbon fiber reinforced composites.
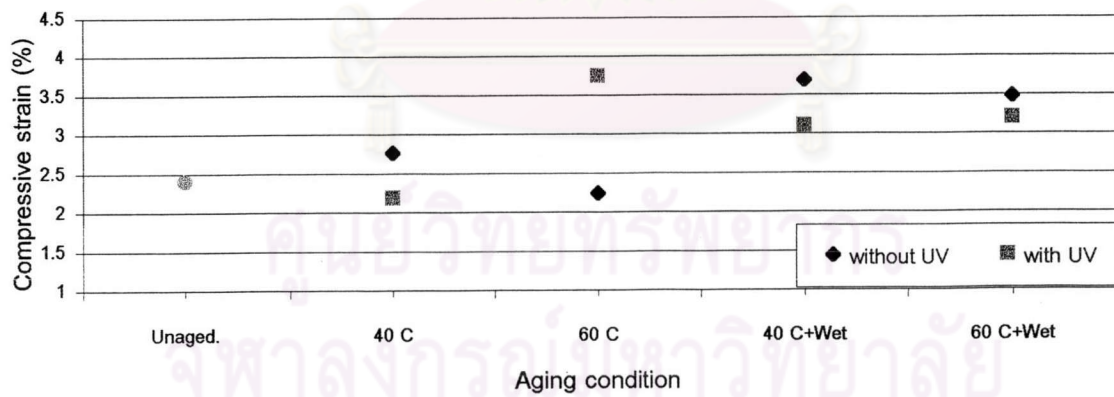
For aramid fiber reinforced epoxy composites in Figures 5.21 (a), (b) and (c), the compressive strain at yield of the specimens aged with high level of aging conditions are nearly equal to those aged with low level of aging conditions. There is only one difference in the specimen aged with UV at a lower temperature in dry condition. The compressive strain at yield of the composites in this condition is higher than any other aging conditions. Thus,
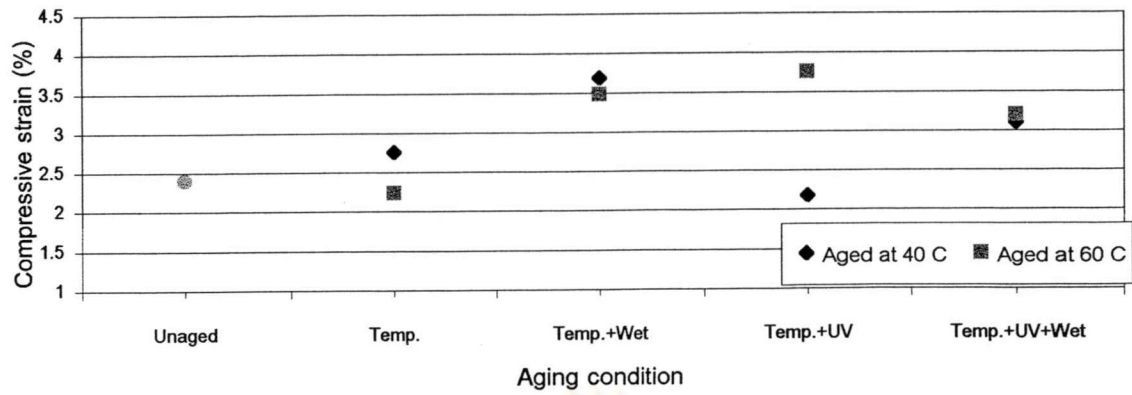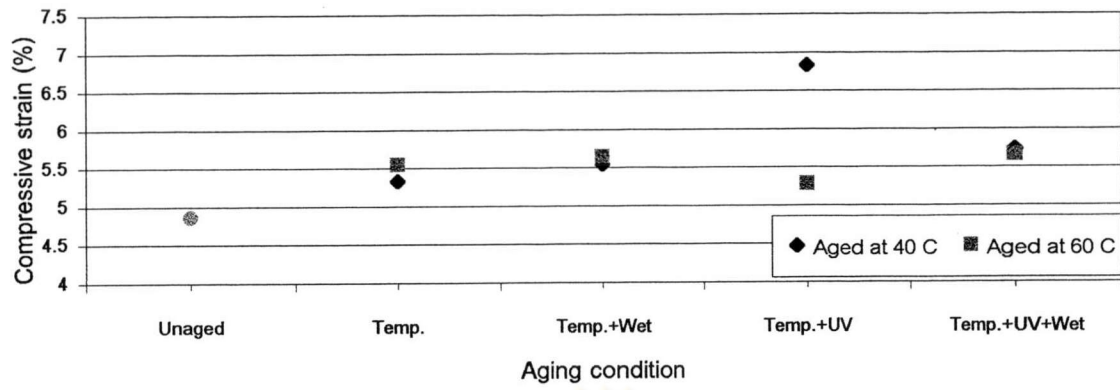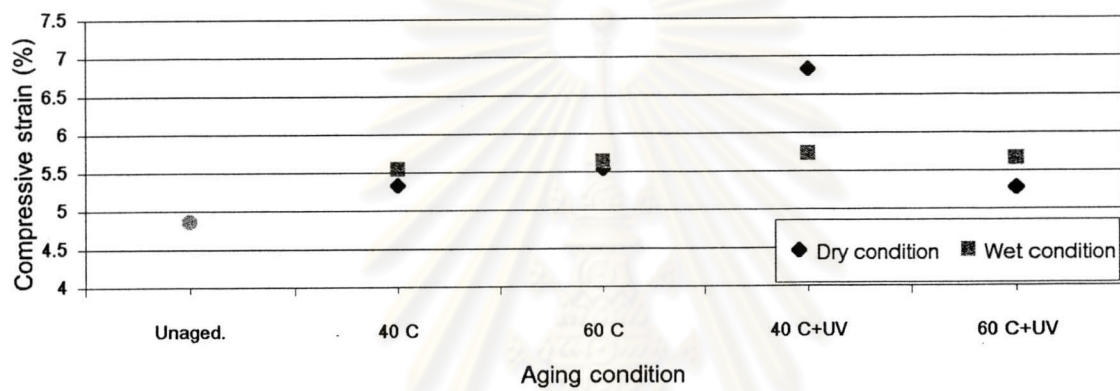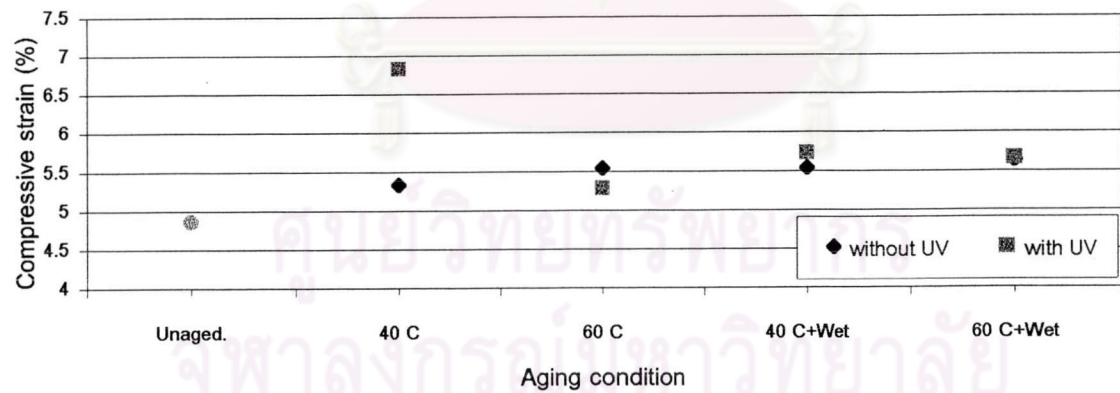
(a)
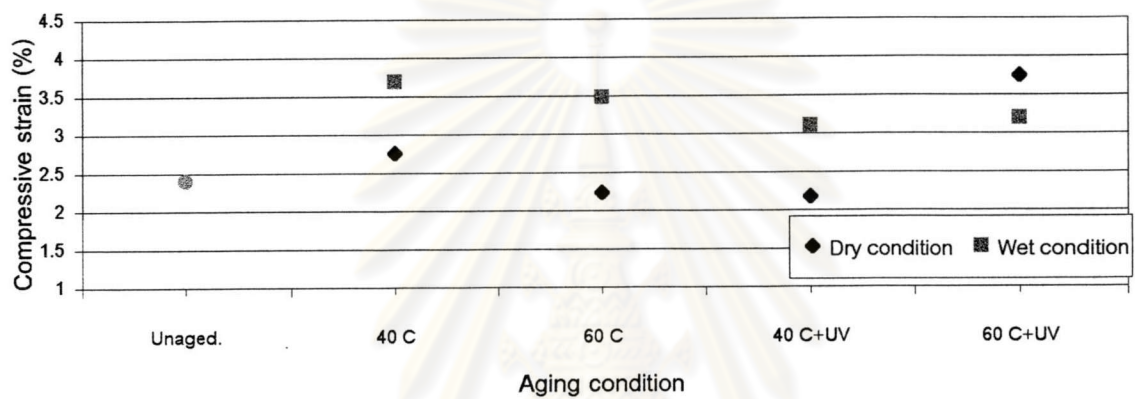
(b)

(c)

Figure 5.20: Effects of temperature (a), humidity (b) and the UV exposure (c) on the compressive strain at yield in direction "1" of carbon fiber reinforced epoxy composites.

(a)

(b)

(c)

Figure 5.21: Effects of temperature (a), humidity (b) and the UV exposure (c) on the compressive strain at yield in direction "1" of aramid fiber reinforced epoxy composites.

only UV exposure may be the significant effect of the compressive strain at yield of aramid fiber reinforced composites.

The effects of various aging conditions on the fracture energy of fiber reinforced epoxy composites under compression are shown in Figure 5.22 and 5.23.

For carbon fiber reinforced epoxy composites, from Figure 5.22, it is apparent that the fracture energy of the specimens aged with high level of aging conditions are higher than those aged with low level of aging conditions. It can be concluded that the aging temperature, humidity and UV are the main effects of the compressive fracture energy of carbon fiber reinforced epoxy composites.
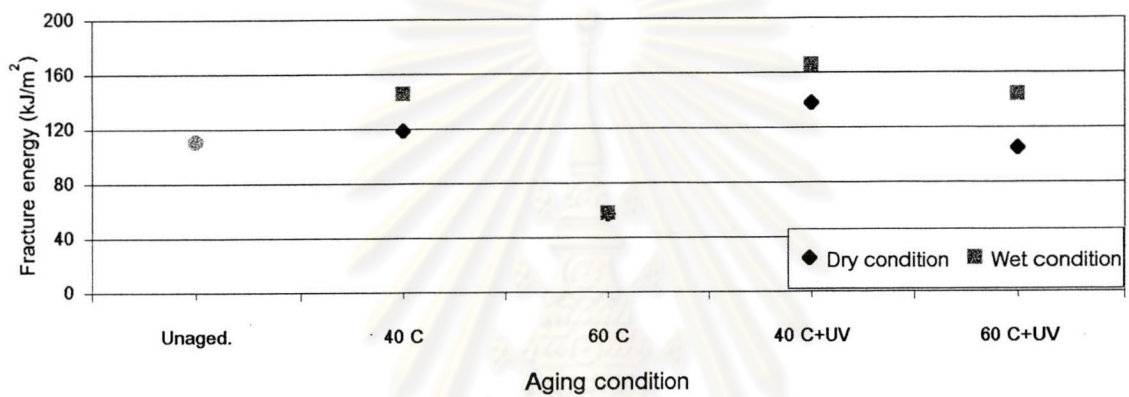
For aramid fiber reinforced epoxy composites, in contrast to carbon fiber reinforced composites, there are some differences between the fracture energy of the specimens aged with high level of aging conditions and those aged with low level of aging conditions. Nevertheless, from Figures 5.23 (b) and (c), it is not clearly seen which factors affect the compressive fracture energy. From Figure 5.23 (a), the fracture energy of the specimens aged at a higher temperature are higher than those aged at a lower temperature except the specimens aged with UV both at a higher and a lower temperature. Thus, the aging temperature influences slightly the fracture energy of aramid fiber reinforced composites.
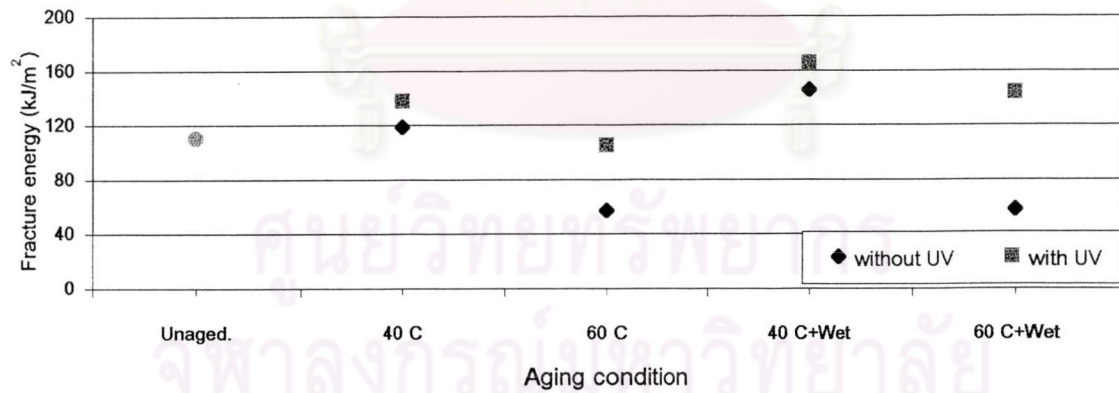
5.2.2.1 Compressive properties in direction "2"

The effects of various aging conditions on the compressive strength of fiber reinforced epoxy composites are shown in Figure 5.24 and 5.25.
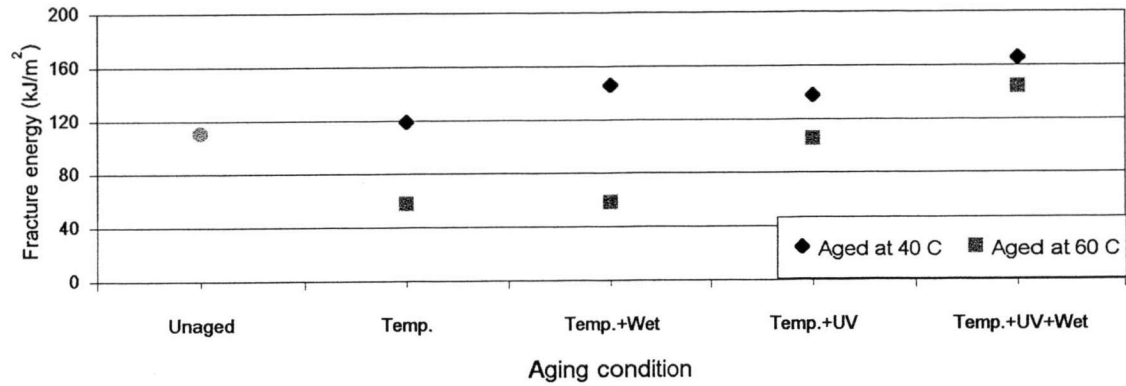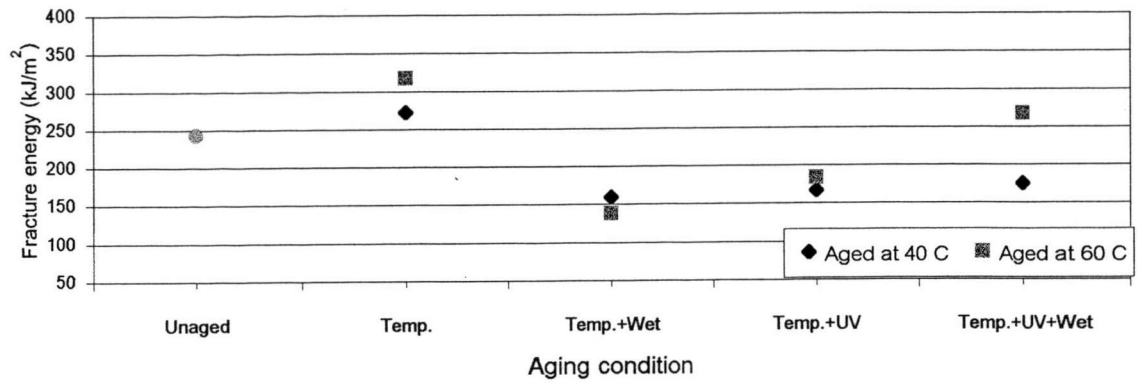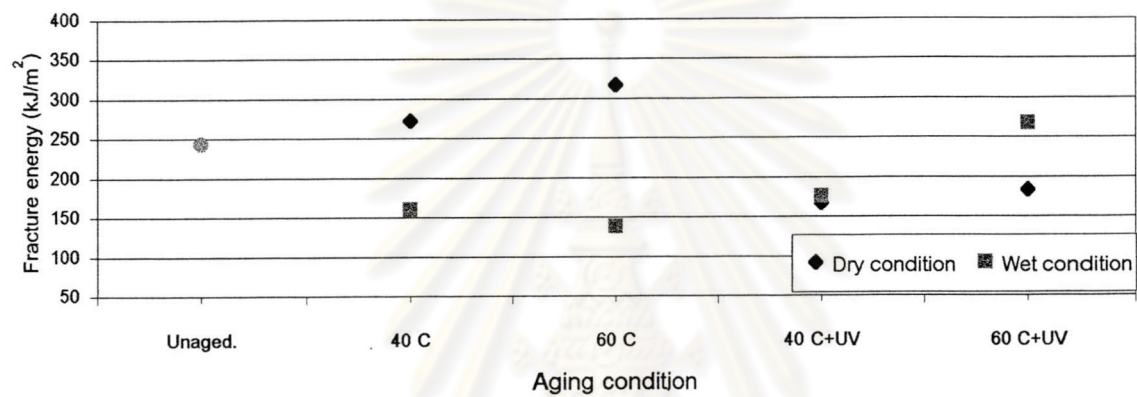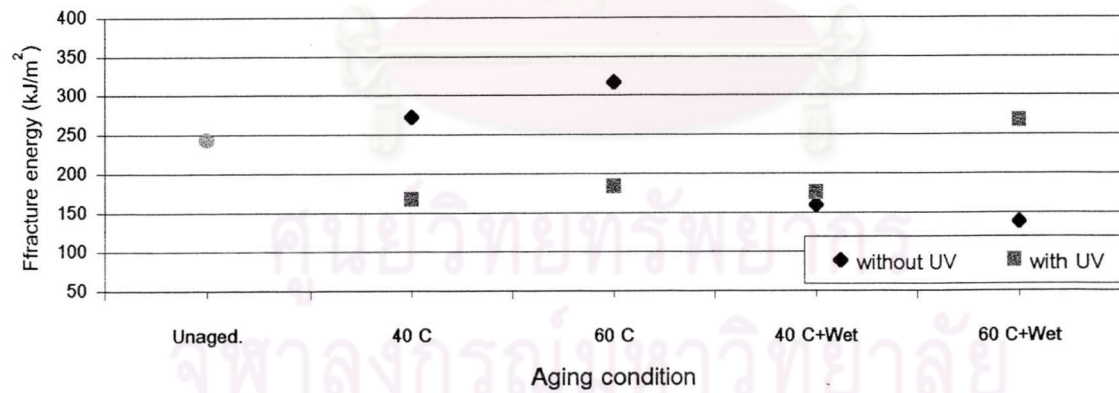
(a)

(b)

(c)

Figure 5.22: Effects of temperature (a), humidity (b) and the UV exposure (c) on the fracture energy in direction "1" of carbon fiber reinforced epoxy composites under compression.
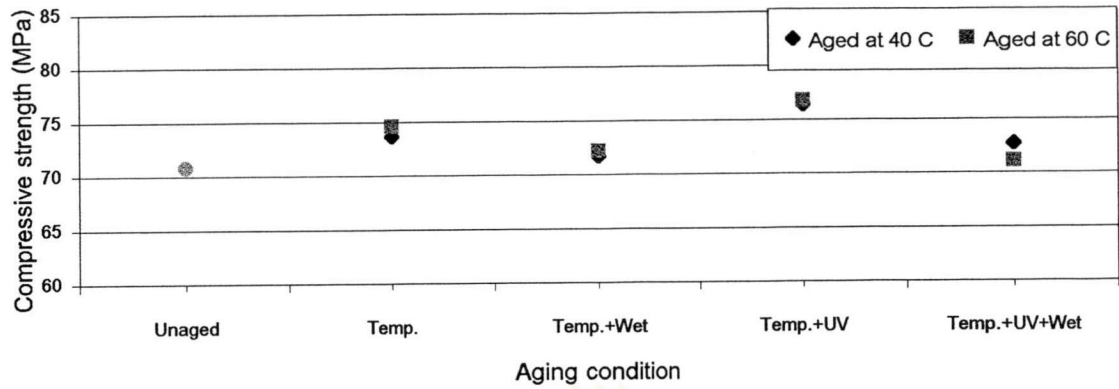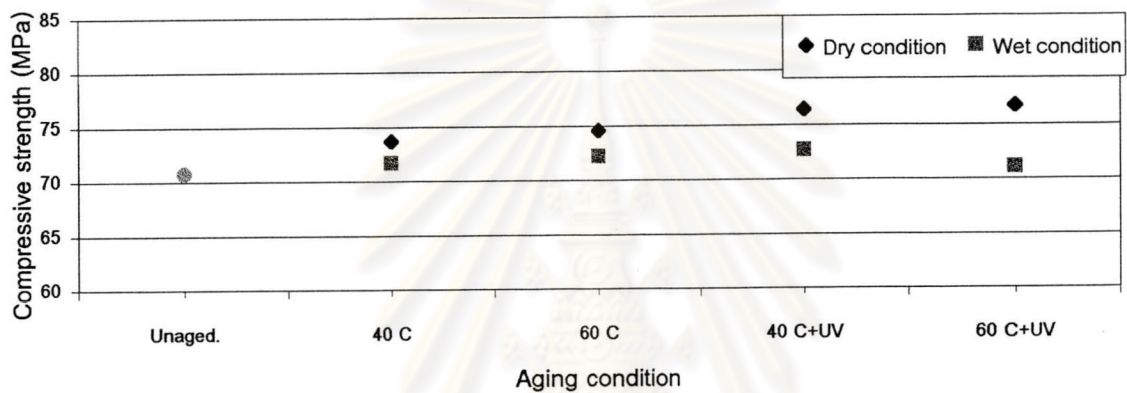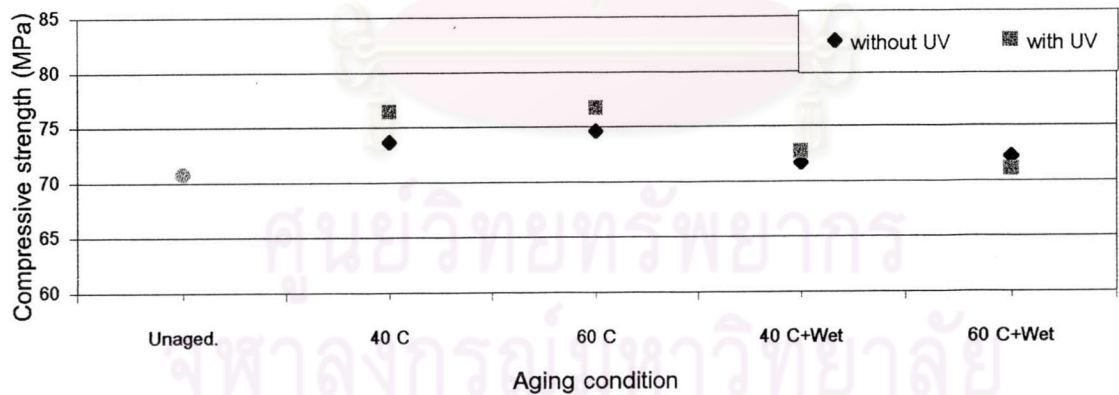
(a)

(b)

(c)

Figure 5.23: Effects of temperature (a), humidity (b) and the UV exposure (c) on the fracture energy in direction "1" of aramid fiber reinforced epoxy composites under compression.
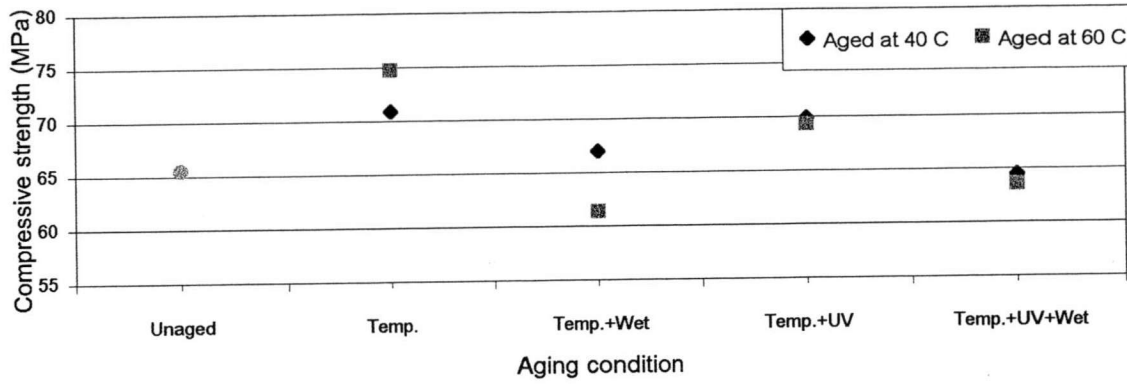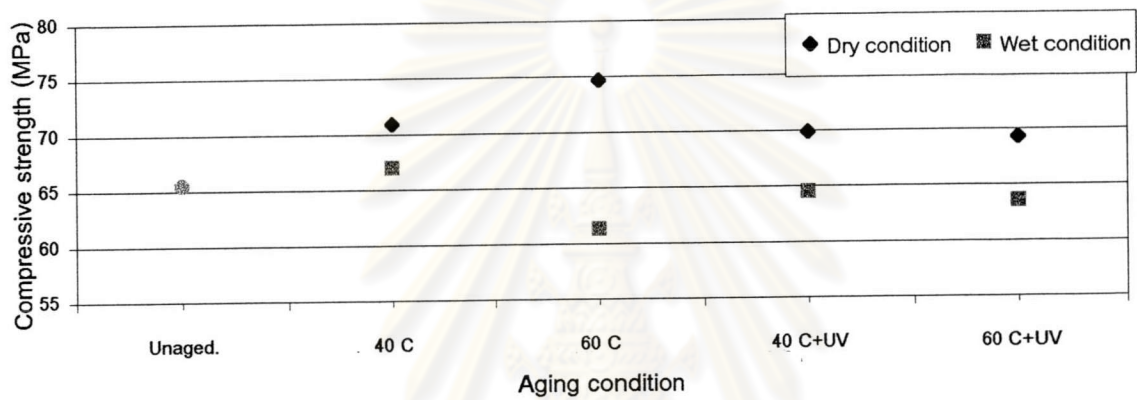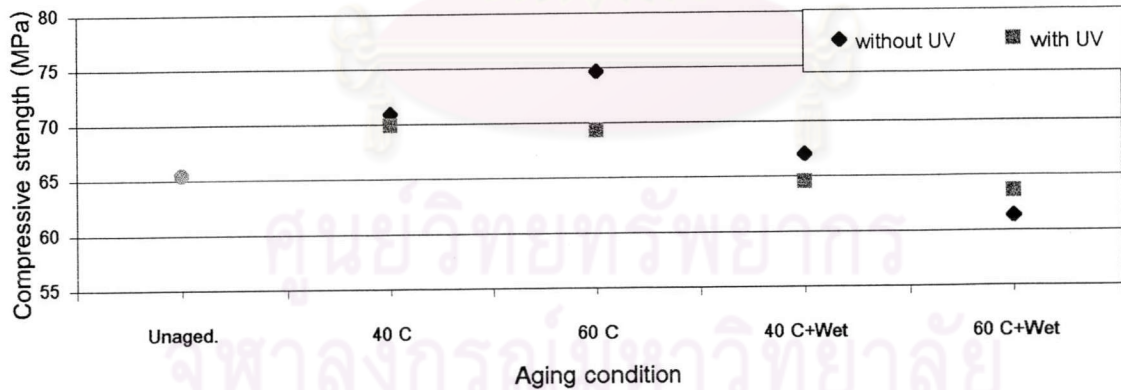
(a)

(b)

(c)

Figure 5.24: Effects of temperature (a), humidity (b) and the UV exposure (c) on the compressive strength in direction "2" of carbon fiber reinforced epoxy composite
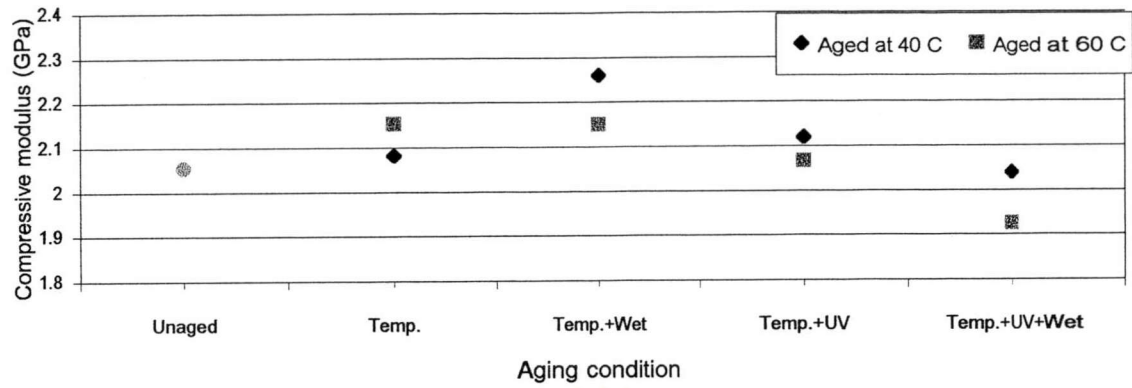
(a)

(b)

(c)

Figure 5.25: Effects of temperature (a), humidity (b) and the UV exposure (c) on the compressive strength in direction "2" of aramid fiber reinforced epoxy composite

For carbon fiber reinforced epoxy composites, from Figures 5.24 (a) and (c), the results show that there is no significant difference in the compressive strength of the specimens aged with high level of aging conditions and those aged with low level of aging conditions. This is because the direction "2" normal to the principal axis of anisotropy is not the direction of fiber alignment. From Figure 5.24 (b), however, the compressive strength of those aged with wet condition decreased slightly and hence were lower than those aged with dry condition. So, humidity slightly affects the compressive strength of the composites.
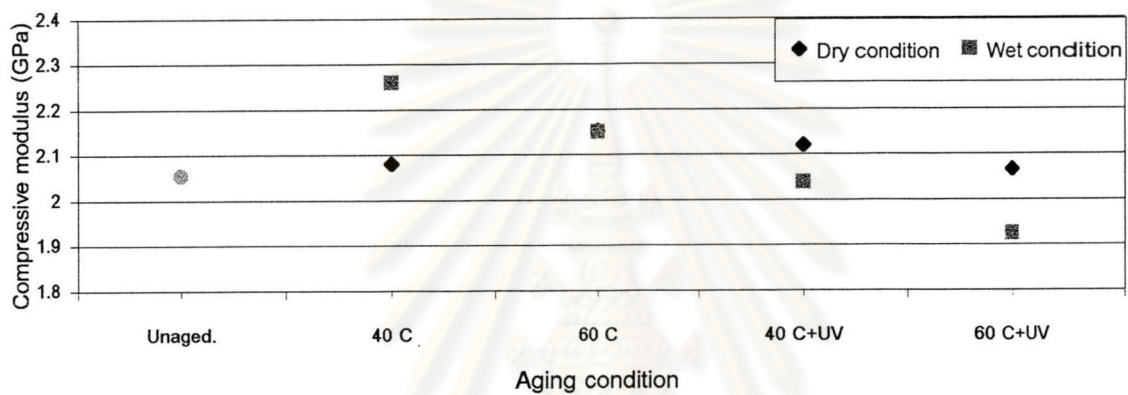
For aramid fiber reinforced epoxy composites, the compressive strength results in Figures 5.25 (a) and (c) do not exhibit significant difference between those aged with high level of aging conditions and aged with low level of aging conditions. From Figure 5.25 (b), it is apparent that the compressive strength of the specimens aged with wet condition are lower than those aged with dry condition. Similar with carbon fiber reinforced composites, humidity is the significant factor affecting the compressive strength of aramid fiber reinforced composites.

The effects of various climatic conditions on the compressive modulus of fiber reinforced epoxy composites are shown in Figure 5.26 and 5.27.
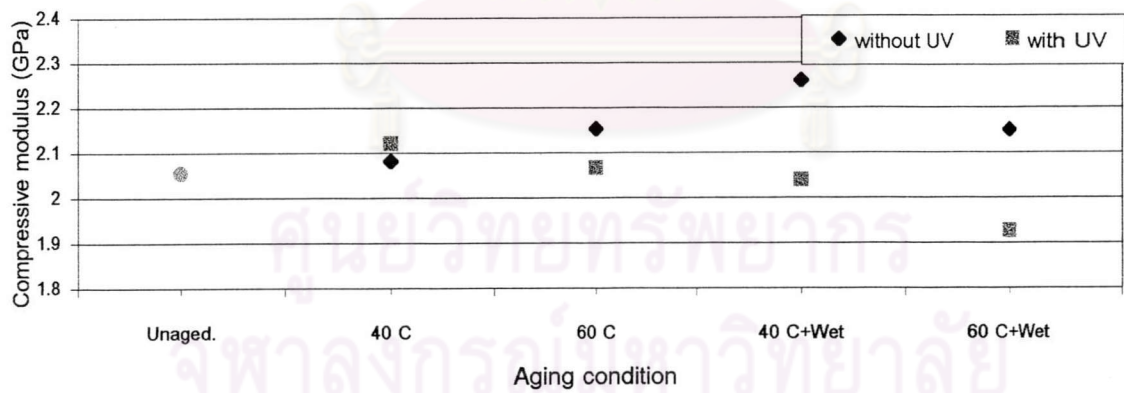
For carbon fiber reinforced epoxy composites, from Figure 5.26, the compressive modulus of the specimens aged with high level of aging conditions are lower than those aged with low level of aging conditions. However, the compressive modulus of the specimens aged at a higher temperature are higher than those aged at a lower temperature as shown in Figure 5.26 (a). The compressive modulus of the specimens aged at a lower temperature with wet condition are higher than those aged at a lower temperature with dry condition as seen from Figure 5.26 (b). Additionally, the compressive modulus of the specimens aged at a lower temperature with UV are higher than those aged at a lower temperature without UV as shown in Figure 5.26 (c). Thus, the aging temperature, humidity and UV may be the
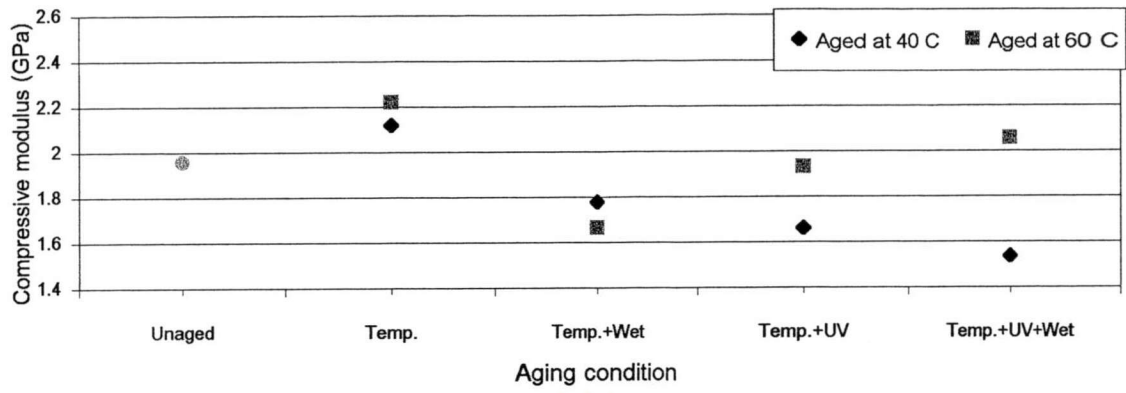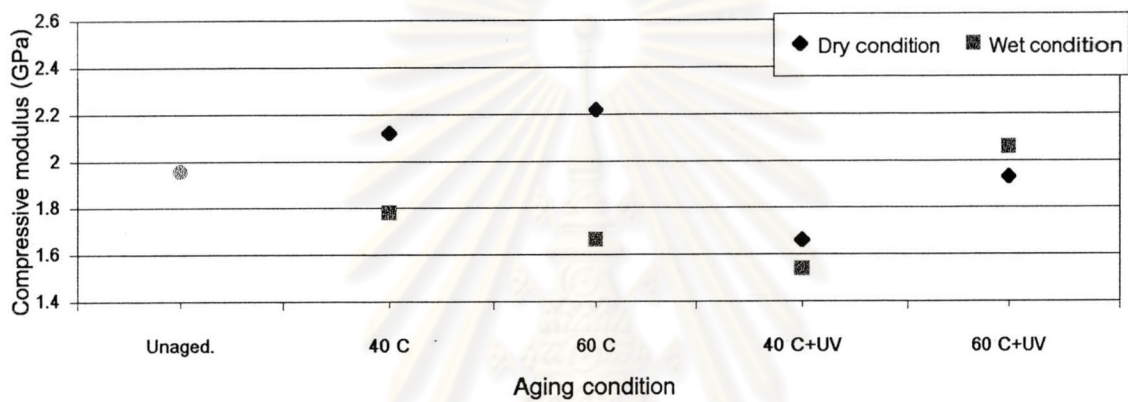
(a)

(b)

(c)

Figure 5.26: Effects of temperature (a), humidity (b) and the UV exposure (c) on the compressive modulus in direction "2" of carbon fiber reinforced epoxy composite

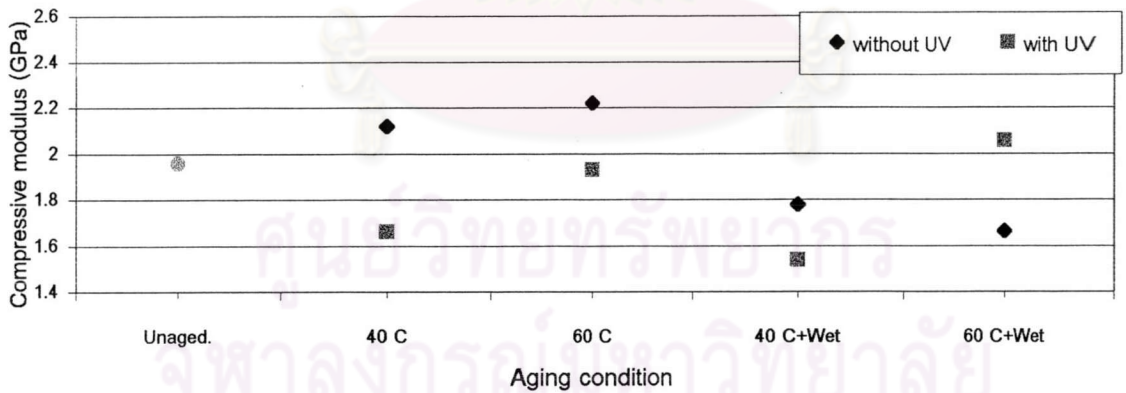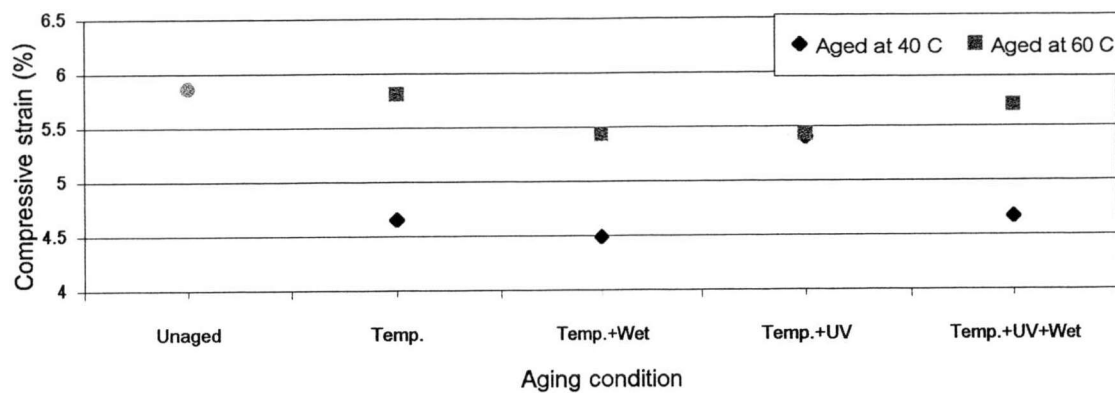(a)

(b)

(c)

Figure 5.27: Effects of temperature (a), humidity (b) and the UV exposure (c) on the compressive modulus in direction "2" of aramid fiber reinforced epoxy composit

significant effect of the compressive modulus of carbon fiber reinforced composites. Moreover, the compressive modulus tends to decrease when the specimens are exposed to more severe conditions.
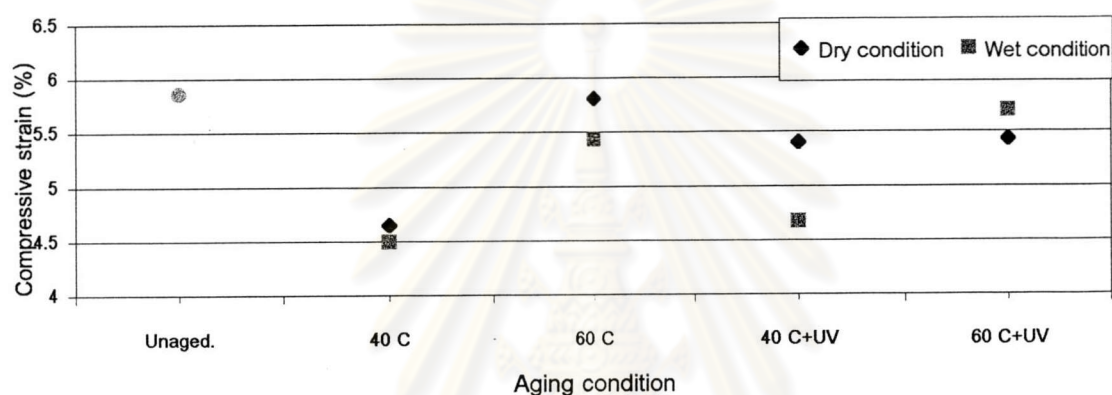
For aramid fiber reinforced epoxy composites, from Figures 5.27 (a), the compressive modulus of the specimens aged at a higher temperature are higher than those aged at a lower temperature except the specimens aged with wet condition at a higher and lower temperature. Hence, the aging temperature plays a significant role affecting the compressive modulus of the aramid fiber reinforced composites. From Figure 5.27 (b), the compressive modulus of the specimens aged with dry condition are higher than those aged with wet condition except the specimens aged at a higher temperature with UV in dry and wet condition. Hence, humidity is another factor affecting the compressive modulus of the aramid fiber reinforced composites. In the same way, from Figure 5.27 (c), the compressive modulus of the specimens aged without UV are higher than those aged with UV except the specimens aged at a higher temperature in wet condition with and without UV. Thus, UV exposure is also one significant factor affecting the compressive modulus of the aramid fiber reinforced composites.

The effects of various environmental conditions on the compressive strain at yield of fiber reinforced epoxy composites are displayed in Figure 5.28 and 5.29.
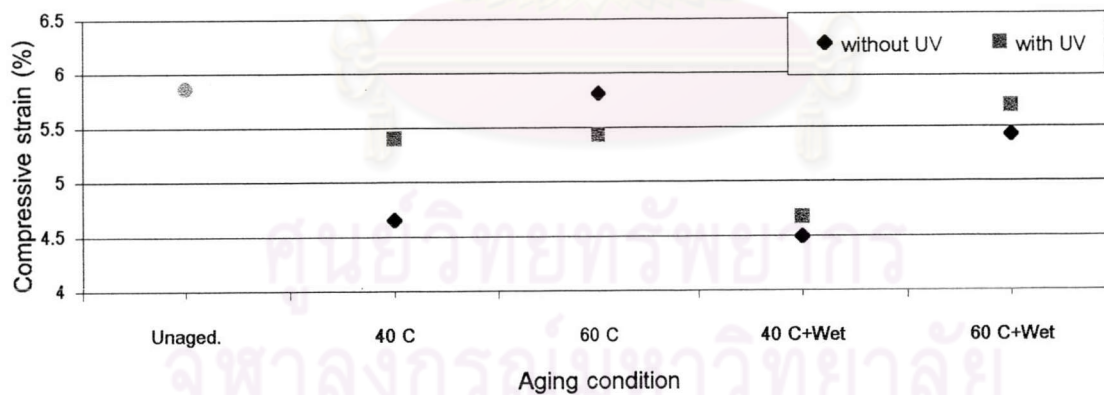
For carbon fiber reinforced composites, from Figure 5.28 (a), it is obvious that the compressive strain at yield of the specimens aged at a higher temperature are higher than those of aged at a lower temperature. This means that aging temperature is the main factor of the compressive strain at yield of carbon fiber reinforced composites. From Figure 5.28 (b), the compressive strain at yield of the specimens aged in wet condition is lower than those aged in dry condition except the specimen aged at a higher temperature with UV in dry and wet condition. From Figure 5.28 (c), the compressive strain at yield of the specimens aged with UV are higher than those aged without UV except for the specimen aged at a higher temperature
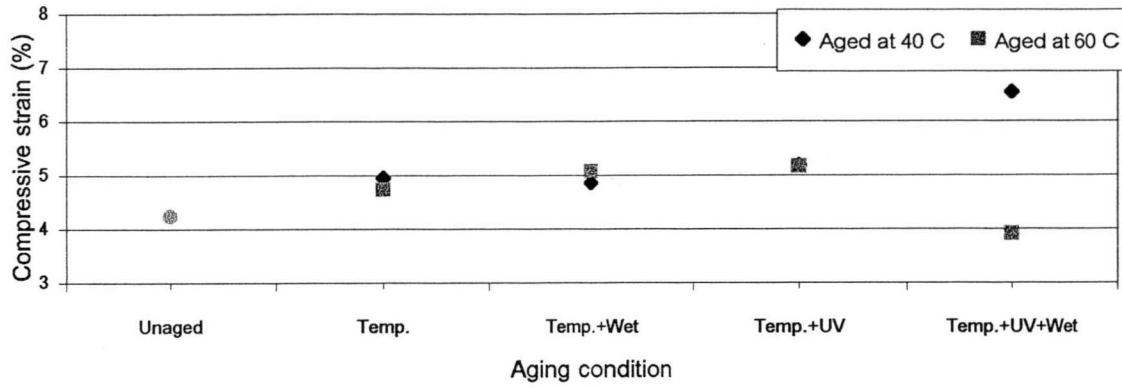
(a)

(b)

(c)

Figure 5.28: Effects of temperature (a), humidity (b) and the UV exposure (c) on the compressive strain at yield in direction "2" of carbon fiber reinforced epoxy composites.

(a)

(b)
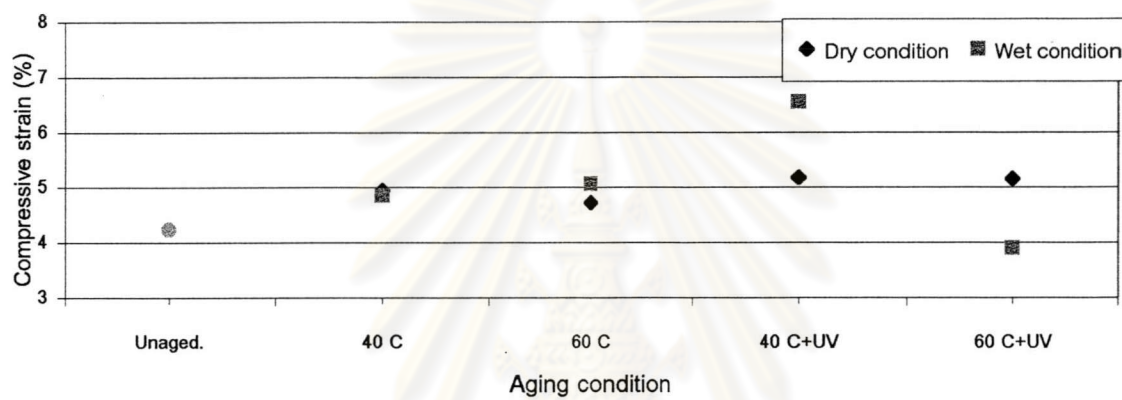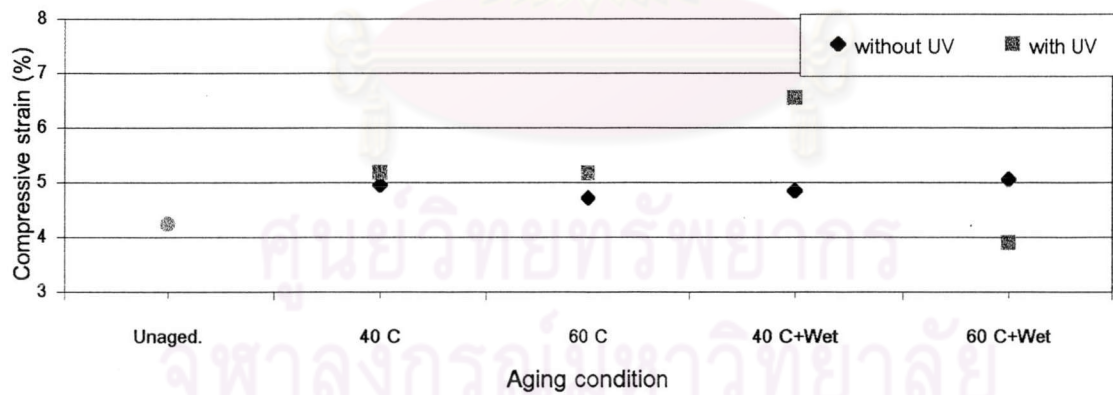
(c)

Figure 5.29: Effects of temperature (a), humidity (b) and the UV exposure (c) on the compressive strain at yield in direction "2" of aramid fiber reinforced epoxy composites.

in dry condition with and without UV. Therefore, humidity and UV are possibly the significant factors of the compressive yield strain of carbon fiber reinforced composites.

For aramid fiber reinforced epoxy composites, from Figures 5.29 (a), (b) and (c), most of the compressive strain at yield of the specimens aged with high level of aging conditions are nearly equal to those aged with low level of aging conditions. There are some differences in the specimens aged with UV in wet condition at a lower and higher temperature. The compressive strain at yield of the composites in this condition apparently differs from other compressive strain at yield of the specimens aged with the rest of aging conditions. Thus, humidity and UV exposure may be the significant factors affecting the compressive yield strain of aramid fiber reinforced composites.
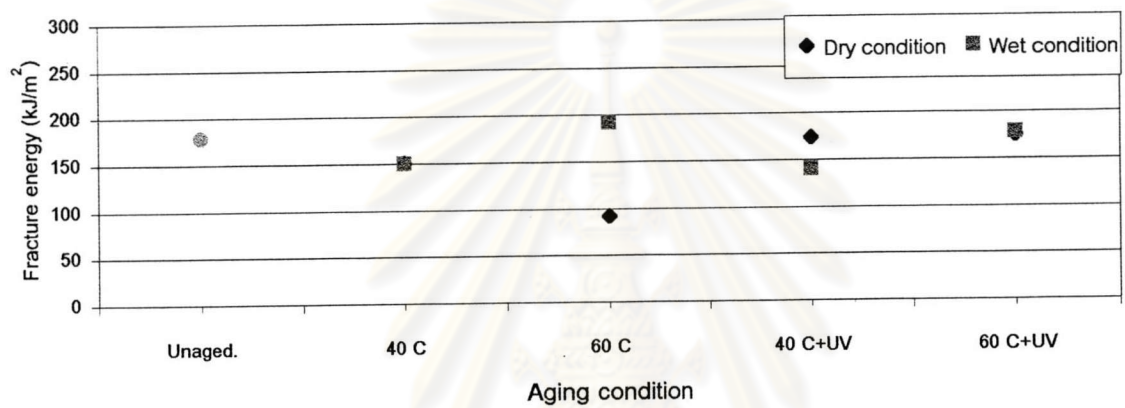
The effects of various aging conditions on the fracture energy of fiber reinforced epoxy composites under compression are shown in Figure 5.30 and 5.31.

For carbon fiber reinforced epoxy composites, from Figure 5.30, it was found that the fracture energy under compression of the specimens aged with high level of aging conditions are almost equal to those aged with low level of aging conditions. From Figure 5.30 (a), the fracture energy of the specimens aged at a higher temperature are higher than those aged at a lower temperature. The aging temperature affects slightly the fracture energy of the carbon fiber reinforced composites. Figures 5.30 (b) and (c), do not exhibit any consistent trend of the compressive fracture energy of carbon fiber reinforce composites.

In contrast with the carbon fiber reinforced composites, the aramid fiber reinforced epoxy composites exhibit some differences between the fracture energy under compression of the ones aged with high level of aging conditions and those aged with low level of aging conditions. However, from Figure 5.31 (a), (b) and (c), it is not clearly seen which factors affect the compressive fracture energy of aramid fiber reinforced composites.
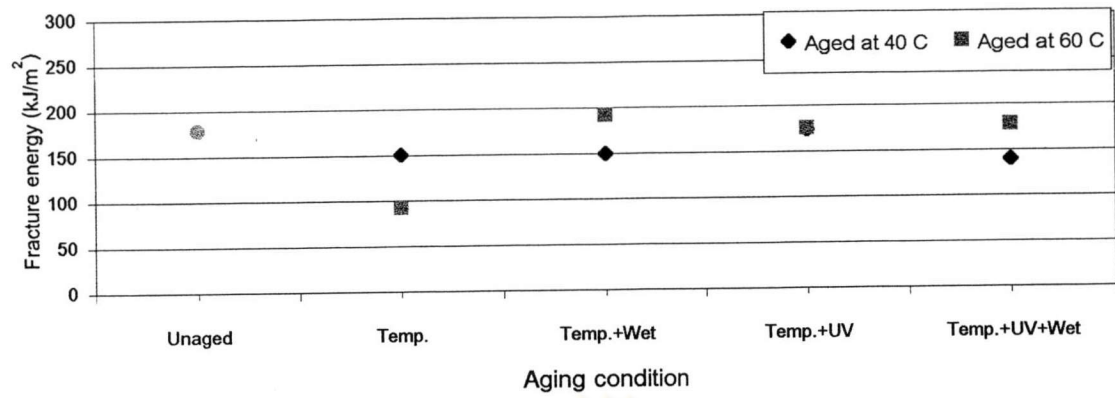
(a)

(b)
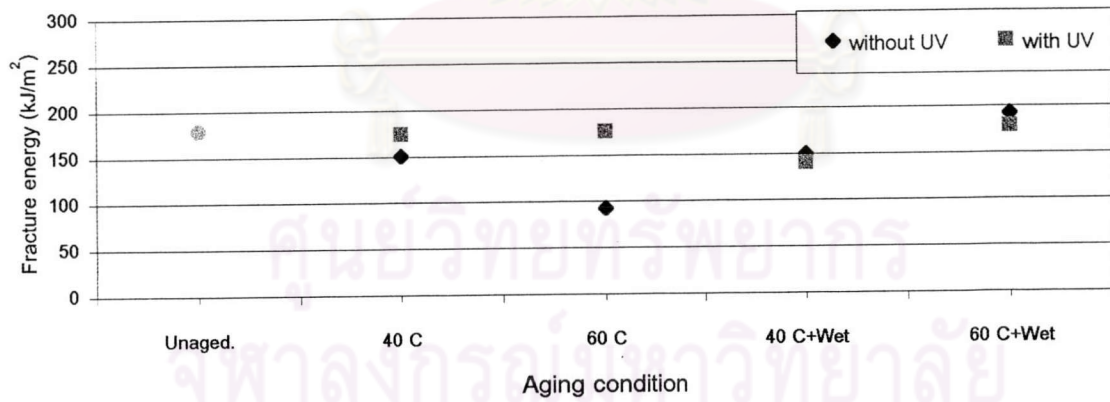
(c)

Figure 5.30: Effects of temperature (a), humidity (b) and the UV exposure (c) on the fracture energy in direction "2" of carbon fiber reinforced epoxy composites under compression.
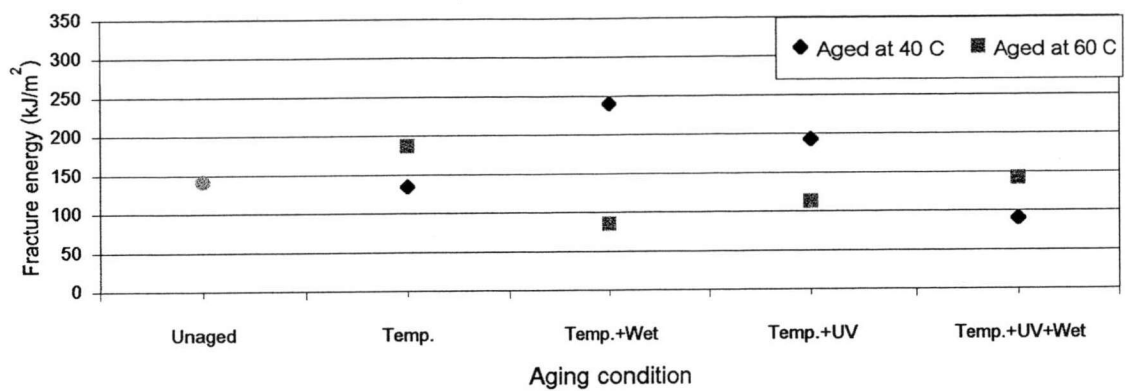
(a)

(b)

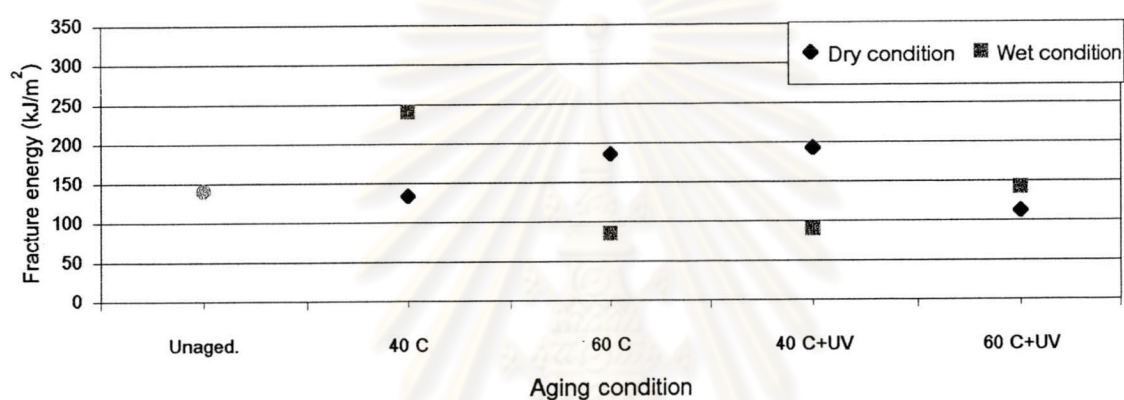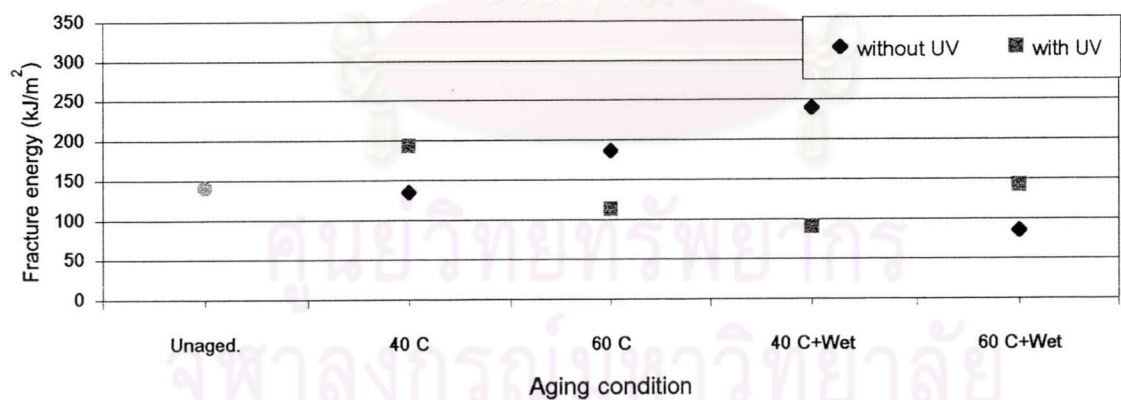(c)

Figure 5.31: Effects of temperature (a), humidity (b) and the UV exposure (c) on the fracture energy in direction "2" of aramid fiber reinforced epoxy composites under compression.
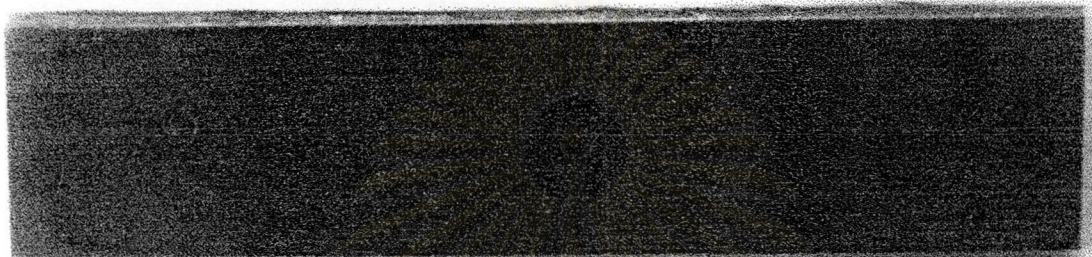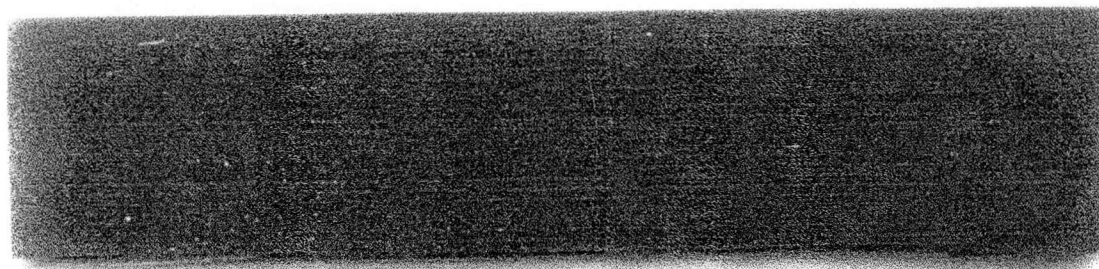
5.2.3 Double torsion test

Double torsion test is applied to estimate the energy required to break the composites, i.e. fracture energy. This test can be done by investigating crack initiation during fracture. The stress field around a sharp crack in a linear elastic material can be defined by a parameter called the stress intensity factor, K. Fracture occurs when the value of K exceeds some critical values, K_{Ic}. For this reason, K is a stress field parameter independent of the material while K_{Ic} is a measure of the material property that is often referred to the fracture toughness. Double torsion-tested specimens of carbon fiber reinforced epoxy composites is shown in Figure 5.32. Epoxy composites was broken along the U-groove that divided the specimen into two halves. The crack propagates slowly from the left end to the right end. Fracture surface of the specimen are investigated microscopically by a scanning electron microscopy (SEM) in Section 5.5.

In the current work, the load at the crack arrest points was measured. The critical stress intensity factor was evaluated by using Equation 5.5 (Truong and Ennis, 1991; Jarun Chutmanop, 1994; Vichaya Vichayapai Bunnag, 2000).

$$K_{Ic} = PW_m \left[\frac{3(1+v)}{Wt^3 t_n} \right]^{\frac{1}{2}} \quad (5.5)$$

where P is the load at the break point, W_m is the moment arm, v is poisson's ratio, W is the width of the test specimen, t is the thickness of the test specimen and t_n is the plate thickness in the plane of the crack.

(a) Epoxy composites broke into 2 pieces.


(b) Fracture surface

Figure 5.32: Carbon fiber reinforced epoxy composites after double torsion test.

The specimen configuration under the double torsion test in the present work satisfied a plane stress condition. Hence, the critical stress intensity factor, the fracture energy, G_{Ic}, can be evaluated by Equation 5.6.

$$G_{Ic} = \frac{K_{Ic}^2}{E} \qquad (5.6)$$

where E is the modulus of elasticity.

The effects of various weathering conditions on the critical stress intensity factor of fiber reinforced epoxy composites are displayed in Figure 5.33 and 5.34.
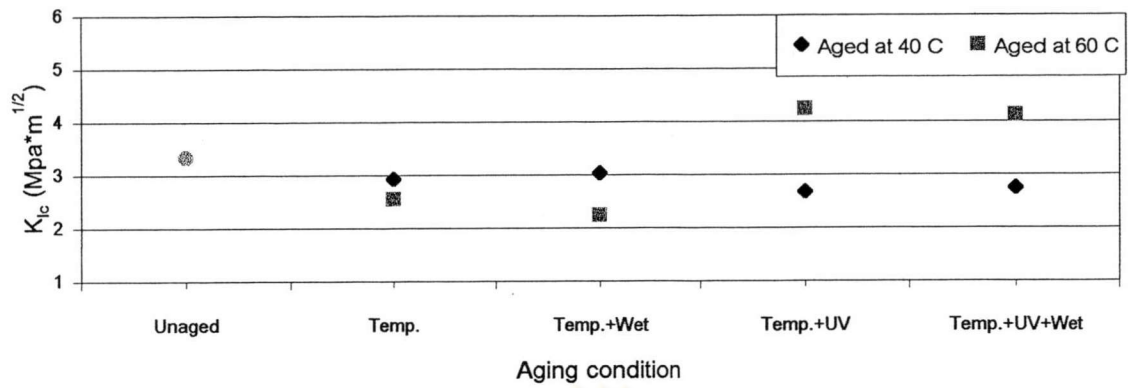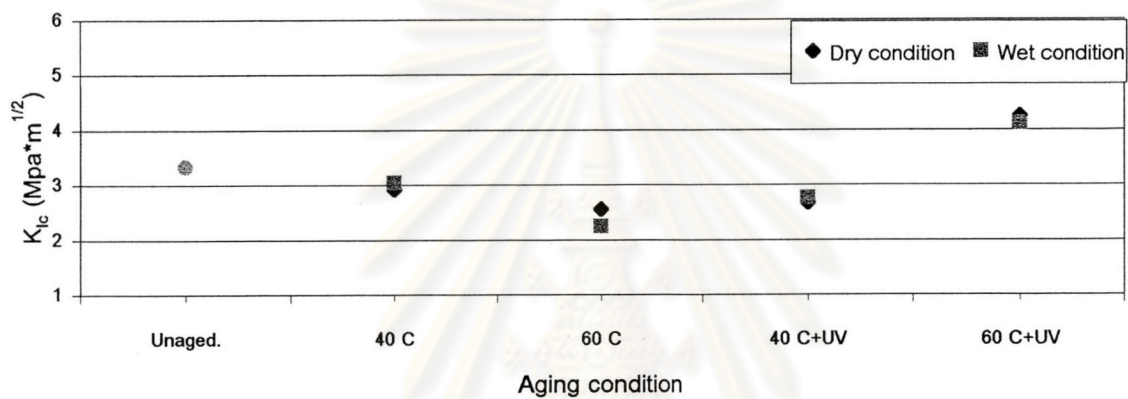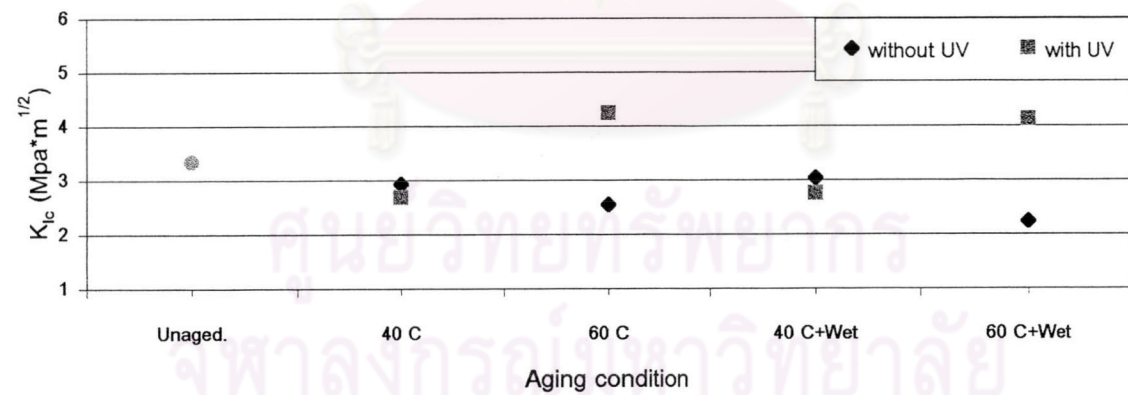
Figure 5.33: Effects of temperature (a), humidity (b) and the UV exposure (c) on the critical stress intensity factor of carbon fiber reinforced epoxy composites.
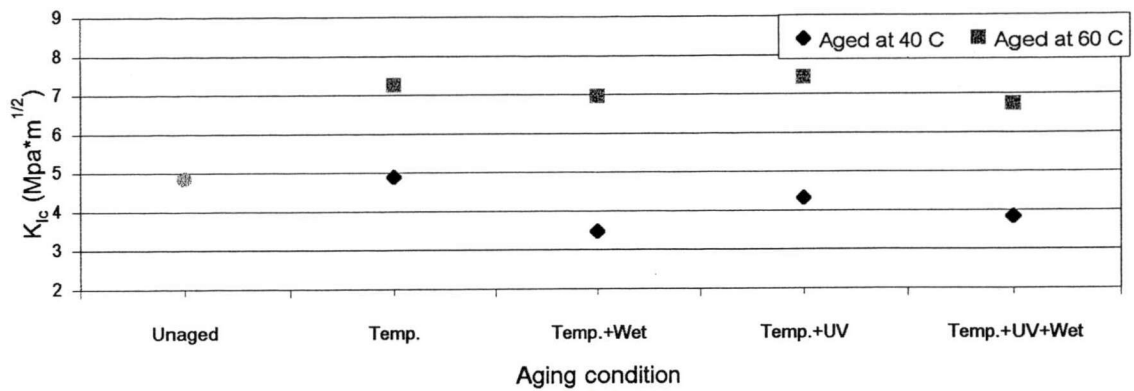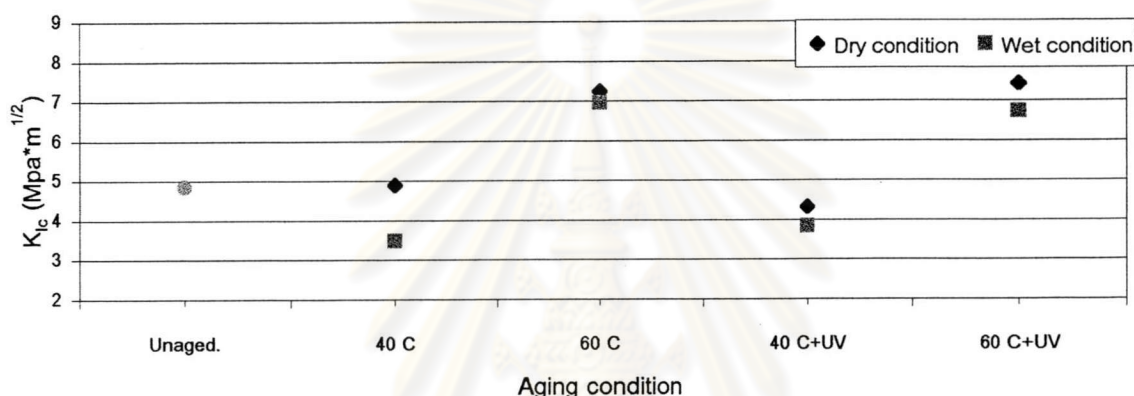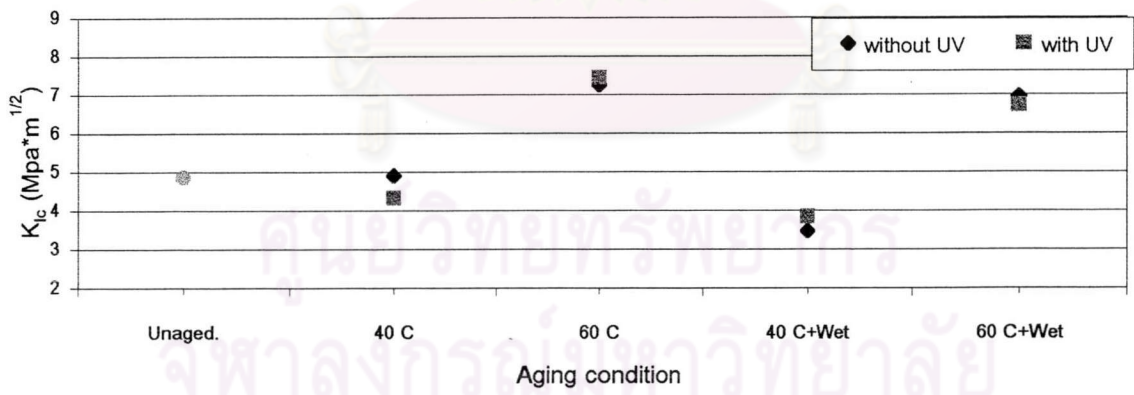
Figure 5.34: Effects of temperature (a), humidity (b) and the UV exposure (c) on the critical stress intensity factor of aramid fiber reinforced epoxy composites.

For carbon fiber reinforced epoxy composites, it is apparent from Figure 5.33 (b) that the critical stress intensity factor of the specimens aged in dry condition are nearly equal to the critical stress intensity factor of those aged in wet condition. So, humidity is not the significant effect for the critical stress intensity factor of carbon fiber reinforced composites. Figures 5.33 (a) and (c) do not show any consistency. However, it was found that the critical stress intensity factor of the specimens aged at a higher temperature with UV both in dry condition and wet condition are higher than those aged with other aging conditions. The interaction of the aging temperature and UV is possibly the significant factor for the critical stress intensity factor. The regression analysis as shown in Figure 5.35 (a) revealed the significant factors affecting the critical stress intensity factor of carbon fiber reinforced composites to be the aging temperature (A), UV exposure (C) and the interaction of aging temperature and UV exposure (AC) respectively.

For aramid fiber reinforced epoxy composites, it is clearly seen from Figure 5.34 (a) that the critical stress intensity factor of the specimens aged at a higher temperature are higher than those aged at a lower temperature. Thus, the aging temperature is one of the significant effects for the critical stress intensity factor. From Figure 5.34 (b), the critical stress intensity factor of the specimens aged in wet condition are lower than those aged in dry condition. So, humidity is one of the significant factors for the critical stress intensity factor. From Figure 5.34 (c), it does not show the consistent trend for all aging conditions. Additionally, the critical stress intensity factor of the specimens aged with UV are nearly equal to the critical stress intensity factor of those aged without UV. From the regression analysis as shown in Figure 5.35 (b), it is found that the significant factors affecting the critical stress intensity factor of aramid fiber reinforced composites are the aging temperature (A), humidity (B) and the combined aging temperature, humidity and UV exposure (ABC) respectively.

(a) carbon fiber reinforced composite

(b) aramid fiber reinforced composite

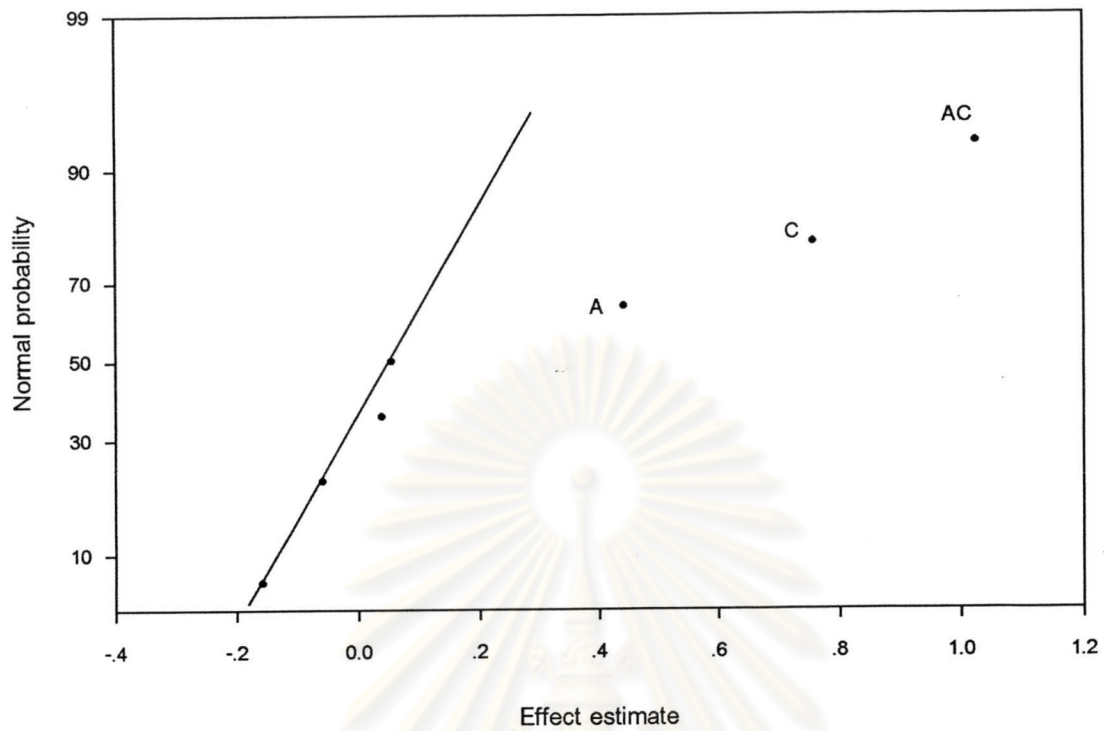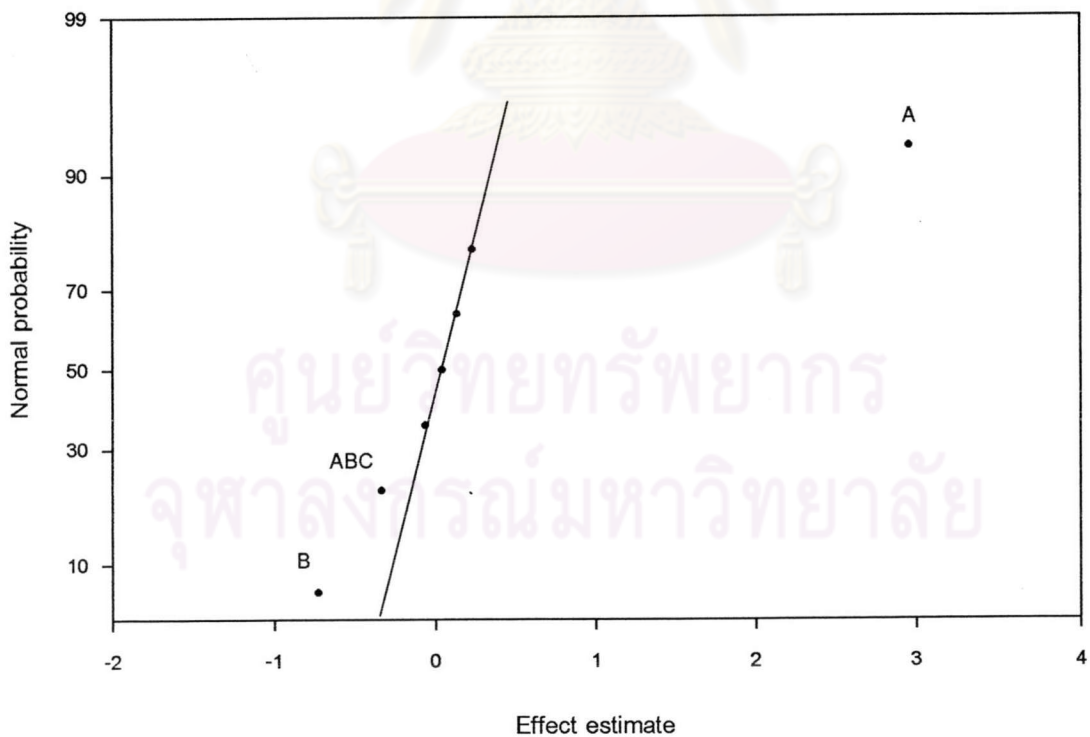**Figure 5.35: Normal probability plots of estimate effect for the critical stress intensity factor of fiber reinforced epoxy composites.**

The effects of various aging conditions on the fracture energy of fiber reinforced epoxy composites are displayed in Figure 5.36 and 5.37.

For carbon fiber reinforced epoxy composites, similar with the critical stress intensity factor, from Figure 5.36 (b), it is obvious that the fracture energy of the specimens aged in dry condition are closely equal to the fracture energy of those aged in wet condition. From Figures 5.36 (a) and (c), it does not show the consistent trend. Nevertheless, it is found that the fracture energy of the specimens aged at a higher temperature with UV both in dry condition and wet condition are higher than the fracture energy of those aged with other aging conditions. The combined effect of the aging temperature and UV may be the significant factor for the fracture energy. From the regression analysis as shown in Figure 5.38 (a), the significant factors affecting the fracture energy of carbon fiber reinforced composites are the aging temperature (A), UV exposure (C) and the combined aging temperature and UV exposure (AC) respectively.
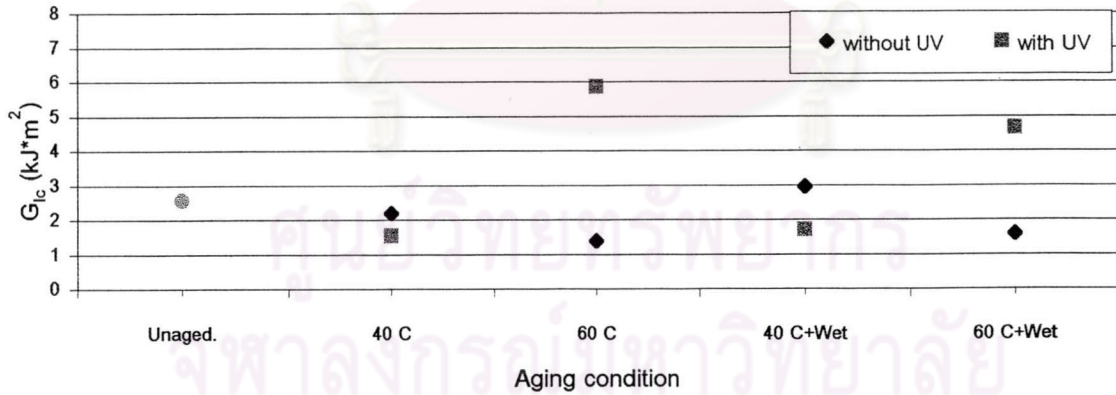
For aramid fiber reinforced epoxy composites, from Figure 5.37 (a), it is apparent that the fracture energy of the specimens aged at a higher temperature are higher than those aged at a lower temperature. Therefore, the aging temperature is one of the significant effects for the fracture energy. From Figure 5.37 (b), the fracture energy of the specimens aged in wet condition are lower than those aged in dry condition but not much. Humidity may be the significant factor of the fracture energy. From Figure 5.37 (c), alike the critical stress intensity factor, it does not show the consistent trend for all aging conditions. From the regression analysis as shown in Figure 5.38 (b), the significant factors affecting the fracture energy of aramid fiber reinforced composites is only the aging temperature (A).
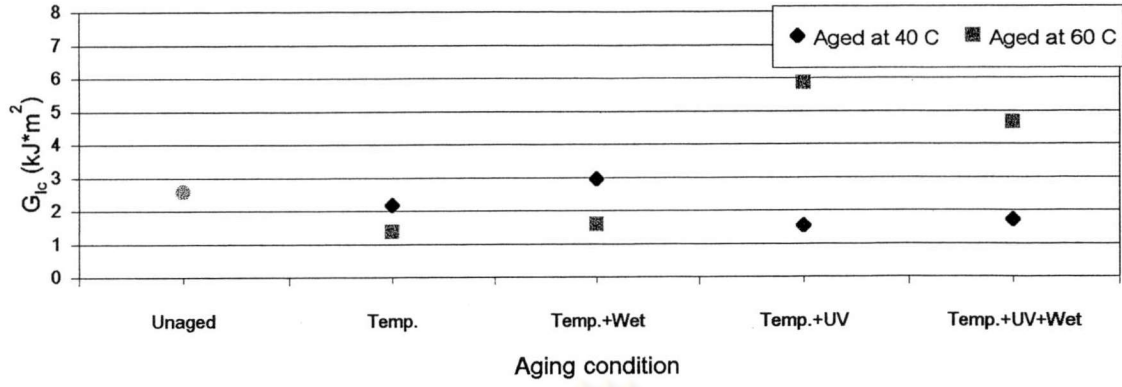
(a)
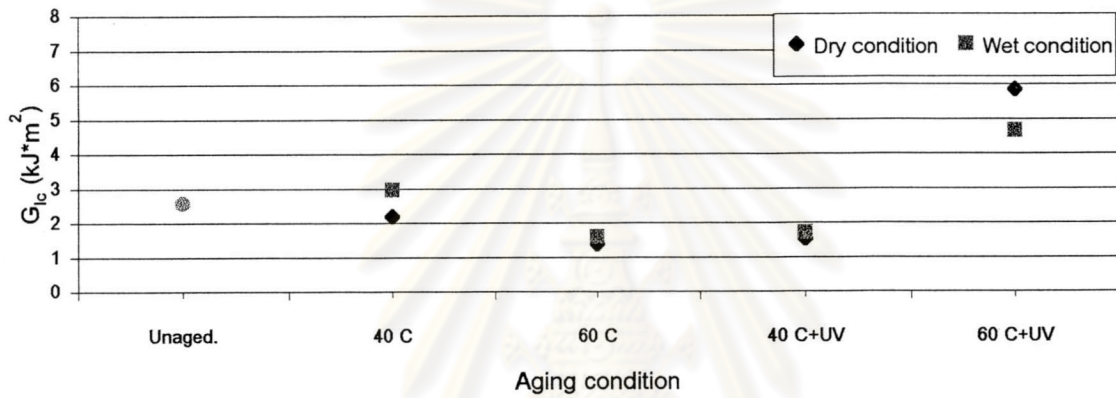
(b)

(c)

Figure 5.36: Effects of temperature (a), humidity (b) and the UV exposure (c) on the fracture energy of carbon fiber reinforced epoxy composites.
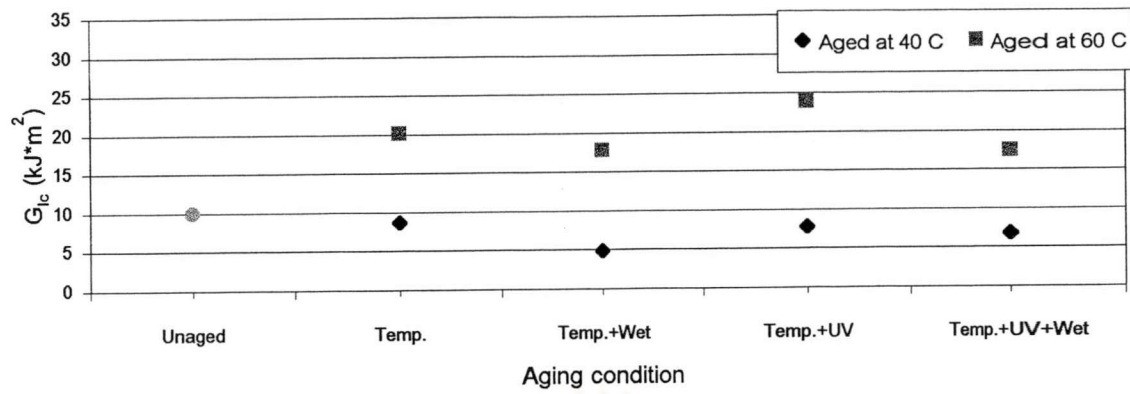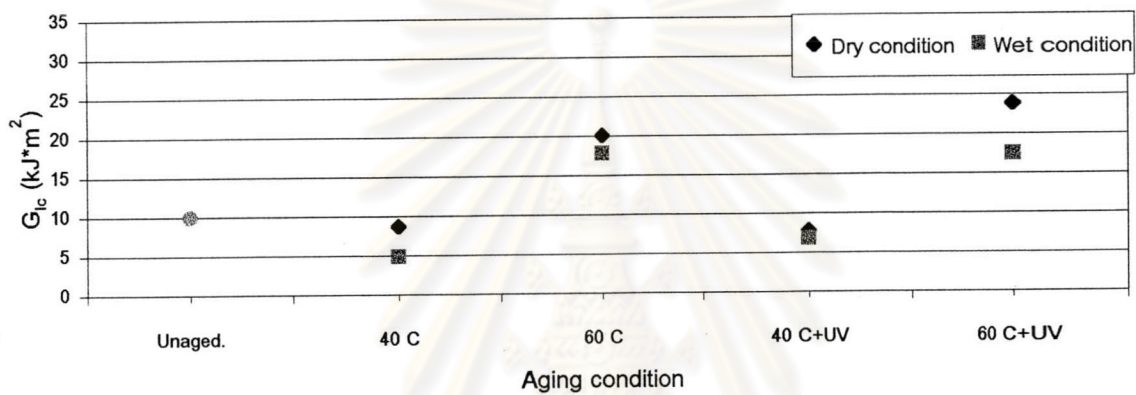
(a)

(b)

(c)

Figure 5.37: Effects of temperature (a), humidity (b) and the UV exposure (c) on the fracture energy of aramid fiber reinforced epoxy composites.
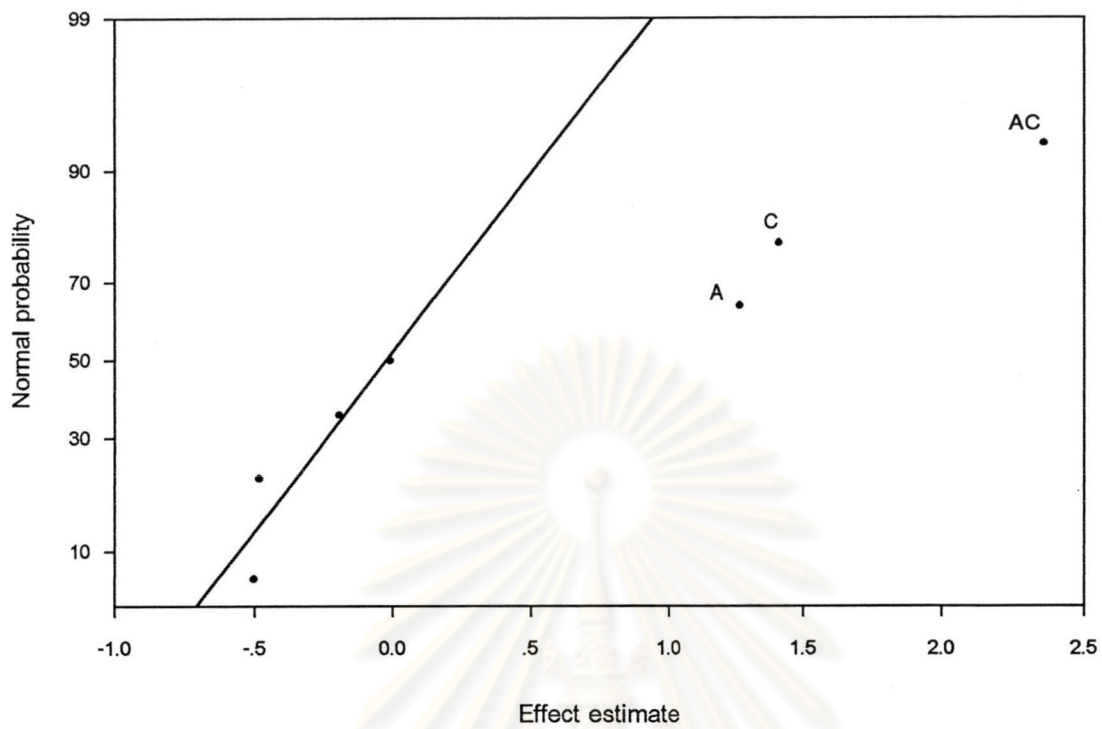
(a) carbon fiber reinforced composite
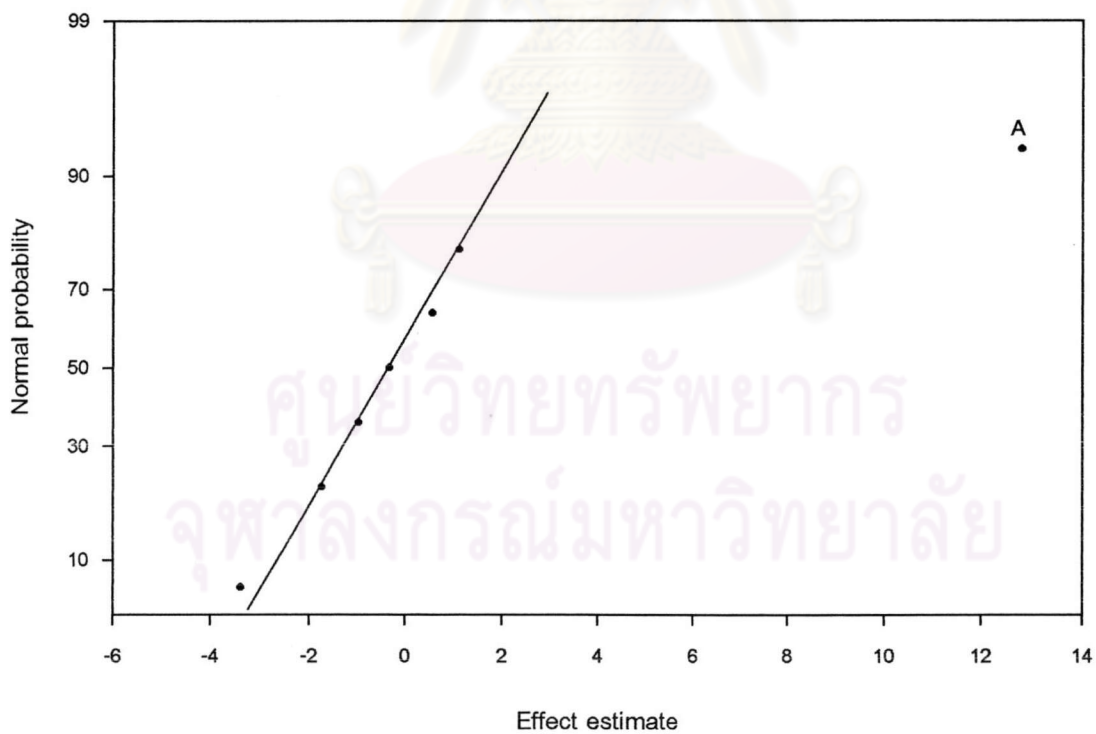
(b) aramid fiber reinforced composite

Figure 5.38: Normal probability plots of estimate effect for the fracture energy of fiber reinforced epoxy composites.

5.3 SAMPLE CHARACTERIZATION

The glass transition temperature (T_g) can be determined by a wide range of techniques such as the measurement of volume (dilatometry), specific heat (calorimetry) and mechanical properties, especially the modulus. Dynamic mechanical analysis (DMA) test can be applied in the study of viscoelastic properties of polymer, for instance, the storage modulus (E'), the loss modulus (E") and the loss factor (tan δ). These properties are generally detected against the change in the temperature as demonstrated in Figure 5.39.
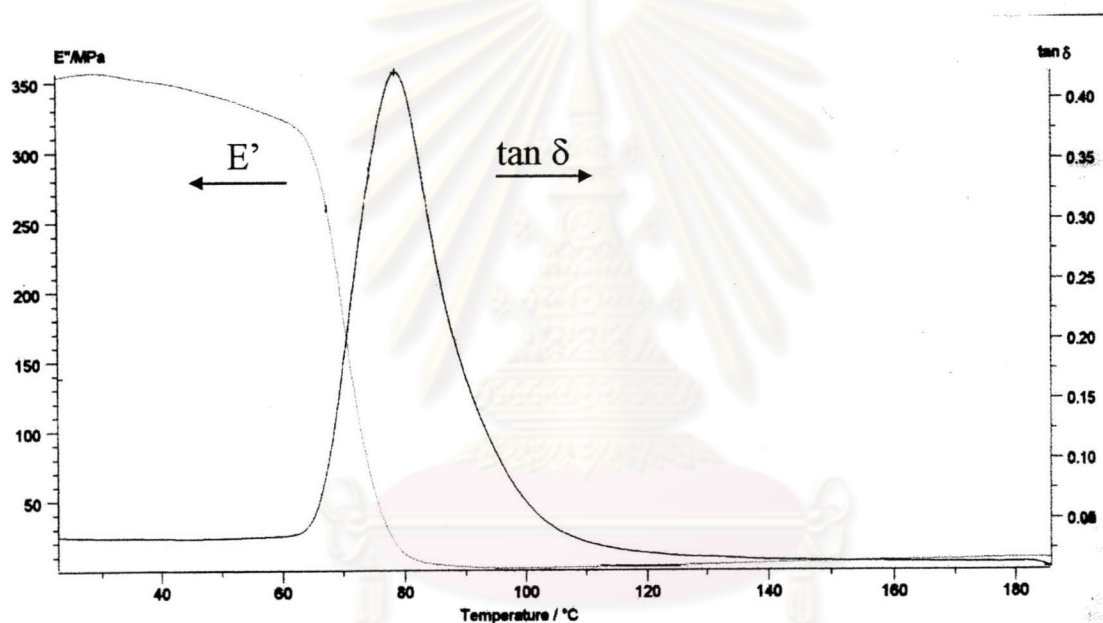
Figure 5.39: Dynamic mechanical properties of unaged aramid fiber reinforced epoxy composites.

In the present study, the effects of various climatic conditions on the T_g's of fiber reinforced composites are displayed in Figure 5.40 and 5.41.

From Figures 5.40 and 5.41, both carbon fiber reinforced composites and aramid fiber reinforced composites seem to have the same thermal behavior. From Figures 5.40 (a) and 5.41 (a), it is obvious that the T_g
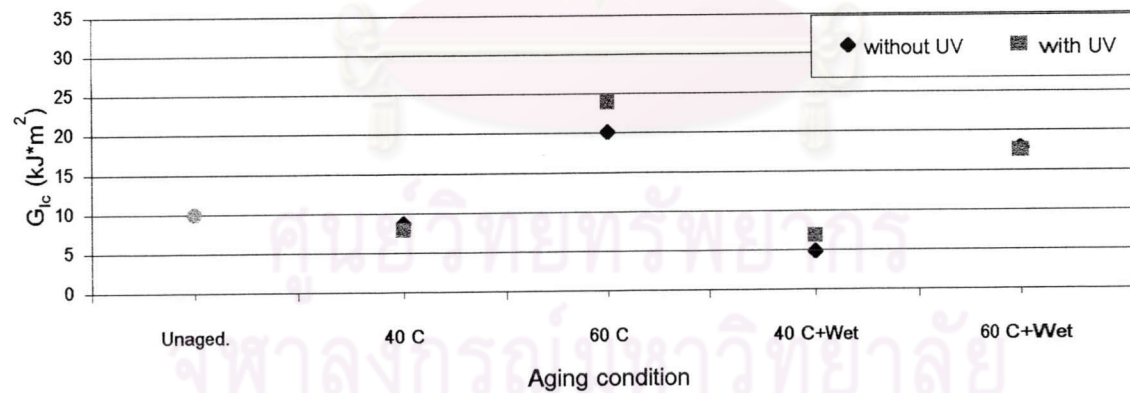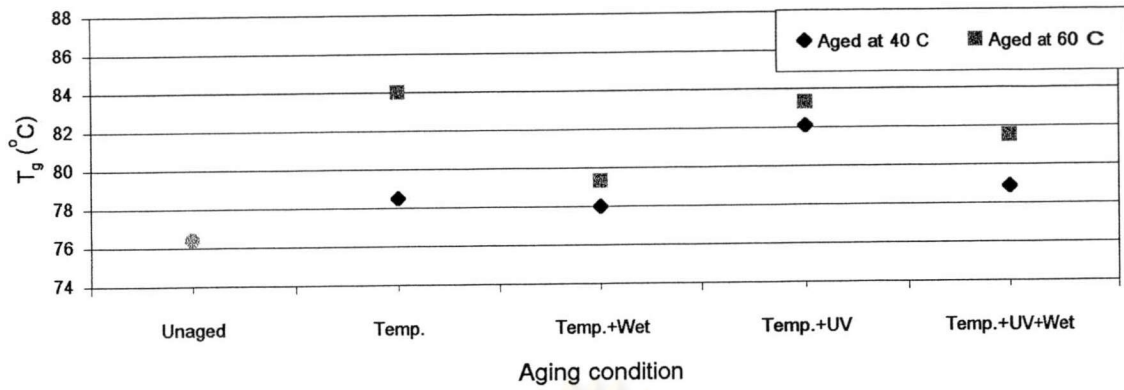
(a)
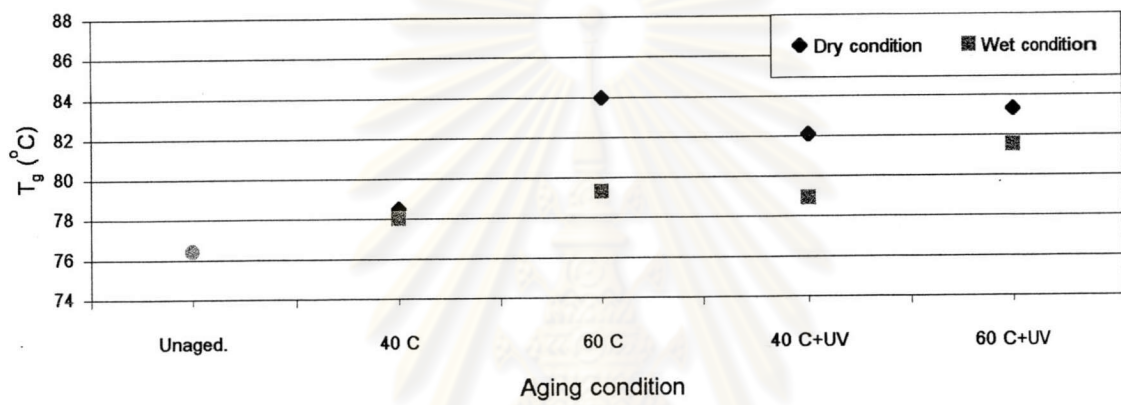
(b)
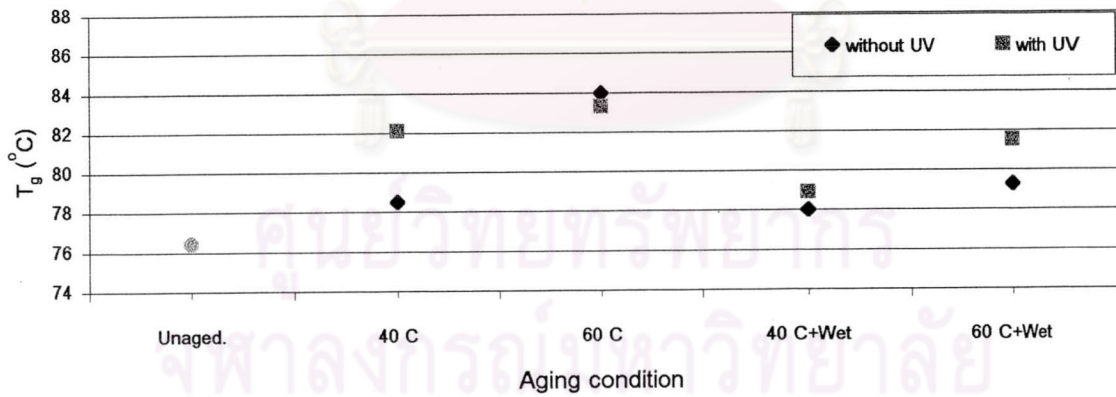
(c)

Figure 5.40: Effects of temperature (a), humidity (b) and the UV exposure (c) on the T_g of carbon fiber reinforced epoxy composites.
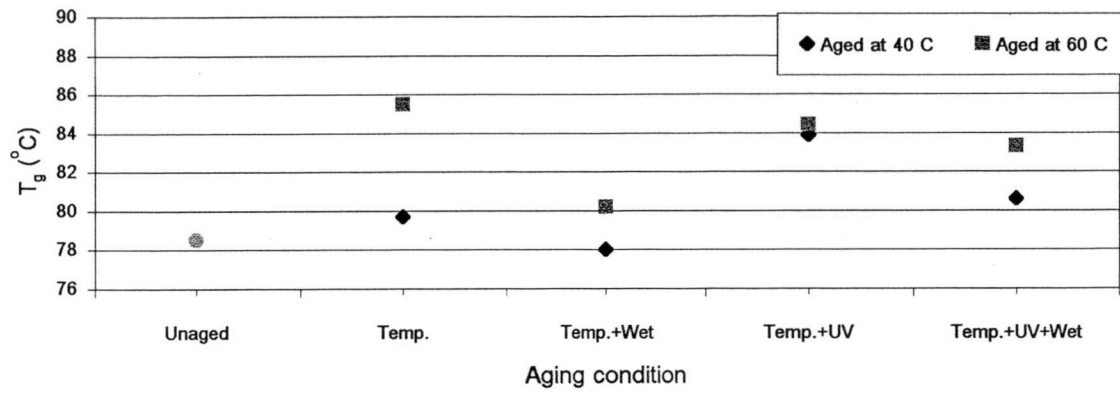
(a)
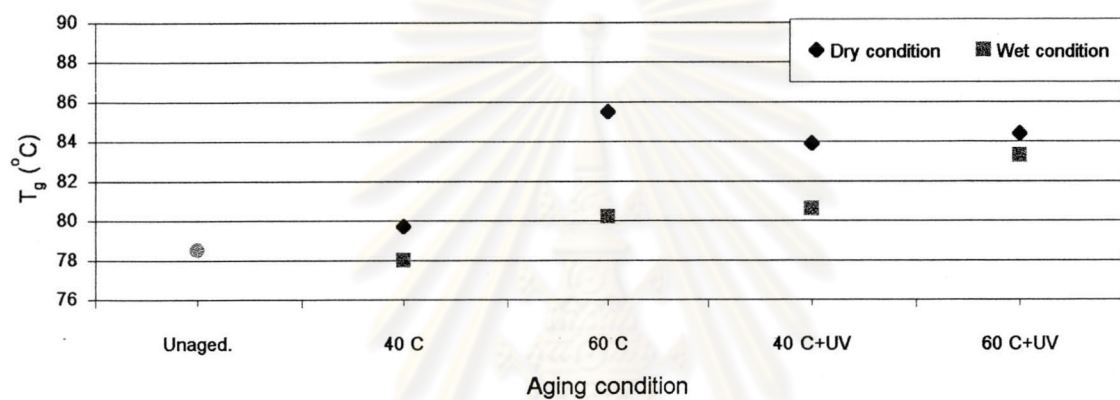
(b)
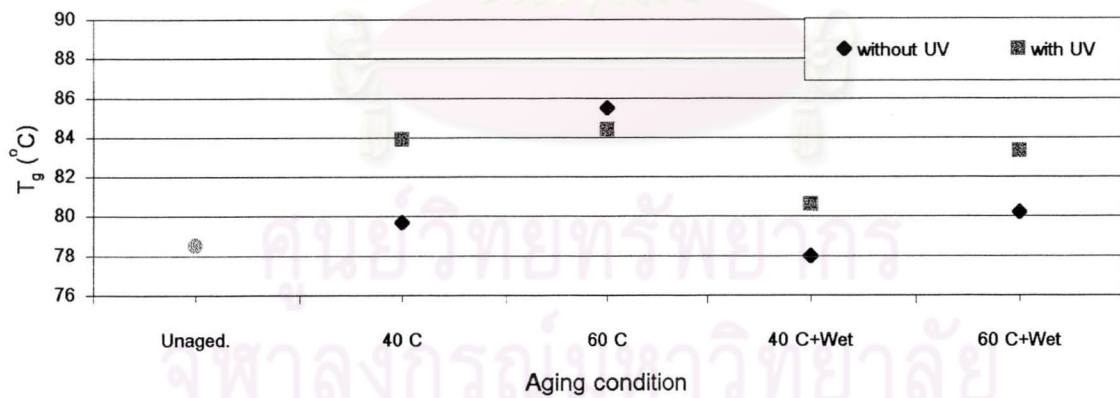
(c)

Figure 5.41: Effects of temperature (a), humidity (b) and the UV exposure (c) on the T_g of aramid fiber reinforced epoxy composites.

of the composites aged at a higher temperature are higher than those aged at a lower temperature. From Figures 5.40 (b) and 5.41 (b), the T_g's of the specimens aged in wet condition are lower than those aged in dry condition. From Figures 5.40 (c) and 5.41 (c), the T_g's of the specimens aged with UV are higher than those aged without UV except for the specimens aged at a lower temperature with and without UV.

Another important property evaluated via the dynamic mechanical test is the molecular weight between crosslink or M_c. High M_c means that epoxy resin has low crosslink density that results in higher possibility of mobility among the epoxy chains.

An analysis on the molecular weight between crosslinks was performed by application of the *Statistical Theory of Rubber Elasticity* under the condition when the epoxy matrix was most elastic and rubber-like. The molecular weight between crosslinks can be calculated by the use of the relationship shown in Equation 5.7 (Collyer, 1992; Anawat Chansaksoong, 1996).

$$\log\left(\frac{G'}{3}\right) = 6 + \left(\frac{293\,\rho}{M_c}\right) \tag{5.7}$$

where G' is the modulus at the temperature that the epoxy was in a rubber-like state, ρ is the density of epoxy and M_c is the molecular weight between crosslinks.

The effects of various aging conditions on the molecular weight between crosslinks of fiber reinforced composites are shown in Figure 5.42 and 5.43.

From Figures 5.42 and 5.43, most of the aged specimens possessed lower molecular weight between crosslinks than those of the unaged ones. This implies an increase in the crosslink density after physical aging. For carbon fiber reinforced epoxy composites, in Figure 5.42 (a) and
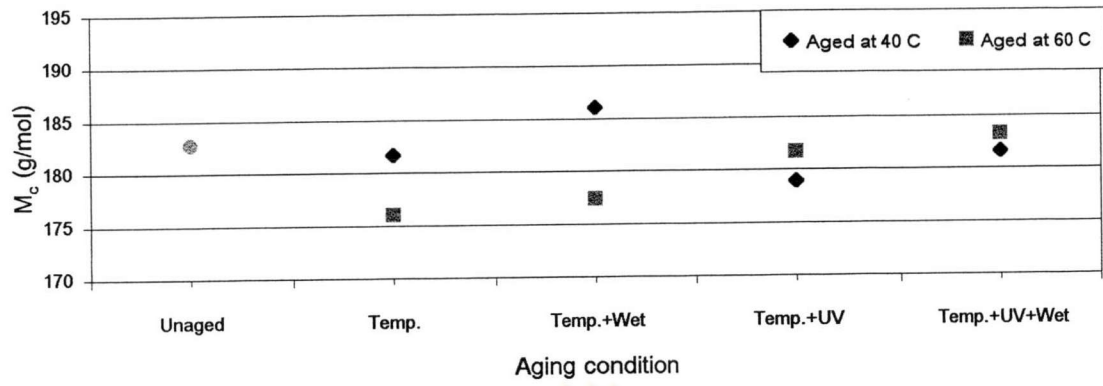
(a)
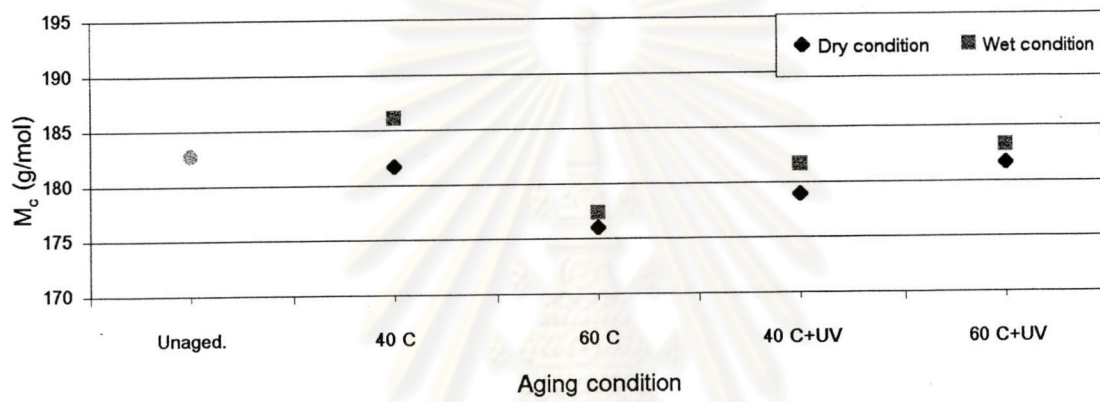
(b)
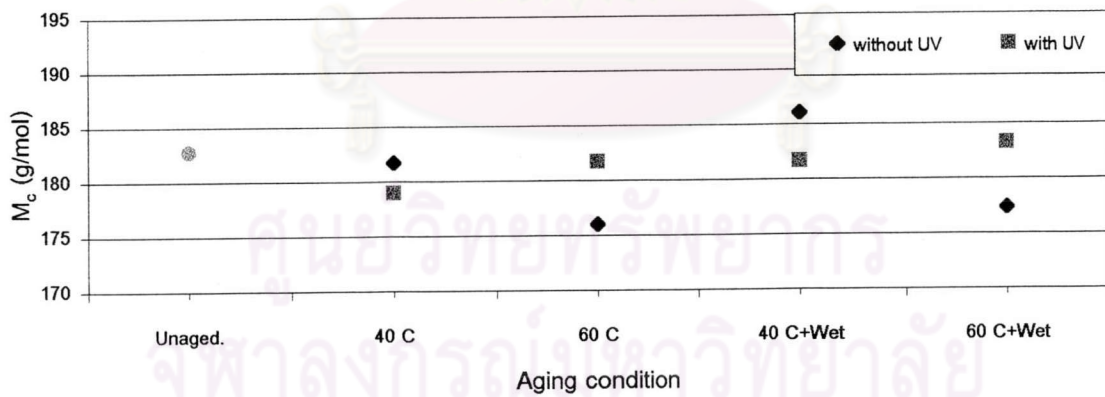
(c)

Figure 5.42: Effects of temperature (a), humidity (b) and the UV exposure (c) on the molecular weight between crosslink of carbon fiber reinforced epoxy composites.

(a)

(b)

(c)

Figure 5.43: Effects of temperature (a), humidity (b) and the UV exposure (c) on the molecular weight between crosslink of aramid fiber reinforced epoxy composites.

(c), no consistent trend was observed for the change in their molecular weight between crosslinks. Although the molecular weight between crosslinks of the specimens aged in wet condition are close to those aged in dry condition as shown in Figure 5.42 (b), the molecular weight between crosslinks of the composites aged in wet condition is consistently greater than those aged in dry condition by a small fraction.

For aramid fiber reinforced epoxy composites, from Figures 5.43 (a), it is apparent that the molecular weight between crosslinks of the specimens aged at a higher temperature are higher than those aged at a lower temperature even in the specimen aged in wet condition with UV. From Figure 5.43 (b), identical with the carbon fiber reinforced composites, the molecular weight between crosslinks of the aramid fiber reinforced composite aged in wet condition in Figure 5.43 (b) are nearly equal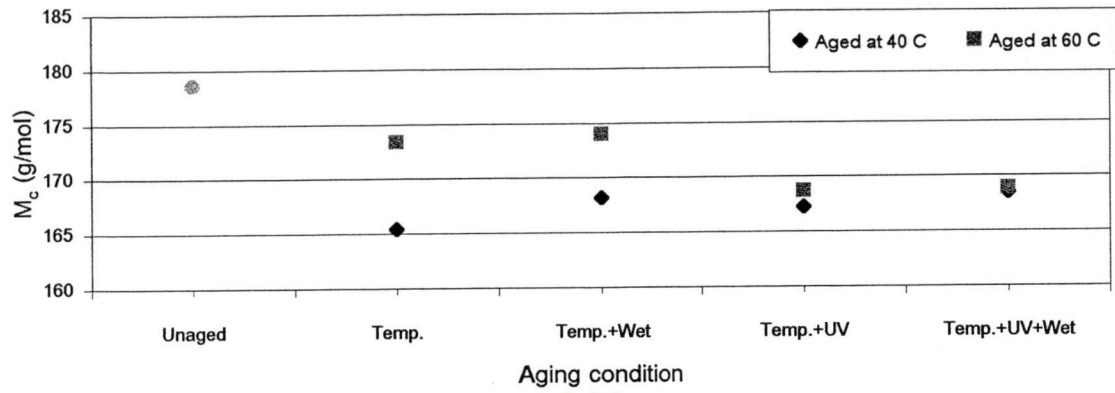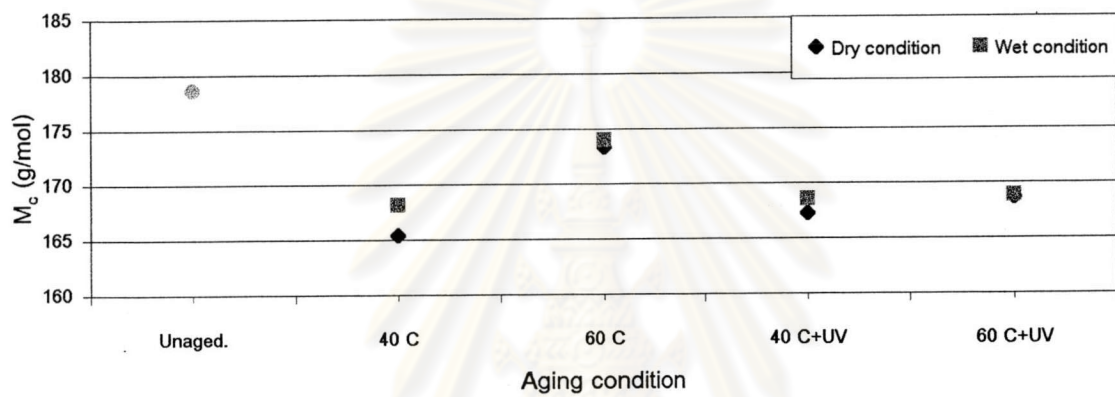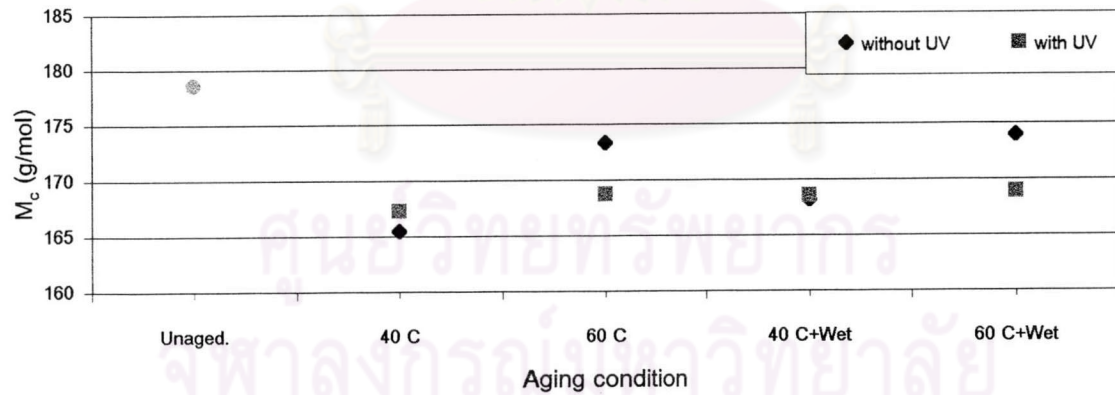 to those aged in dry condition but the molecular weight between crosslinks of the composites aged in wet condition is still higher. Figure 5.43 (c) shows that UV has significant effect on the molecular weight between crosslinks of aramid fiber reinforced epoxy composites aged at higher temperature conditions.

5.4 EFFECTS OF HUMIDITY AND UV ON THE MECHANICAL PROPERTIES AND THERMAL PROPERTY OF THE FIBER REINFORCED EPOXY COMPOSITES.

From the experimental results in the present study, it was found that the flexural strength and the compressive strength of the carbon fiber and aramid fiber reinforced epoxy composites had been decreased upon physical aging, especially in the humidity and humidity-related aging conditions except for the interaction of humidity and UV. This is because humidity is trapped between the epoxy matrix and the reinforcing fiber, resulting in a poor adhesion within the composites.

For aramid fiber reinforced epoxy composite, it can produce the hydrogen bonding with water at the amide functional group as shown in Figure 5.44. This brings about additional obstacles to molecular mobility within the composite when it was stressed. Hydrogen bonding formed with the water also influences adversely on the stability of the molecule of aramid fiber resulting in the strength reduction of the composite. Another explanation is that the hydrogen bonding formed in the aramid fiber molecule causes the separation of the chains and increases their general mobility. This is the effect of plasticisation that will cause a reduction in the T_g.
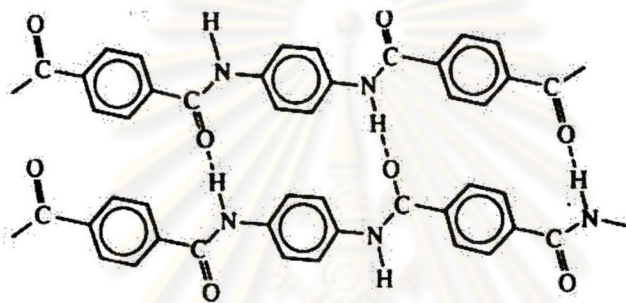
Figure 5.44: Functional groups in aramid fiber that can form the hydrogen bonding.

UV leads to weakening and embrittlement of composites. It is believed to have brought about thermal oxidation in the epoxy resin as was verified by the Fourier Transform Infrared Spectroscopic study (FTIR) in Figure 5.45. Carbonyl group (C=O) was found at the wavenumber range of 1715 ± 10 cm^{-1} only in the aged specimens. This existence of the C=O group, found only in the aged composites, confirms that thermal oxidation of the epoxy resin took place within the composites after UV exposure.
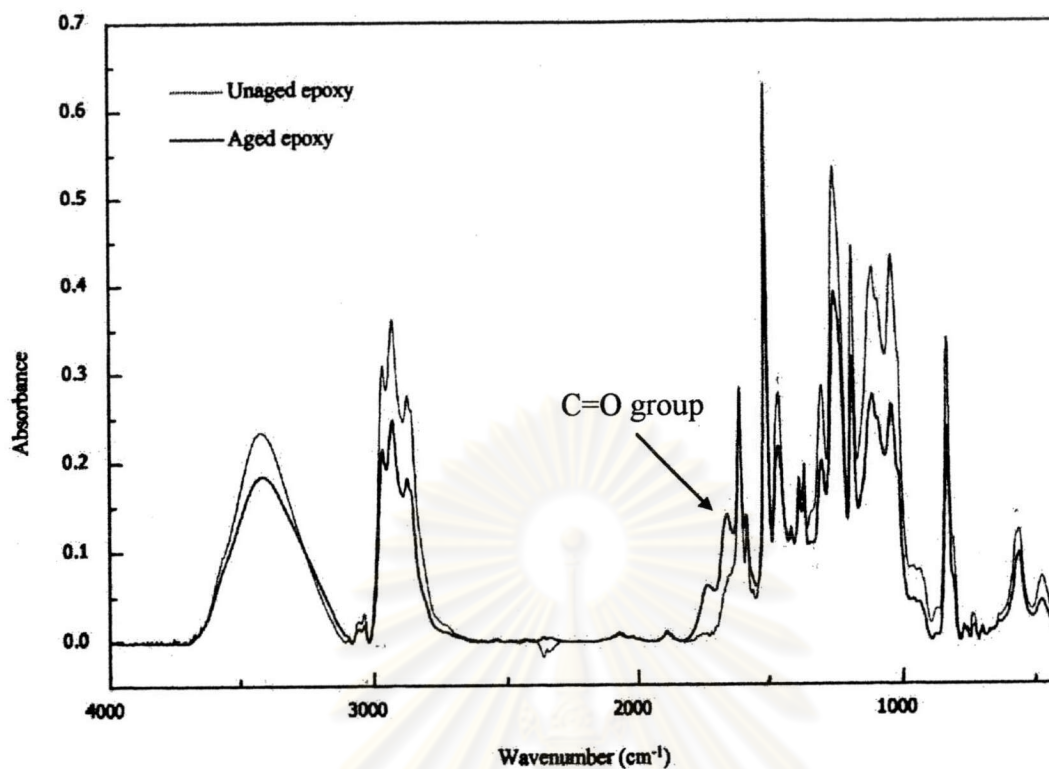
Figure 5.45: FTIR Spectra of unaged and aged epoxy resin.

5.5 WLF EQUATION

From the thermal information of fiber reinforced epoxy composites derived from the DMA test, it can be further analyzed to predict the relaxation modulus of the composites for short or long term behaviors by application of the principle of time-temperature superposition. The temperature dependence of the shift factor can be represented by the Williams-Landel-Ferry or WLF equation.

The temperature dependence of the shift factor based on the WLF equation is given by Equation 5.8 (Williams, 1955).

$$\log a_T = -\frac{C_1(T - T_S)}{C_2 + T - T_S} = \log \frac{t_T}{t_S} \qquad (5.8)$$

where C_1 and C_2 are constants, T_S is the reference temperature and T is the experimental temperature. When T_g is adopted for T_S, it is well known that C_1 = 17.44 and C_2 = 51.6 (Ferry, 1980) for a wide variety of polymers and glass-forming liquids. By changing two parameters, C_1 and C_2, the temperature dependence of the shift factor (log a_T) can be determined experimentally under the various aging conditions. Since the deformation mode utilized in the DMA test is deformed by flexural loading, the thermal data of flexural properties is chosen for the calculation of a_T. Corresponding significant factors in flexural properties are hence selected, namely the aging temperature (A), humidity (B) and the combined factors of aging temperature and UV (AC) for carbon fiber composite, humidity (B) and the combination of aging temperature and humidity (AB) for aramid fiber composite.

The shift factor can be estimated according to Equation 5.9 (Ferry, 1980) where t_{303} means the time when the relaxation modulus reaches a given value at 303 K and t_T is the time at a given temperature T. The calculated log a_T's over a temperature ranges from 303 to 373 K are shown in Figure 5.46 (a) and (b) where the reference temperature is 303 K. The temperature used in the calculation of t_T are ranged from 303, 313, 323,..., 373 K. The t_T and t_{303} can be found from the DMA data for each significant factors.

$$\log a_T = \log\left(\frac{t_T}{t_{303}}\right) \tag{5.9}$$

When a temperature other than T_g is applied as the reference, the shift factor, log S_T, is given in Equation 5.10.

$$\log S_T = \log\frac{t_T}{t_S} \tag{5.10}$$

$$= \log\frac{t_T}{t_g} - \log\frac{t_S}{t_g}$$

$$= -\frac{17.44(T - T_g)}{51.6 + T - T_g} + \frac{17.44(T_S - T_g)}{51.6 + T_S - T_g} \qquad (5.11)$$
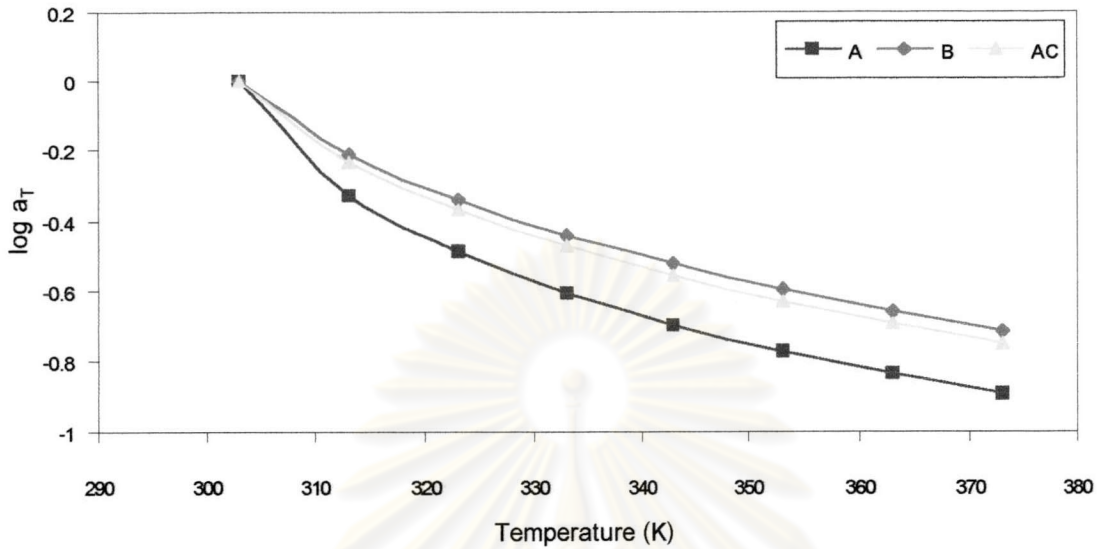
(a) Carbon fiber reinforced composite.
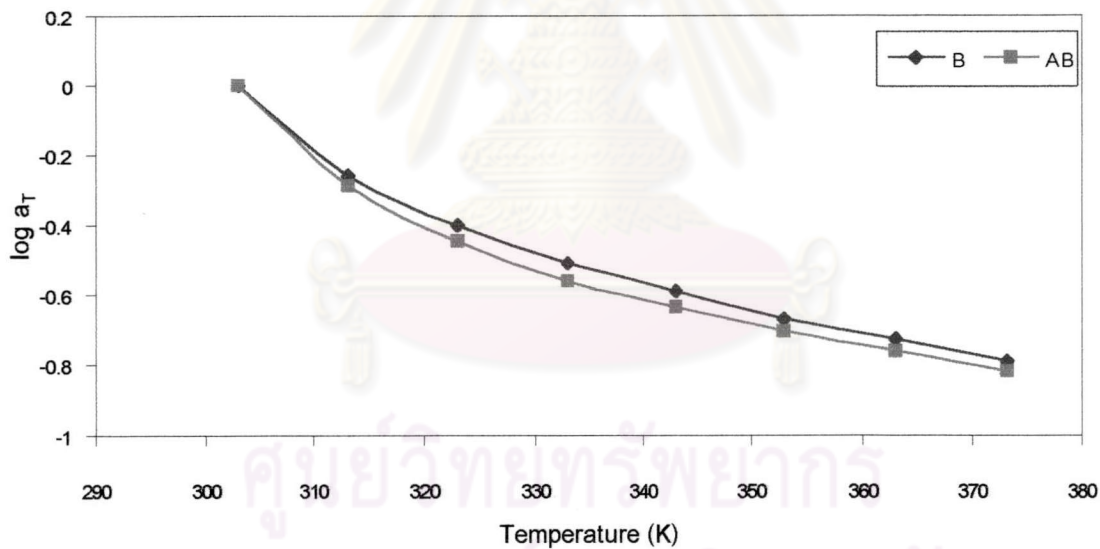
(b) Aramid firber reinforced composite.

Figure 5.46: Temperature dependence of shift factor for fiber reinforced epoxy composites when the reference temperature is fixed at 303 K.

The temperature dependence of the shift factor according to Equation 5.11 is exhibited in Figure 5.47.

Figure 5.47: Comparison of the shift factor of carbon fiber reinforced composite obtained from the present experimental study and those predicted by the WLF equation using T_g as the reference temperature.

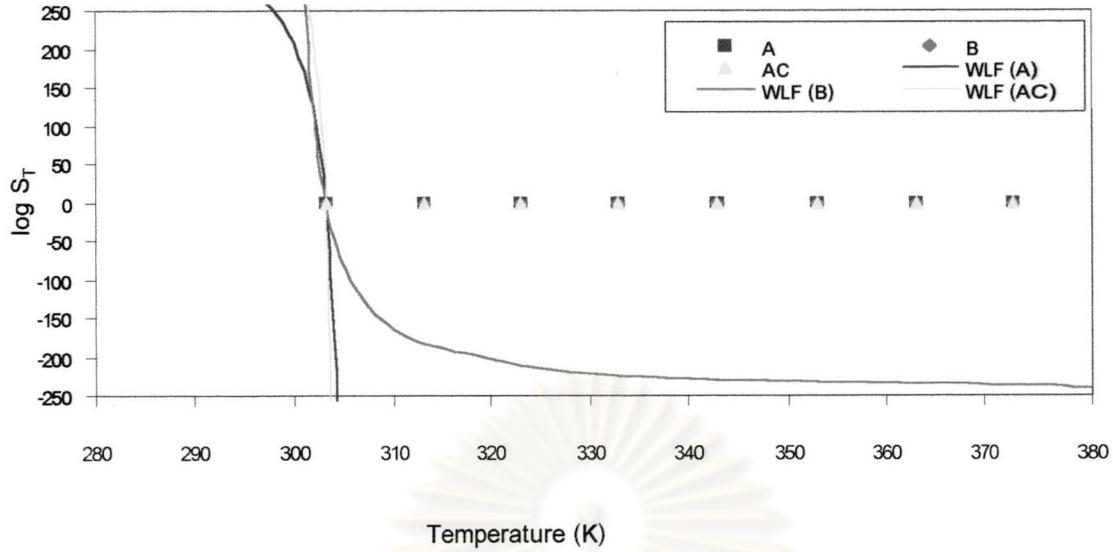As indicated by experimental points, the experimental shift factors are very different from the curves predicted by the usual **WLF** equation. Therefore, the parameters C_1 and C_2 in Equation 5.8 have to be requantified. Equation 5.10 is commonly rewritten to be Equation 5.12 (Ferry, 1980). New parameters C_1' and C_2'' corresponding to C_1 and C_2 are added, yielding Equation 5.12.

$$\because \log S_T = \log \frac{t_T}{t_g} - \log \frac{t_S}{t_g}$$

$$\log S_T + \log S_S = \log \frac{t_T}{t_g} = -\frac{C_1' (T - T_g)}{C_2' + T - T_g}$$

$$\therefore \frac{(T - T_g)}{\log S_T + \log S_S} = \frac{C_2'}{C_1'} - \frac{(T - T_g)}{C_1'} \tag{5.12}$$

where $\log S_S$ is given by Equation 5.13.

$$\log S_S = -\frac{C_1'(T-T_g)}{C_2'' + T_S - T_g} = \log\frac{t_S}{t_g} = \text{Constant} \tag{5.13}$$

where t_g means the time when the relaxation modulus is measured at T_g and t_S is the time when the relaxation modulus is measured at a given reference temperature T_S. In other words, $\log S_S$ is the actual shift factor from T_g to T_S. Equation 5.12 can be plotted to demonstrate the relationship between $-(T-T_g)/(\log S_T + \log S_S)$ versus $(T-T_g)$ as illustrated in Figure 5.48.

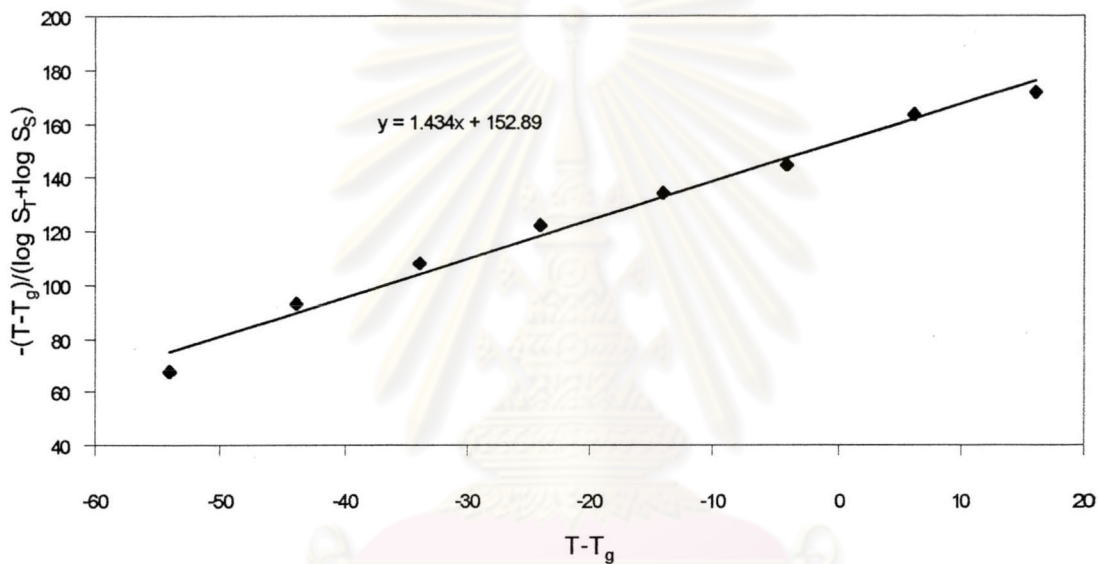**Figure 5.48: The plot between $-(T-T_g)/(\log S_T + \log S_S)$ and $(T-T_g)$ to illustrate the effect of aging temperature (A) of carbon fiber reinforced epoxy composites at $T_S = 303$ K.**

The slope α and the intercept β of the line in Figure 5.42 can be correlated with C_1' and C_2' following Equation 5.14 and 5.15.

$$C_1' = \frac{1}{\alpha} \tag{5.14}$$

$$C_2' = \frac{\beta}{\alpha} \tag{5.15}$$

As a result, both the C_1' and C_2' are estimated based on the experimental shift factors. Figure 5.49 shows the comparison between the experimental shift factors and the curves predicted by WLF equation in which one pair of the modified parameters (C_1'=0.7409, C_2'=112.6188) are applied.
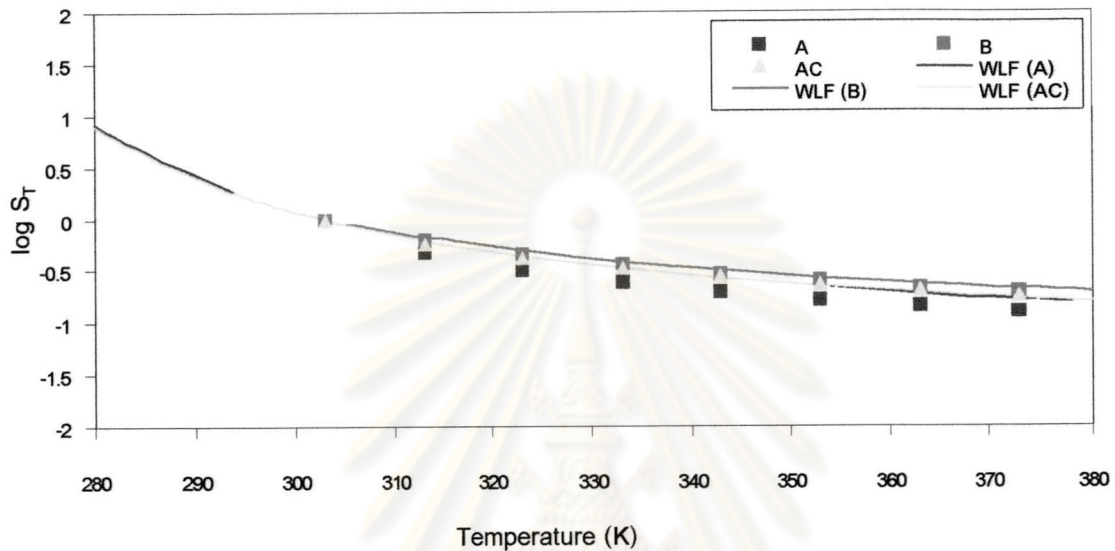

Figure 5.49: Comparison of the shift factor of carbon fiber reinforced composite obtained from the present experimental study and those predicted by the WLF equation using the modified C_1' and C_2'.

Equation 5.9 is independent of the choice of T_S. It is often useful to choose a second reference temperature and repeat the graphical evaluation that provides new parameters C_1'' and C_2'' for a new T_g ($\cong T_g'$) (Ferry, 1980; Ogawa et al., 1998). Thus, C_1' and C_2' can be given by Equations 5.16 and 5.17.

$$C_1'' = C_1'C_2' / (C_2' + T_g - T_g') \tag{5.16}$$

$$C_2'' = C_2' + T_g - T_g' \tag{5.17}$$

So, C_1'' and C_2'' can be determined from C_1', C_2' and T_g for the arbitrary T_g'. The shift factor for any T_g, log S_T, can be represented when C_1' and C_2' are known for a given T_g. For this reason, C_1'' and C_2'' are given as a function of T_g' in Equations 5.18 and 5.19 for carbon fiber reinforced epoxy composites.

$$C_1'' = \frac{83.6555}{467.3854 - T_g'} \tag{5.18}$$

$$C_2'' = 467.3854 - T_g' \tag{5.19}$$

The comparison between the experimental shift factors and those predicted by WLF equation using C_1'' and C_2'' are displayed in Figure 5.50 (a). The experimental shift factors according to T_g are in good agreement with the predicted curves, verifying that the relaxation modulus of the carbon fiber reinforced epoxy composites can be predicted.

By the same process, the experimental shift factors of the aramid fiber reinforced epoxy composites can be determined. The corresponding C_1'' and C_2'' are given in Equations 5.20 and 5.21. The comparison between the experimental shift factors and the curves predicted by WLF equation is illustrated in Figure 5.50 (b).

$$C_1'' = \frac{53.029}{443.1501 - T_g'} \tag{5.20}$$

$$C_2'' = 443.1501 - T_g' \tag{5.21}$$

There are not significant differences between Figures 5.49 and Figure 5.50. But the advantage of the curve predicted by Equation 5.18, 5.19, 5.20 and 5.21, as shown in Figures 5.50 (a) and (b), is that the modified parameter C_1'' and C_2'' are related to the glass transition temperature, the important material property that can be measured.
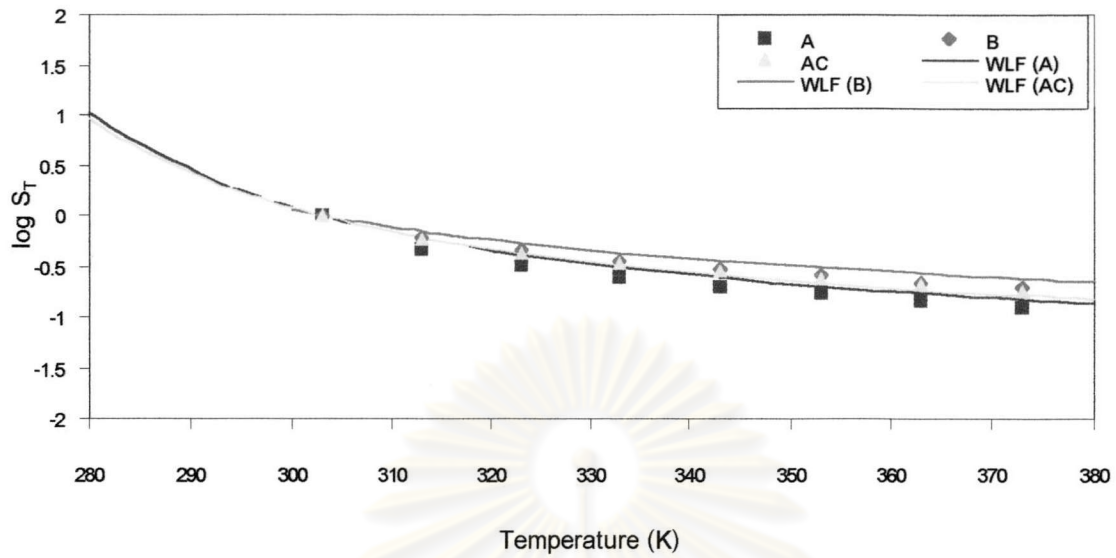
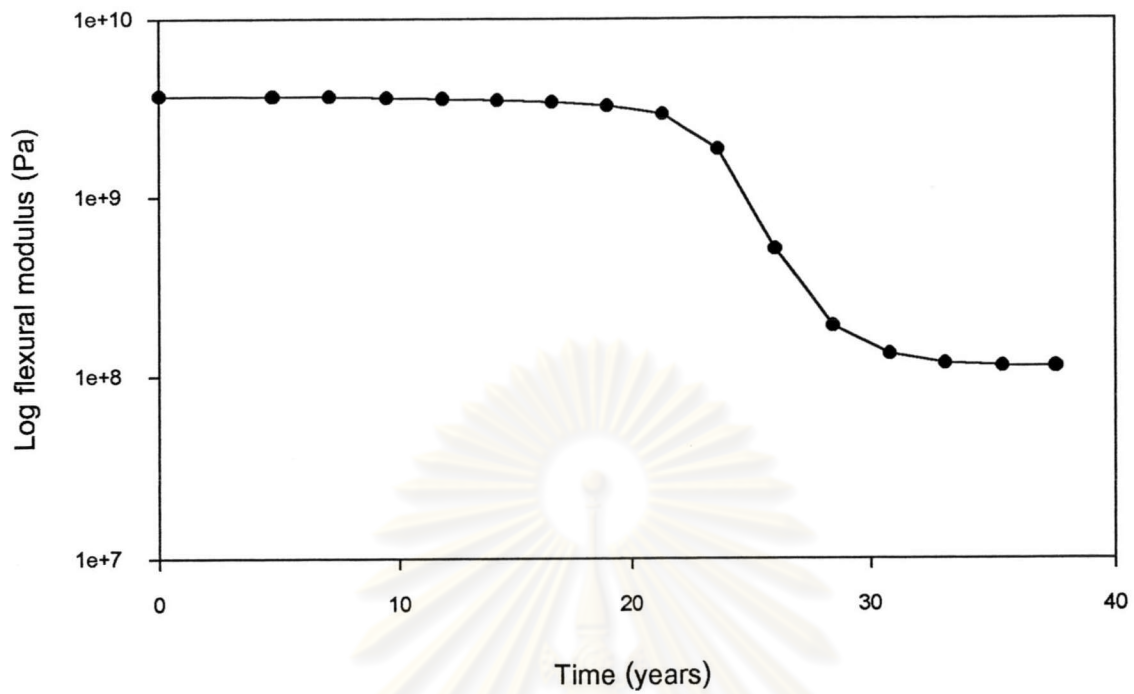(a) Carbon fiber reinforced composites
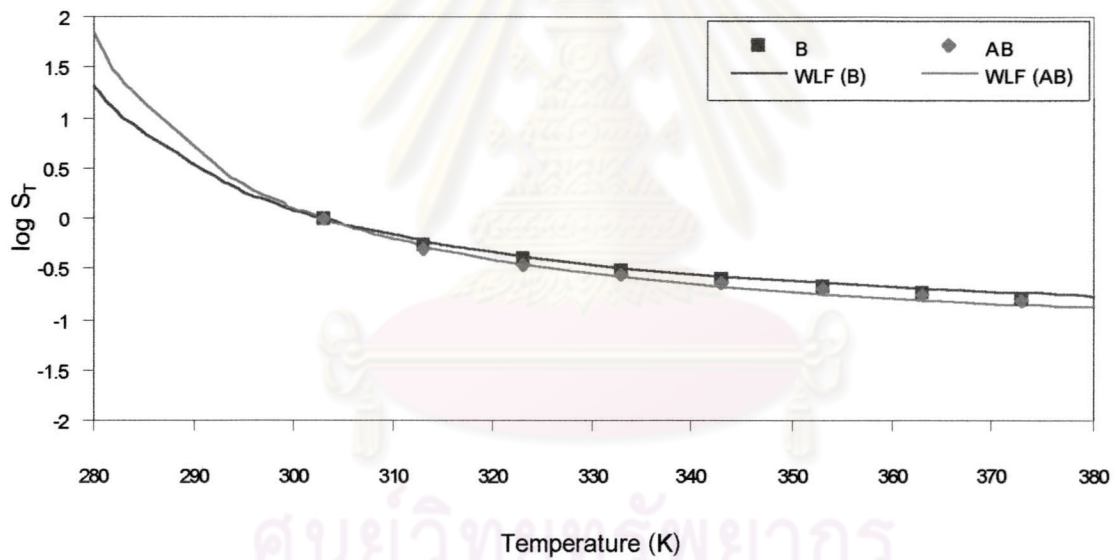
(b) Aramid fiber reinforced composites

Figure 5.50: Comparison of the shift factors of fiber reinforced epoxy composites obtained from the present experimental study and those predicted by the WLF equation using the modified C_1'' and C_2''.

The life span prediction of the fiber reinforced composites in the present study can be performed by using the DMA data and the flexural data. Thus, the short term dynamic behavior of the fiber reinforced composite can be utilized to estimate their long term behavior. Figures 5.51 shows the relationship between the flexural modulus and the expected service life of the fiber reinforced composites studied in the present work. This predicted behavior revealed that a change of modulus would be drastic at the onset of the twenty first year for carbon fiber reinforced composite and the twenty fourth year for aramid fiber reinforced composite. Critically abrupted change in the modulus is predicted between the 21st – 26th year for carbon fiber reinforced composite and the 24th – 29th year in aramid fiber reinforced composite. A change in the modulus by close to 50% in the fiber reinforced composite will occur after the carbon fiber reinforced epoxy composite has been used for about 24 years while that of the aramid fiber reinforced epoxy composite will after about 27 years.

(a) carbon fiber reinforced epoxy composite
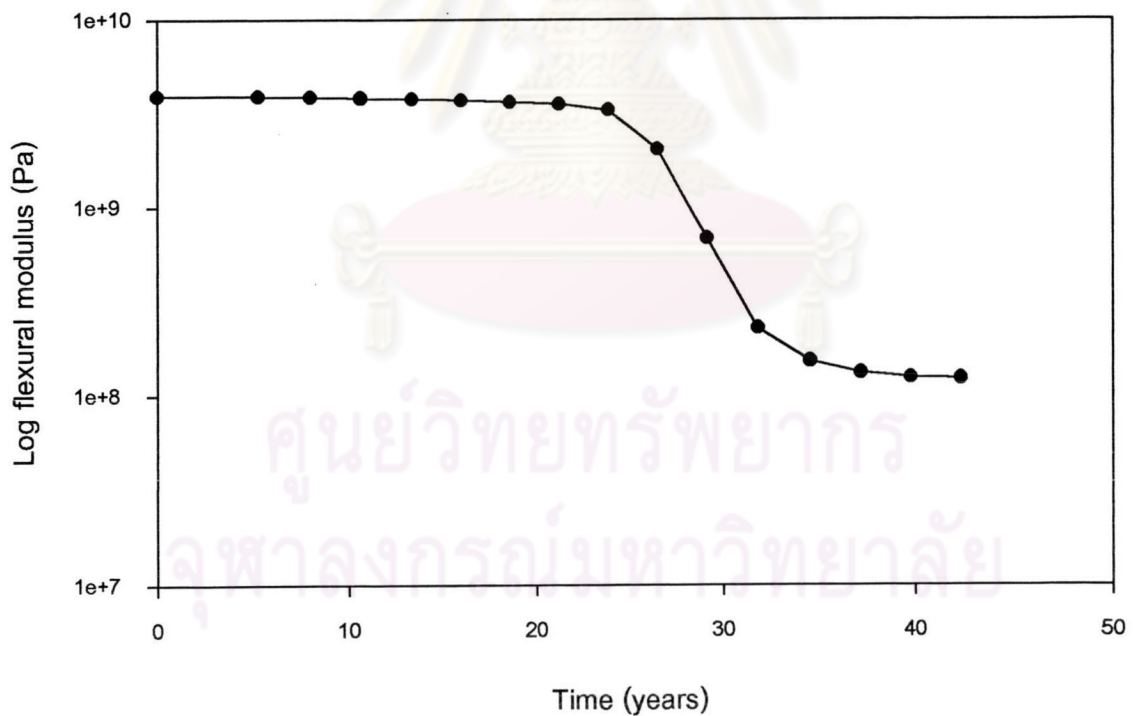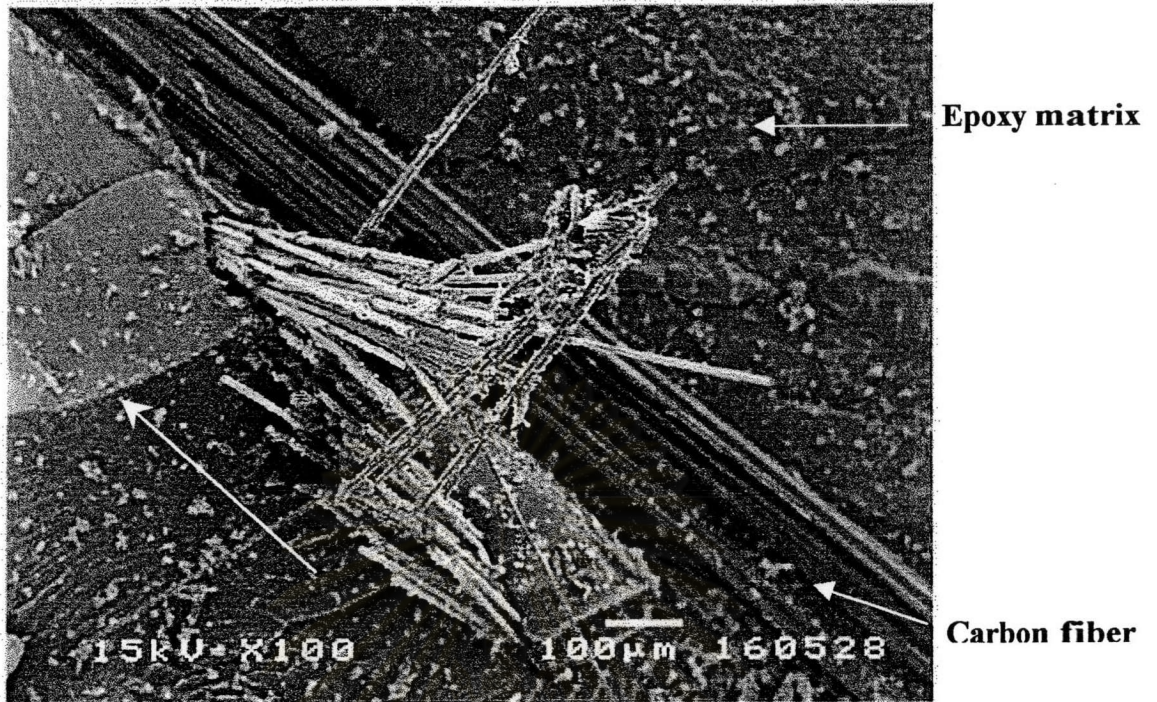

(b) aramid fiber reinforced epoxy composite

Figure 5.51: Predicted flexural modulus along the service life of fiber reinforced epoxy composites.

5.6 MICROSCOPIC OBSERVATION

The fracture surface of fiber reinforced epoxy composites are depicted microscopically in their fractographs in Figures 5.52 to 5.54 broken by torsion.

Figure 5.52 (a) shows a broad view of the fracture surface of carbon fiber reinforced epoxy composite cracked in the double torsion test. Fracture surface of the carbon fiber reinforced composite seems rough, implying that it is quite a tough material. The surfaces of the aramid fiber reinforced epoxy composites, also fractured in the double torsion test, is shown in Figures 5.52 (b). Similar to those of carbon fiber reinforced epoxy composites, the epoxy matrix formed a very rough surface, also indicating that the composite is a tough material. It can be seen from the Figure 5.52 that the fracture surface of the aramid fiber reinforced composite is rougher than that of carbon fiber reinforced composite, implying that the aramid fiber reinforced composite was tougher than the carbon fiber reinforced composite. This was reflected by the greater fracture toughness observed quantitatively in the aramid fiber reinforced composite in Figures 5.33 and 5.34.

Further observation revealed river markings formed abundantly in the epoxy matrix, as shown in Figure 5.53. Specifically, the fracture surface shown in Figure 5.53 was the epoxy layer at the middle of crack. River markings were observed both in the carbon fiber reinforced composite and in the aramid fiber reinforced composite. It is obvious that the formation of the river markings resulted from local plastic deformation (Jarun Chutmanop, 1994). It is an important morphological clue for locating local crack propagation. It can be utilized to indicate the direction of local crack propagation.
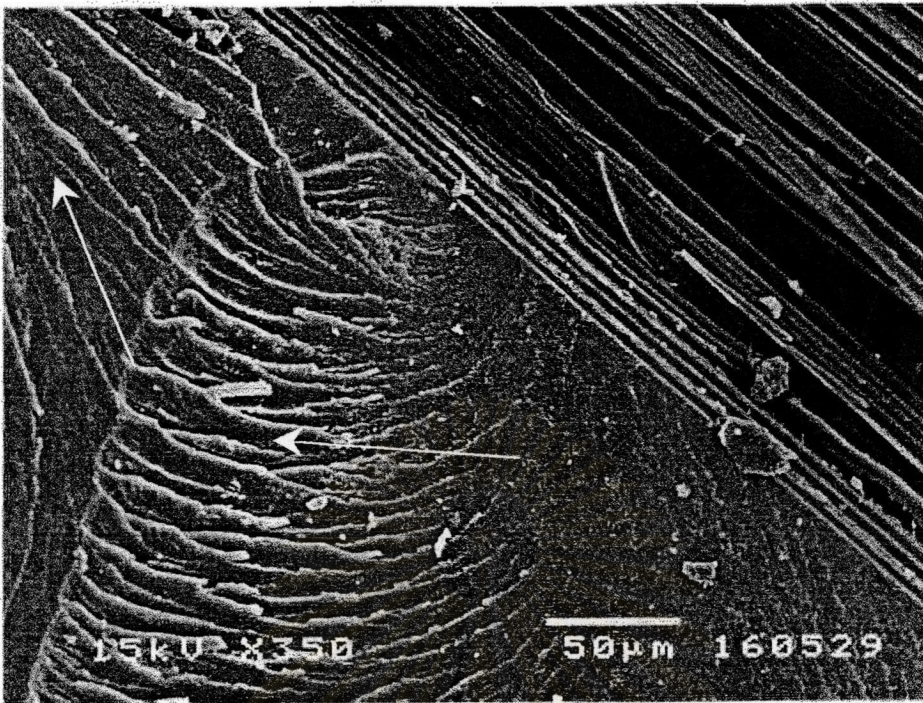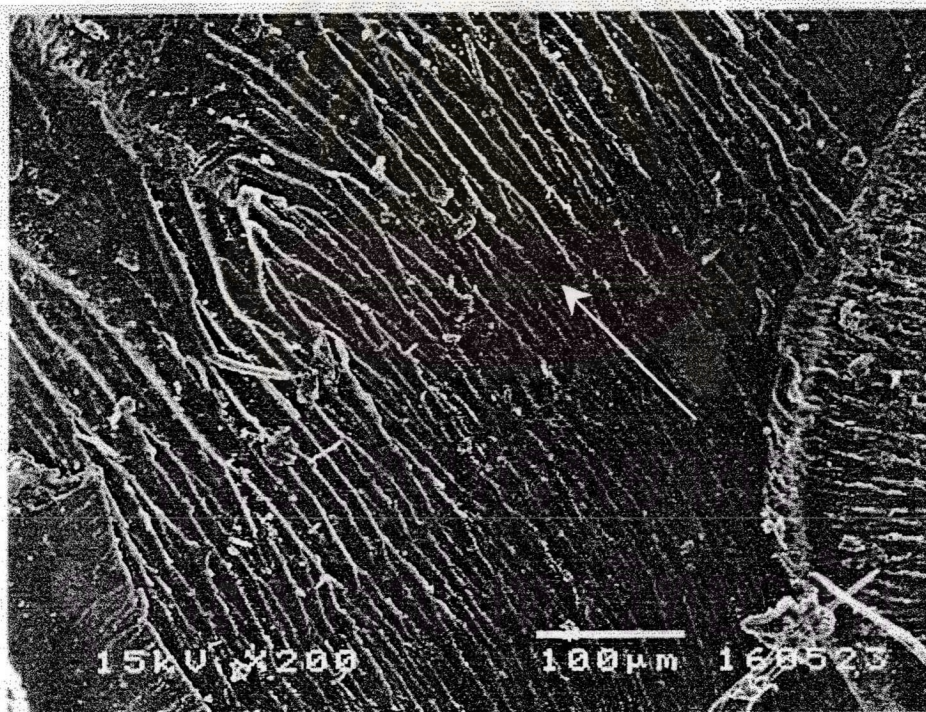
(a) carbon fiber reinforced composite

(b) aramid fiber reinforced composite

Figure 5.52: Fracture surface of fiber reinforced epoxy composites. Arrow indicates the direction of crack propagation.
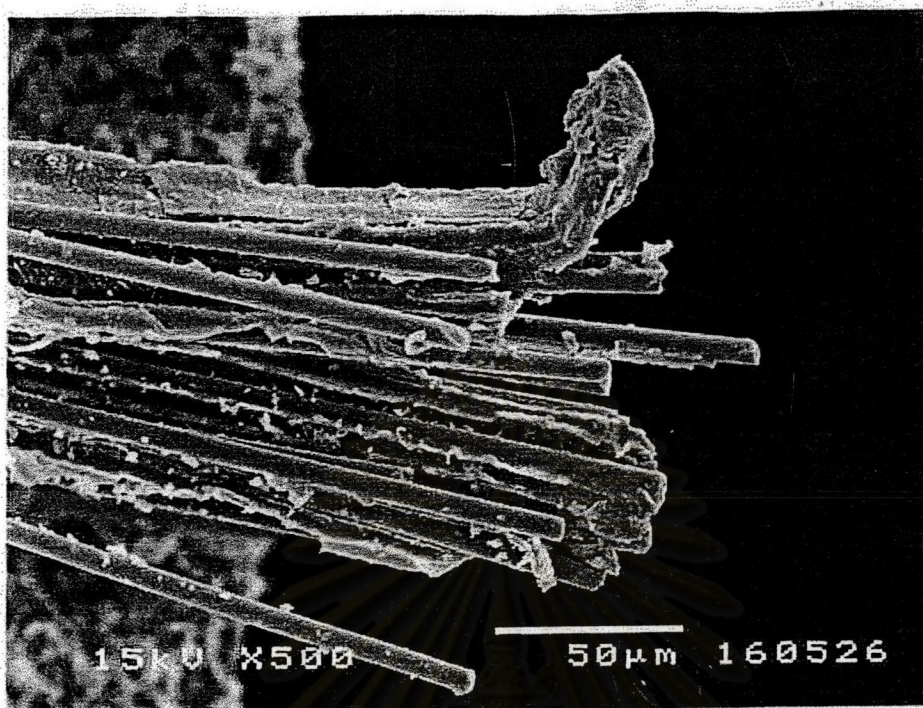
(a) carbon fiber reinforced composite

(b) aramid fiber reinforced composite

Figure 5.53: River markings in the epoxy matrix of fiber reinforced epoxy composites. Arrow indicates the direction of crack propagation.

Figures 5.54 demonstrate the adhesion between the fiber and the epoxy matrix. The epoxy resin seems to adhere well to both carbon fiber and aramid fiber. From Figure 5.54 (b), the epoxy matrix of the aramid fiber reinforced epoxy composite has an elongated groove, representing a morphological clue on the matrix and revealing the position where a fiber had been placed prior to fractures. A part of the aramid fiber still lies on the fracture surface of the specimen. This is a clue that indicates the quality of adhesion between the epoxy matrix and the aramid fiber.

(a) carbon fiber reinforced composite

(b) aramid fiber reinforced composite

Figure 5.54: Adhesion between fibers and epoxy resin in the epoxy composites failed by double torsion test.